

**PEP7 is a ligand for receptor kinase  
SIRK1 to regulate aquaporins and root  
growth**

**Dissertation for Obtaining the Doctoral Degree of  
Natural Sciences (Dr. rer. nat.)**

**Faculty of Natural Sciences  
University of Hohenheim**

Institute of Biology  
Department of Plant Systems Biology

Submitted by

**Jiahui Wang**

Shuozhou, Shanxi, V.R. China

2021

Dean: Prof. Dr. Uwe Beifuß  
1st reviewer / examiner: Prof. Dr. Waltraud Schulze  
2nd reviewer / examiner: Prof. Dr. Andreas Schaller  
3rd examiner: Prof. Dr. Andreas Kuhn

Date of submission: July 6th, 2021  
Date of oral examination: September 29th, 2021

This work was accepted by the Faculty of Natural Sciences at the University of Hohenheim on July 19<sup>th</sup>, 2021 as “Dissertation for Obtaining the Doctoral Degree of Natural Sciences”.

# Contents

List of Figures and Tables.....	III
Abbreviations.....	IV
Summary.....	VI
Zusammenfassung.....	VIII
1. Introduction.....	1
1.1 General Introduction.....	1
1.2 Plant Receptor-like Kinases.....	2
1.2.1 Diversity and Functions of RLKs.....	2
1.2.2 Ligand-Sensing Structural Mechanism and Signal Transduction Mechanism of RLKs.....	3
1.3 Peptide Signaling.....	5
1.4 The PROPEP-PEP-PEPR System.....	7
1.5 AE-MS Provides Sensitive Detection of Protein-Protein Interactions under Limited Conditions.....	9
1.6 Previous Work on SIRK1 (Sucrose-Induced Receptor Kinase).....	11
1.7 Aim of the Research.....	13
2. Material and Methods.....	14
2.1 Plant Materials and Growth Conditions.....	14
2.2 Acquisition of Native Membrane Proteins.....	14
2.2.1 Seeds Sterilization and Vernalization.....	14
2.2.2 Hydroponic Culture.....	14
2.2.3 Microsomal Fraction Isolation.....	15
2.3 Production of Recombinant Protein.....	15
2.3.1 Transient Expression of Recombinant SIRK1 in <i>Nicotiana benthamiana</i> .....	15
2.3.2 Protein Extraction and Strep-Tag Purification.....	15
2.3.3 SDS-PAGE and Western Blot.....	16
2.4 Protein Concentration Measurement.....	17
2.4.1 BCA Assay.....	17
2.4.2 Bradford Assay.....	17
2.5 Pull-downs of GFP-tagged SIRK1.....	17
2.6 In Vitro SIRK1 Kinase Activity Assay.....	17
2.7 Detection of Ligand-Receptor Interactions.....	18
2.7.1 Binding Assays.....	18
2.7.2 Competitive Binding Assay.....	19
2.7.3 Microscale Thermophoresis.....	19
2.8 Sample Preparation for LC-MS/MS.....	19
2.8.1 in Solution Trypsin Digestion.....	19
2.8.2 Phosphopeptide Enrichment.....	20
2.8.3 Peptide Desalting over C18-Stage Tips.....	20
2.9 LC-MS/MS Analysis of Peptides and Phosphopeptides.....	20
2.10 Mass Spectrometric Data Analysis.....	20
2.10.1 Peptide and Protein Identification.....	20
2.10.2 Label-Free Peptide and Protein Quantitation.....	21

2.10.3 Statistical Analyses and Data Visualization.....	21
2.11 Phenotype Experiment.....	21
2.11.1 Drought Stress in Soil.....	21
2.11.2 Osmotic Stress in Plate.....	21
2.11.3 Protoplast Swelling Assay.....	22
2.11.4 Plate Assay for Primary Root Elongation.....	24
3. Results.....	25
3.1 SIKK1 and QSK1 Co-responded to Abiotic Osmotic Stress at the Whole Plant Level.....	25
3.1.1 The <i>sirk1qsk1</i> Double Mutant Showed the Most Superior Survival Ability in Response to Drought Stress in Soil.....	25
3.1.2 The Roots of <i>sirk1qsk1</i> Double Mutant Showed a Strong Osmotic Stress Tolerance Capacity in Response to Osmotic Stress in Plates.....	26
3.2 Characterization of PEP7 as a Ligand Candidate.....	28
3.2.1 Identification of SIKK1 Ligand Candidates.....	28
3.2.2 PEP7 Induced Kinase Activity of SIKK1 in a Concentration-Dependent Manner.....	29
3.3 PEP7 Bound to SIKK1 Ectodomain.....	31
3.3.1 In Vitro Inverse Binding Assay Enables Detection of PEP7-SIKK1 Interactions.....	31
3.3.2 Pre-bound SIKK1-PEP7 Complex could be Competitively Released by Free PEP7.....	33
3.3.3 Microscale Thermophoresis Uncovered the Ligand-Receptor Binding of PEP7 to SIKK1.....	34
3.4 PEP7 was Capable of Activating the SIKK1 Signaling Cascades.....	37
3.4.1 Experimental Design and Workflow.....	37
3.4.2 PEP7 Induced SIKK1 Signaling Complex Formation.....	39
3.4.3 PEP7 Induced Phosphorylation of SIKK1 Substrates.....	41
3.5 PEP7 Affected Water Influx to Protoplasts via SIKK1.....	44
3.6 PEP7/SIKK1 Signaling Pathway Affected Root Growth.....	47
4. Discussion.....	49
4.1 PEP7 as a Specific Member of the Danger Signal Peptide Family.....	49
4.2 Linkage between Sucrose and PEP7.....	50
4.2.1 Sucrose Supply Induces the Secretion and Accumulation of PEP7.....	50
4.2.2 Sucrose Affects Gene Expression Level and Phosphorylation Status of PROPEP7.....	50
4.2.3 Processing of PEP7.....	52
4.2.4 Possible Feedback Regulation of PEP7/SIKK1 Signaling.....	52
4.3 Receptor-Ligand Binding.....	53
4.4 The Possible Role(s) of the PEP7-SIKK1/QSK1-PIPs System in Plant Drought Tolerance.....	54
5. Conclusions and Perspective.....	55
6. Supplementary Data.....	56
7. Bibliography.....	67
8. Acknowledgments.....	79
9. Declaration.....	80
10. Curriculum Vitae.....	81

## List of Figures and Tables

Figure 1: Typical RLK signal cascade steps, adapted from (Hohmann et al., 2017).....	5
Figure 2: Comparison of AP-MS and AE-MS, modified from (Walhout et al., 2012; Keilhauer et al., 2015). .....	10
Figure 3: Scheme of functional model of the SIRK1/QSK1 complex at the plasma membrane, adapted from (Wu et al., 2019). .....	11
Figure 4: SIRK1 and QSK1 confer distinct regulatory effects on PIP2F, adapted from (Wu et al., 2019).	12
Figure 5: water flux density calculation.....	23
Figure 6: Phenotypes comparison of <i>sirk1</i> , <i>qsk1</i> , <i>sirk1qsk1</i> and wild type plant under drought conditions in soil.....	26
Figure 7: Root phenotypes of Col-0, <i>sirk1</i> , <i>qsk1</i> , and <i>sirk1qsk1</i> under osmotic stress (generated by PEG) and normal condition (CK) on agar plates. ....	27
Figure 8: Screen for peptide ligands, data collected from Stefanie König's master's thesis. ....	29
Figure 9: Kinase activity of SIRK1-GFP induced by different signaling peptides.....	30
Figure 10: Binding assays of PEP7 to immobilized SIRK1. ....	32
Figure 11: Competitive binding assays.....	33
Figure 12: Purification and identification of SIRK1-ECD. ....	35
Figure 13: Microscale thermophoresis assay.....	36
Figure 14: Proteomics (phosphoproteomics) experimental design and workflow.....	38
Figure 15: Interactome of SIRK1 induced by PEP7 and Sucrose.....	40
Figure 16: PEP7-induced alterations of phosphorylation of SIRK1 substrates. ....	43
Figure 17: Volume change of protoplasts over time.....	45
Figure 18: Water influx density of protoplasts induced by osmotic changes. ....	46
Figure 19: Root growth phenotype. ....	48
Figure 20: Normalized ion intensity of PEP7 in apoplasmic fractions under different nutrient supply. ....	50
Figure 21: Phosphorylation of PROPEP7 in context of internal and external sucrose. ....	51
Figure 22: PEP7 inducible SIRK1 kinase activity in relationship with the concentration of PEP7 at different internal sucrose concentrations. ....	53
Figure S1: Identification of double mutant of <i>sirk1pep7</i> as a result of crossing single mutants <i>sirk1</i> (SALK_125543) and <i>pep7</i> (SALK_025824).....	56
Figure S2: Expression of SIRK1 was detected by western blotting. ....	56
Table 1: Overview of the buffers used in the protoplast swelling assays. ....	23
Table S1: Synthetic peptides used in the experiment.....	56
Table S2: Interaction partners recruited by SIRK1 under different treatments. ....	57
Table S3: List of identified phosphopeptides.....	61

## Abbreviations

<b>aa</b>	amino acid
<b>ABA</b>	Abscisic Acid
<b>ACN</b>	Acetonitrile
<b>ADP</b>	Adenosine Diphosphate
<b>AE-MS</b>	Affinity Enrichment Mass Spectrometry
<b>AP-MS</b>	Affinity Purification Mass Spectrometry
<b>ATP</b>	Adenosine Triphosphate
<b>BAK1</b>	BRI1-Associated Receptor Kinase 1
<b>BAM1</b>	Barely Any Meristem 1
<b>BR</b>	Brassinolide
<b>BRI1</b>	Brassinosteroid Insensitive1
<b>BSA</b>	Bovine Serum Albumin
<b>CEP</b>	C-terminally Encoded Peptides
<b>CEPR</b>	C-terminally Encoded Peptides Receptor
<b>CERK</b>	Chitin Elicitor Receptor Kinase
<b>cGMP</b>	cyclic GMP
<b>ECD</b>	Ectodomain
<b>ED</b>	End of Day
<b>EFR</b>	EF-TU Receptor
<b>EF-TU</b>	Elongation Factor TU
<b>EN</b>	End of Night
<b>EPF</b>	Epidermal Pattern Factor
<b>FDR</b>	False Discovery Rate
<b>Flg22</b>	A 22-amino acid peptide fragment of the N-terminal region of Flagellin
<b>FLS2</b>	Flagellin-Sensing 2
<b>GRP</b>	Glycine-Rich Protein
<b>HSL</b>	HAESA-Like
<b>IDA</b>	Inflorescence Deficient in Abscission
<b>ID</b>	IDA-Like
<b>JA</b>	Jasmonic Acid
<b>Kd</b>	Dissociation Constant
<b>LC-MS/MS</b>	Liquid Chromatography-tandem Mass Spectrometry
<b>LFQ</b>	Label Free Quantification
<b>LRR</b>	Leucine Rich Repeat
<b>LRR-RLK</b>	Leucine Rich Repeat Receptor-Like Kinase
<b>LysM</b>	Lysin Motif

<b>MAPK</b>	Mitogen-Activated Protein Kinase
<b>MC</b>	Metacaspase
<b>MF</b>	Microsomal Fraction
<b>MST</b>	Microscale thermophoresis
<b>NO</b>	Nitric Oxide
<b>PEG</b>	Polyethylene Glycol
<b>PEP</b>	Plant Elicitor Peptide
<b>PEPR</b>	PEP Receptor
<b>PERK</b>	Proline-rich Extensin-like Receptor Kinase
<b>PIC</b>	Protease Inhibitor Cocktail
<b>PIP</b>	Plasma Membrane Intrinsic Proteins
<b>PROPEP</b>	Precursor of Plant Elicitor Peptide
<b>PSK</b>	Phytosulfokine
<b>PSKR</b>	Phytosulfokine Receptor1
<b>PTI</b>	Pattern-Triggered Immunity
<b>PTM</b>	Posttranslationally Modified
<b>PXY</b>	Phloem Intercalated With Xylem
<b>QSK</b>	Qiān Shǒu (Chinese: 千手 ‘thousand hands’ ) Kinase
<b>RALF</b>	Rapid Alkalinization Factor
<b>RLK</b>	Receptor-Like Kinase
<b>ROS</b>	Reactive Oxygen Species
<b>SERK</b>	Somatic Embryogenic Receptor Kinase
<b>SIRK</b>	Sucrose Induced Receptor Kinase
<b>SYR</b>	Systemin Receptor
<b>WAK</b>	Wall-Associated Kinase
<b>WT</b>	Wild Type

## Summary

Plant cells have evolved a wide array of sensors to monitor changes in plant endogenous and external environmental cues for proper plant development. Among those sensors, the receptor kinases constitute the largest protein family in regulating various responses to external and internal biotic and abiotic signals. In general, the activation of receptor kinases requires the binding of their corresponding ligands. However, for a large number of receptor kinases, their ligands remain unknown. In recent years, more and more small peptides have been discovered as signals controlling plant development and response to external stimuli by activating specific receptor kinases. A consensus is emerging that receptor kinases are prime candidates for recognition of various biologically active peptides. However, to date, still only few receptor kinases have been precisely assigned with peptide signaling functions, and the identification of ligand-receptor pairs has become a big challenge in the field of plant biology.

The major objective of this thesis was to determine the ligand for the known receptor kinase SIRK1 (Sucrose-Induced Receptor Kinase 1). Previously, the role of SIRK1 and QSK1 (qiān shǒu, Chinese: 千手 ‘thousand hands’ kinase) as a receptor/co-receptor pair in regulating aquaporins in response to osmotic changes induced by sucrose was demonstrated. Moreover, a large-scale ligand screening assay helped to narrow down the candidate ligands for SIRK1 to a few small peptides, and after exposing SIRK1 to such different small peptides in a kinase assay, only PEP7, a member of the PEP (Plant Elicitor Peptide) family, was able to increase the kinase activity of SIRK1. Therefore, the hypothesis that PEP7 acts as a ligand for SIRK1 has been proposed. To test this hypothesis, a series of experiments using the synthetic peptide PEP7 were conducted in this project, focusing on exploring the mutual recognition of PEP7 and SIRK1, the activation of the SIRK1 signaling complex by PEP7, and the biological function of PEP7/SIRK1 as a ligand/receptor pair in response to osmotic stress. In the assays to detect the binding of PEP7 and SIRK1, PEP7 was captured by the immobilized SIRK1-ECD (SIRK1 Ectodomain), while reverse pull-down experiments revealed that PEP7 likewise captured SIRK1 from different solutions, including heterologous expression of SIRK1-ECD and native SIRK1 from microsomal fractions. The binding affinity of PEP7 and SIRK1-ECD was determined by microscale thermophoresis, and a binding constant of approximately 19  $\mu\text{M}$  was determined in the absence of co-receptor QSK1. After confirming the binding of PEP7 to SIRK1-ECD, we investigated the activation of the SIRK1 signaling pathway by PEP7. The induction of the SIRK1 signaling complex formation by PEP7 was analyzed with the aid of an AE-MS (affinity enrichment mass spectrometry) approach. As did sucrose, external PEP7 treatment induced the formation of signaling complexes involving SIRK1, QSK1 and aquaporins. In addition, phosphoproteomic studies revealed that PEP7 induced phosphorylation of SIRK1 substrates, including aquaporins. These results supported our hypothesis, that PEP7/SIRK1 is involved in the regulation of aquaporins as a ligand/receptor pair. In order to ascertain the biological function of this regulation, mutant analyses were performed in conjunction with the physiological experiments. It was shown that the knockout mutants of receptor SIRK1 (*sirk1* plants) were insensitive to external PEP7 treatment. Only in the presence of SIRK1, PEP7 was able to regulate aquaporins and alter their activity, thus affecting water influx into the protoplasts. While analyzing the effect of PEP7 on the receptor SIRK1 at the whole plant level, we observed that PEP7/SIRK1 as a

ligand/receptor pair can also affect root growth. Thus, the role of PEP7/SIRK1 as a ligand-receptor pair for regulating water influx into protoplasts and affecting root growth was validated. In experiments conducted with PEP7, the two other members of the PEP family, PEP6 and PEP4, were also included. Binding to the receptor SIRK1 and induction of physiological responses was specific to PEP7. Other members of the PEP-family (PEP6, PEP4) were unable to induce SIRK1 kinase activity, aquaporin phosphorylation, or protoplast water influx activity.

In addition, phenotypic analyses of SIRK1 and QSK1 knockout mutants was carried out at the whole-plant level. Observations on drought-stressed rosette leaves (in soil) and simulated drought-stressed roots (in plates) demonstrated that the double mutant *sirk1qsk1* exhibited the greatest resistance to osmotic stress. This illustrated that SIRK1/QSK1 co-regulates plant water uptake at the whole plant level, and also suggested the stabilizing and enhancing function of QSK1 as a co-receptor for SIRK1.

In summary, this work showed that PEP7 is a ligand for the receptor kinase SIRK1 regulating aquaporins and root growth. Biochemical assays demonstrated that PEP7 binds to the extracellular domain of SIRK1. Proteomic (phosphoproteomic) studies revealed the activation of the SIRK1 signaling complex by PEP7, including PEP7-induced formation of the SIRK1 signaling complex and PEP7-induced phosphorylation of SIRK1 substrates. The biological function of PEP7/SIRK1 as a ligand-receptor pair for regulating water influx into protoplasts and affecting root growth became evident. Our work presents and functionally characterizes a novel ligand-receptor pair, contributing some new insights to the still vastly unknown field of plant receptor kinases and small signaling peptides. Nevertheless, there are still many unanswered questions in the proposed PEP7/SIRK1 signaling pathway, for example, we do not know exactly how sucrose resupply caused the binding of PEP7 to SIRK1, and whether the PEP7/SIRK1 signaling pathway also affects plant water uptake at the whole plant level and thus plant stress tolerance.



## Zusammenfassung

Pflanzenzellen haben ein breites Spektrum an Sensoren entwickelt, um Veränderungen in Antwort auf endogene Signale der Pflanze und externe Reize aus der Umwelt für die richtige Pflanzenentwicklung zu überwachen. Unter diesen Rezeptorsystemen bilden die Rezeptorkinasen die größte Proteinfamilie. Im Allgemeinen erfordert die Aktivierung von Rezeptorkinasen die Bindung eines entsprechenden Liganden. Die Liganden einer großen Anzahl von Rezeptorkinasen sind jedoch immer noch unbekannt. In den letzten Jahren wurden mehr und mehr kleine Peptide entdeckt, die die pflanzliche Entwicklung und die Reaktion auf externe Stimuli steuern, indem sie spezifische Rezeptorkinasen aktivieren. Es zeichnet sich ab, dass Rezeptorkinasen die Hauptkandidaten für die Erkennung verschiedener biologisch aktiver Peptide mit Signalfunktion sind. Jedoch konnten bisher nur wenige dieser vermuteten direkten Interaktionen zwischen Rezeptorkinasen und Peptidliganden mit Sicherheit bestätigt werden. Die Identifizierung von Liganden-Rezeptor-Paaren ist damit zu einer großen Herausforderung im Bereich der Pflanzenbiologie geworden.

Das Hauptziel dieser Arbeit war es, den Liganden der bekannten Rezeptorkinase SIRK1 (Sucrose-Induced Receptor Kinase 1) zu bestimmen. Zuvor wurde die Rolle von SIRK1 und QSK1 (qiān shǒu, chinesisch: 千手 'tausend Hände' Kinase) als Rezeptor/Co-Rezeptor-Paar nachgewiesen, und eine Rolle bei der Regulierung von Aquaporinen als Reaktion auf osmotische Veränderungen gezeigt. Darüber hinaus half ein groß angelegtes Liganden-Screening-Assay dabei, die Liganden-Kandidaten für SIRK1 auf einige wenige kleine Peptide einzugrenzen. Nachdem SIRK1 solchen verschiedenen kleinen Peptiden in einem Kinase Assay ausgesetzt wurde, konnte nur PEP7, ein Mitglied der PEP (Plant Elicitor Peptide) -Familie, die Kinase-Aktivität von SIRK1 erhöhen. Daher stellten wir die Hypothese auf, dass PEP7 als Ligand für SIRK1 fungiert. Um diese Hypothese zu testen, wurden innerhalb dieser Dissertation eine Reihe von Experimenten mit einem synthetischen PEP7 Peptid durchgeführt. Der Fokus lag dabei auf der Erforschung der gegenseitigen Erkennung von PEP7 und SIRK1, der Aktivierung des SIRK1-Signalkomplexes durch PEP7 und der biologischen Funktion von PEP7/SIRK1 als Ligand/Rezeptor-Paar in Reaktion auf osmotischen Stress. In der Tat wurde PEP7 von der immobilisierten SIRK1-ECD (SIRK1 Ectodomain) gebunden, und Reverse-Pull-Down-Experimente zeigten, dass PEP7 ebenfalls SIRK1 bindet, einschließlich der heterolog exprimierten und gereinigten SIRK1-ECD und nativem SIRK1 aus mikrosomalen Fraktionen. Die Bindungsaffinität von PEP7 und SIRK1-ECD wurde mittels Microscale Thermophorese bestimmt, wobei sich in Abwesenheit des Co-Rezeptors QSK1 eine Bindungskonstante von ca. 19  $\mu\text{M}$  ergab. Nachdem die Bindung von PEP7 an SIRK1-ECD gezeigt wurde, untersuchten wir die Aktivierung des SIRK1-Signalweges durch PEP7. Die Induktion der SIRK1-Signalkomplexbildung durch PEP7 wurde mit Hilfe eines AE-MS-Ansatzes (Affinitätsanreicherungs-Massenspektrometrie) analysiert. Sowohl Saccharose, als auch die externe PEP7-Behandlung, induzierten die Bildung von Signalkomplexen, an denen SIRK1, QSK1 und Aquaporine beteiligt waren. Zusätzlich zeigten Untersuchungen des Phosphoproteoms, dass PEP7 die Phosphorylierung von SIRK1-Substraten induzierte, darunter auch Aquaporine. Diese Ergebnisse unterstützten unsere Hypothese, dass PEP7/SIRK1 als Ligand/Rezeptor-Paar an der Regulation der Aquaporine beteiligt ist. Um die biologische Funktion dieser Regulation näher zu ermitteln, wurden physiologische Experimente mit Mutanten durchgeführt. Knockout-Mutanten des

SIRK1 Rezeptors (*sirk1*-Pflanzen) zeigten sich unempfindlich gegenüber externer PEP7-Behandlung. Nur in Anwesenheit von SIRK1 war PEP7 in der Lage, Aquaporine zu regulieren und deren Aktivität zu verändern und damit den Wassereinstrom in die Protoplasten zu beeinflussen. Bei der Analyse der Wirkung von PEP7 auf den Rezeptor SIRK1 auf der Ebene der gesamten Pflanze haben wir beobachtet, dass PEP7/SIRK1 als Ligand/Rezeptor-Paar auch das Wurzelwachstum beeinflussen kann. Somit wurde die Rolle von PEP7/SIRK1 als Liganden-Rezeptor-Paar für die Regulierung des Wassereinstroms in Protoplasten und die Beeinflussung des Wurzelwachstums validiert. In Experimenten, die mit PEP7 durchgeführt wurden, haben wir als Kontrolle auch zwei andere Mitglieder der PEP-Familie, PEP6 und PEP4, einbezogen. Die Bindung an den Rezeptor SIRK1 und die Induktion von physiologischen Reaktionen war jedoch spezifisch für PEP7. Andere Mitglieder der PEP-Familie (PEP6, PEP4) waren nicht in der Lage, SIRK1-Kinase-Aktivität, Aquaporin-Phosphorylierung oder Protoplasten-Wassereinstrom-Aktivität zu induzieren.

Weiterhin wurden phänotypische Analysen von SIRK1- und QSK1-Knockout-Mutanten auf Ebene der gesamten Pflanze durchgeführt. Untersuchungen an Rosettenblättern von Pflanzen in trockenheitsgestresster Erde und an Wurzeln in Platten, in denen Trockenstress simuliert wurde zeigten, dass die Doppelmutante *sirk1qsk1* die größte Resistenz gegen osmotischen Stress aufwies. Dies deutet darauf hin, dass SIRK1/QSK1 die Wasseraufnahme der Pflanze nicht nur auf zellulärer Ebene reguliert, sondern Auswirkungen auf der Ebene der gesamten Pflanze hat. Dabei konnte die stabilisierende und verstärkende Funktion von QSK1 als Co-Rezeptor für SIRK1 erneut veranschaulicht werden.

Insgesamt zeigt diese Arbeit, dass PEP7 ein Ligand für die Rezeptorkinase SIRK1 ist, die für die Regulierung der Aquaporine und des Wurzelwachstums wichtig ist. Biochemische Experimente zeigten, dass PEP7 an die extrazelluläre Domäne von SIRK1 bindet. Proteomic-Studien (Phosphoproteomics) zeigten die Aktivierung des SIRK1-Signalkomplexes durch PEP7, einschließlich der PEP7-induzierten Bildung des SIRK1/QSK1-Signalkomplexes und der PEP7-induzierten Phosphorylierung von SIRK1-Substraten. Die biologische Funktion von PEP7/SIRK1 als Ligand-Rezeptor-Paar zur Regulierung des Wassereinstroms in pflanzliche Zellen und zur Beeinflussung des Wurzelwachstums wurde ebenfalls belegt. Diese Arbeit stellt ein neuartiges Liganden-Rezeptor-Paar vor und charakterisiert es funktionell, um damit neue Erkenntnisse auf dem immer noch immer weitestgehend unbekanntem Gebiet der pflanzlichen Rezeptorkinasen zu liefern. Nichtsdestotrotz gibt es noch immer viele unbeantwortete Fragen im hier vorgeschlagenen PEP7/SIRK1 Signalweg. Zum Beispiel wissen wir weiterhin nicht genau, wie die Saccharose die Bindung von PEP7 an SIRK1 auslöst und inwieweit der PEP7/SIRK1 Signalweg auch die Wasseraufnahme auf der Ebene der gesamten Pflanze und somit auch die Stressresistenz der Pflanze beeinflusst.

(Translated by Sven Gombos, modified by Max Gilbert)

# 1. Introduction

## 1.1 General Introduction

Cells in various organisms are able to sense their environment and adapt themselves in response to changes. The sessile lifestyle of plants requires more active cellular physiology to adapt to altering environmental conditions in terms of light intensity, temperature variation, water and nutrient availability, wounding, pathogens attacking and even changes in neighboring plants. All these stimuli become signal inputs to the plant cells, as extracellular information that are precisely recognized at cell surface and integrated with intracellular (metabolic) signals.

The plasma membrane, as the boundary compartment for the separation of the cell's inner "life" from the environment, therefore constituting a communication platform that allows the precise integration of environmental and developmental signals. Receptors are generally protein molecules that are localized at the membrane (internal or peripheral), mainly responsible for signal transduction, including the role of detecting pericellular changes and further translating them into adequate cellular responses. The protein composition as well as their position within membranes is dynamic and stimulus-dependent (Demir et al., 2013; Szymanski et al., 2015). Cell surface receptors are of various types and can perceive diverse signals and stimuli from the environment. Unlike most of the cell surface receptors in animals that are G protein-linked (with a cytosolic domain that associates with a trimeric G protein), most of those found in plants to date are enzyme-linked (with a cytosolic domain that either has an intrinsic enzyme activity or associates directly with an enzyme) (Alberts et al., 2002a, b). In plants, receptor kinases (RKs or RLKs) constitute the largest receptor family, accounting for more than 600 members in *Arabidopsis* (Shiu and Bleecker, 2001b). RLKs are usually transmembrane proteins, comprised of an extracellular domain that confers signal perception specificity, a transmembrane span, and an intracellular serine/threonine kinase domain exposed to the cytoplasm. The diversity in RLKs ectodomains contributes to the involvement of receptor kinases in a wide range of plant developmental processes as well as in responses to biotic and abiotic stresses (Shiu and Bleecker, 2001b, 2003; Osakabe et al., 2013).

In the RLK signal transduction system, ligand-binding is required to induce the RLK activation and initiate the response (Becraft, 2002). In plants, ligands were usually demonstrated as hormones, polypeptides, and small proteins (Ullrich and Schlessinger, 1990; Chinchilla et al., 2006; Yamaguchi et al., 2010; He et al., 2018). To date, the emerging picture shows that peptide signaling predominates in plant development, and appears to be involved in RLKs activation (Lindsey et al., 2002). The involvement of receptor-like kinases in peptide signaling in plants has been reviewed elsewhere previously (Cock et al., 2002; Matsubayashi, 2003; Tichtinsky et al., 2003). It becomes apparent that receptor kinases are primary candidates for the recognition of the variety of signaling peptides, however currently for most of the receptor kinases the precise ligand remains unknown. Therefore, the identification and characterization of ligand-receptor pairs is of high interest in order to gain a more comprehensive understanding of the activation cascade of plant receptor kinases.

## 1.2 Plant Receptor-like Kinases

### 1.2.1 Diversity and Functions of RLKs

The plant receptor kinases are typically serine/threonine kinases but show functional and structural relationships to receptor tyrosine kinases in animals (Shiu and Bleecker, 2001b). Receptor kinases are overrepresented in land plant genomes compared to animals and early differentiating plants such as algae. The relative expression of RLKs is conserved across multiple lineages of land plants, thus it is likely that the expansion of this receptor family predates the differentiation of land plants (Shiu and Bleecker, 2001b, 2003). In *Arabidopsis*, receptor kinases include more than 600 members, representing nearly 2.5% of the protein-coding sequences in the genome, and constitute the largest phylogenetic kinase family in the aggregated *Arabidopsis* kinome (Shiu and Bleecker, 2003).

Plant RLKs are commonly classified into 23 subfamilies on the basis of their extracellular domain (Shiu and Bleecker, 2001b). Of these, receptors containing leucine-rich repeats (LRR) at the extracellular region includes more than 200 members. These LRR-RLKs constitute a third of *Arabidopsis* RLKs subfamilies, and comprise the largest group of transmembrane/cell surface receptors (Diévar and Clark, 2003; Gou et al., 2010; Shinohara et al., 2016). Based on the LRR tandem repeats and the whole sequences origination, the LRR-RLKs are further subdivided into 14 subfamilies (Shiu and Bleecker, 2001b; Gou et al., 2010; Zulawski et al., 2014). Members of this family include many plant developmental regulators, for example, BRI1 as a receptor kinase for the plant steroid hormone brassinolide (BR) (Wang et al., 2001). They participate in many developmental processes such as hypocotyl elongation, meristem development and rosette leaves expansion (Li and Chory, 1997; Wang, 2012); Receptor HASEA was described to bind the IDA (Inflorescence Deficient in Abscission) peptide and is identified in controlling floral organ abscission (Jinn et al., 2000; Santiago et al., 2016). CLAVATA1 (CLV1) is characterized as receptor perceiving the CLAVATA3 peptide to mediate cell differentiation and proliferation in shoot and floral meristems (Clark et al., 1997; Hazak and Hardtke, 2016; Nimchuk, 2017). ERECTA (ER), ERECTA-LIKE1 (ERL1) and ERL2, as members of ERECTA family, are characterized as receptor kinases with function in organogenesis including regulation of inflorescence architecture, organ shape, and epidermal stomatal patterning (Torii et al., 1996; Shpak et al., 2005; Pillitteri and Torii, 2012; Bemis et al., 2013; Escocard de Azevedo Manhães et al., 2021). The LRR-RLKs family also includes some well-characterized immunity regulators, for example, FLS2 as the receptor perceiving flagellin, is a well-known receptor kinase with function in defense against pathogens (Chinchilla et al., 2006; Sun et al., 2013; Janda et al., 2019). EFR (EF-TU RECEPTOR) as a receptor for bacterial EF-TU, is characterized to play a role in plant immunity (Zipfel et al., 2006).

In addition, there are many well-studied receptor kinases belonging to other kinase subfamilies. PERK4 (proline-rich extensin-like receptor kinase 4) belongs to the PERK family and has been identified to be involved in plant abiotic stress response such as ABA responses (Bai et al., 2009). Members of the wall-associated kinase (WAK) subfamily are able to bind cell wall components like pectin through their extracellular domains, and one of the members has been reported to bind a secreted glycine-rich protein (GRP), and may be involved in regulating cell expansion during development (Anderson et al., 2001).

FERONIA is one classical example of a member of the CrRLK1-Like (*Catharanthus roseus* RLK1-like) subfamily which binds to the ligand peptide RALF (Rapid Alkalinization Factor) (Haruta et al., 2014). FERONIA mediates male-female interactions during pollen tube reception (Escobar-Restrepo et al., 2007), root development and plant immune responses (Stegmann et al., 2017; Yu et al., 2020; Zhang et al., 2020). CERK1 (CHITIN ELICITOR RECEPTOR KINASE 1) is a member of Lysine motif (LysM) RLK subfamily and is involved in the plant immune response as a major Chitin-binding receptor (Iizasa et al., 2010; Petutschnig et al., 2010; Liu et al., 2012). Lectin-containing RLKs (LecRLKs) recognize specific sugar moieties present in cell walls of pathogens and nematodes and are associated with jasmonate-mediated defense against pathogens (Balagué et al., 2017; Yekondi et al., 2018).

Receptor-like kinases form a large gene family in plants and the role of kinases in plants covers almost all aspects of plant developmental processes and stress responses (Shiu and Bleecker, 2001a; Diévarit and Clark, 2004; Osakabe et al., 2013). Notably, aside from those typical well-known RLKs, there are a large number of uncharacterized kinases. Characterization of RLKs and their biological functions will provide important information on how plants attempt to maintain "normal" growth and development under various environmental conditions.

### **1.2.2 Ligand-Sensing Structural Mechanism and Signal Transduction Mechanism of RLKs**

In recent years, three-dimensional structural studies of RLK-ligand complexes by X-ray crystallography have provided us with a deeper understanding of the molecular mechanisms underlying the signal recognition. To date, most structural evidence has been obtained for members of the LysM (lysin motif) RLK and LRR RLK receptor families (Hohmann et al., 2017; Wang et al., 2018a). In Arabidopsis, CHITIN ELICITOR RECEPTOR KINASE 1 (*AtCERK1*) is a structurally well-studied member of LysM-RLK family. Ectodomains of *AtCERK1* contain three LysM motifs, the three LysM domains fold tightly against one another in which the LysM2 domain is specifically responsible for reading out a chitin, however, the chitin binding does not induce significant conformational changes (Iizasa et al., 2010; Hohmann et al., 2017). LRR-RLKs like FLS2, PEPR and HAESA bind small peptides in an extended conformation along several of their LRRs through multiple hydrophilic and hydrophobic interactions between the RLK and the peptide's backbone, some of the studies also highlight the importance of the peptide C-terminal residues as well as its post-translational modifications for ligand perception (Chinchilla et al., 2006; Tang et al., 2015; Santiago et al., 2016). In the case of BRI1 and PSKR (receptor of phytosulfokine), their LRR repeats can be interrupted by non-LRR amino acid sequences (called island domains) that protrude from the typical LRR horseshoe arrangement, creating a cleft for ligand binding, where the direct ligand binding triggers a conformational change in the island domain (Matsubayashi et al., 2002; Torii, 2004; She et al., 2011; Hohmann et al., 2017; Wang et al., 2018a).

The signal transduction pathways of receptor kinases usually follow a relatively conserved yet distinct mechanism: classically, the extracellular domain of the receptor kinase recognizes its ligand, ligand perception induces autophosphorylation of the RLK in the kinase domain, and the activated receptor kinase is able to recruit and transphosphorylate its downstream signaling elements, consequently activating the signaling cascade (Figure 1) (Shiu and Bleecker, 2001a; Yang et al., 2012; Hohmann et al., 2017). The

activation mechanism of RLKs vary and can be classified into two types according to available reports on LysM-RLKs and LRR-RLKs: (1) Ligand-induced homodimerization activation mechanism and (2) Ligand-induced heterodimerization activation mechanism. In the first case, as in the case of *At*CERK1, the chitin (at least 7 N-acetyl-D-glucosamine units) is expected to promote homodimerization of *At*CERK1 thereby initiating the activation (Liu et al., 2012; Wong et al., 2015). While LysM RLKs can form homodimers upon chitin binding, the LRR-RLKs normally form heterodimers with another LRR-RLK (so called co-receptor) upon ligand binding, or in some cases, the formation of heterodimer (receptor and co-receptor) is also crucial for ligand binding (Ogawa et al., 2008; She et al., 2011; Sun et al., 2013; Wang et al., 2015; Santiago et al., 2016). LRR-RLKs like the mentioned FLS2, PEPR1, HAESA, BRI1 and PSKR are all known to recruit members of SOMATIC EMBRYOGENIC RECEPTOR KINASE (SERK) family of LRR RLKs as their co-receptors to form heterodimers, and the structural studies suggest that activation of LRR-RLKs is dependent on their shape-complementary co-receptor (Postel et al., 2010; She et al., 2011; Sun et al., 2013; Wang et al., 2015; Santiago et al., 2016). Therefore, the ability of SERK proteins to establish specific interactions with the ligand-perceiving ectodomains of the abovementioned LRR RLKs, suggests that this small family of LRR RLKs is versatile in forming complexes with the ligand-perceiving receptors (Hohmann et al., 2017). Taken together the structures, genetics, biochemistry and evolutionary knowledge about LRR-RKs, we have actually clustered the two groups of LRR-RKs based on their ECD lengths (Xi et al., 2019): the co-receptor group that contain the short ECDs (less than 400aa), and the ligand-perceiving receptor group with long ECDs (more than 400aa). In heterodimers, ligand-perceiving receptors are able to pinpoint certain biological pathways, while co-receptors help anchor the ligand in the extracellular domain and mediate signal transitions within the cell along with the ligand-binding receptor (Zhang et al., 2016a; Hohmann et al., 2018).

To date, structural biology has provided us with a detailed insight of the activation mechanisms of some RLKs in plants, in particular two important subfamilies, LysM-RLKs and LRR-RLKs. Understanding the activation mechanisms of RLKs at the molecular level is extremely important, however, only a few receptor activation mechanisms have been structurally elucidated so far, and this aspect deserves further exploration.

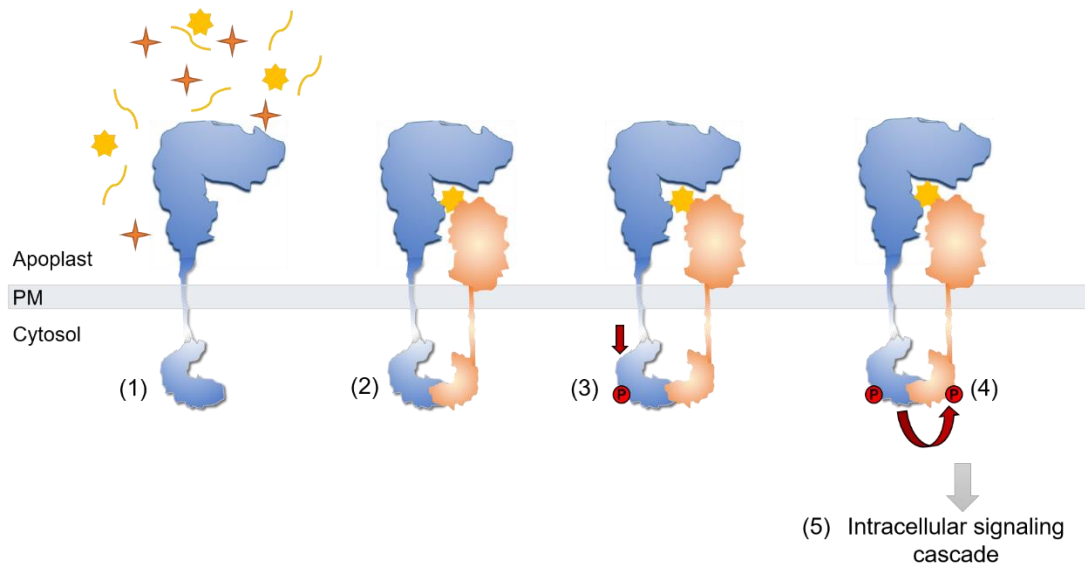


**Figure 1: Typical RLK signal cascade steps, adapted from (Hohmann et al., 2017).**

(1) RLKs sense ligands with their extracellular domain. RLKs specifically sense their specific ligands (small molecules, peptides, and/or proteins) among many possible ligands present in the extracellular space. (2) Ligand binds to the extracellular domain of RLK, this binding may include co-receptor. (3) Binding of the ligand and co-receptor to RLK induces the autophosphorylation of RLK in the kinase domain. (4) Subsequently, the activated receptor kinase transphosphorylates its co-receptor (and other downstream signaling element). (5) Consequently causing intracellular signaling cascade. As in Figure, each protein structure shows the extracellular structure, the transmembrane domain and the cytoplasmic kinase structure. Potential ligands are shown as orange four-pointed stars, yellow seven-pointed stars and yellow sticks, while the sites of protein phosphorylation are shown as red circles.

### 1.3 Peptide Signaling

Various peptides along with steroids are known to regulate intercellular communication in eukaryotes. In plants, mobile phytohormones, such as auxin, cytokinin and brassinosteroids, are responsible for managing various cellular communication pathways. However, the role of plant peptides with multiple functions that mediate multiple signaling pathways as ligands in plant development have only recently come into view (Fukuda and Higashiyama, 2011). In 1991, systemin was discovered as the first peptide with signaling function in plants (Pearce et al., 1991). This peptide with 18 amino acids was found to be involved in both plant defense, wound response, biotic, and abiotic stress responses (Pearce et al., 1991; Ryan et al., 2002). Since 1999, receptors for sensing systemin have been continuously discovered in different species. From the earliest SR160 (a 160-kDa Systemin-binding protein was isolated from membranes of *Solanum peruvianum* suspension cultured cells) (Scheer and Ryan, 1999), but more recently binding of systemin to SYR1 and SYR2 (Systemin Receptors, from tomato RLKs) was experimentally shown (Wang et al., 2018b). After the discovery of systemin, an increasing number of signaling peptides have been identified involved in cell-to-cell communication, developmental processes and stress responses (Matsubayashi, 2014; Tavormina et al., 2015). Examples of these identified signal peptides are phytosulfokine (PSK), LUREs, CLAVATA3 (CLV3), CEP1, and others (Matsubayashi and Sakagami, 1996; Brand et al., 2000; Ohyama et al., 2008; Okuda et al., 2009). In Arabidopsis, studies predict that there are over 1000 genes that may

encode secreted peptides, which suggest that plants also employ peptides as intercellular signaling molecules, similarly as other eukaryotes (Lease and Walker, 2006; Chakraborty et al., 2019).

In most cases, plant polypeptides are secreted from cells and act in a non-cell-autonomous manner on neighboring cells (Fukuda and Higashiyama, 2011). The most well studied peptides as examples are CLAVATA3 and CEPs. The peptide CLAVATA3 has been well studied in its role during meristem maintenance (Clark et al., 1996; Fletcher et al., 1999), and has been recognized as a ligand for the LRR-receptor kinase CLAVATA1 which is expressed in neighboring cell files (Clark et al., 1997; Trotochaud et al., 2000). CEPs (The Arabidopsis C-terminally encoded peptides) is another amazing example of small peptides that are secreted in nitrogen starved roots and then translocate to the shoot, and finally are received by their receptors which also belong to leucine-rich repeat receptor kinases (LRR-RKs) (Tabata et al., 2014). This indicates that the small peptide can even be translocated throughout the plant. It is expected that the CEP-CEPR ligand receptor pairs are involved in mediating systemic N-demanding signaling (Tabata et al., 2014). In the case of PSK signaling, hormones act in a cell or tissue-type specific manner. PSK and its receptor PSKR are expressed by the same cell type where the receptor activation occurs; however, with the diffusible property of PSK, the ligand can influence both nearby cells and long-distance targets (Hartmann et al., 2013). Thus, plant signaling peptides are normally secreted to the extracellular space and can be recognized by adjacent cells locally, or as a long-distance signals to modulate cellular signaling pathways systemically.

The biologically active peptides are generally defined as polypeptide chains with less than 100 amino acids (Matsubayashi, 2011). Majority of identified plant peptides so far are derived from nonfunctional larger precursor proteins (Tavormina et al., 2015). Generally, plant peptides can be categorized into three groups, small PTM (posttranslationally modified) peptides, cysteine-rich peptides, and non-Cys-rich/non-PTM peptides (peptides that undergo no PTM process, and meanwhile lacking of cysteine-rich presentation) (Matsubayashi, 2014; Tavormina et al., 2015; Hu et al., 2018). The active peptides usually undergo a proteolytic process of maturation that consists of two steps: the cleavage of an N-terminal signal sequence necessary for secretion of the protein to the apoplast, and release of the active peptide by cleavage of the prodomains (Matsubayashi, 2014). Afterwards, peptides that undergo complex posttranslational modifications are defined as posttranslationally modified (PTM) small peptides; peptides that form intramolecular disulfide bridges are defined as cysteine-rich peptides (Matsubayashi, 2014). The plant PTM peptides are typically modified through hydroxylation, glycosylation as well as Tyr sulfatation (Matsubayashi, 2011). The PSK, CLEs, IDA (INFLORESCENCE DEFICIENT IN ABSCISSION) and IDL (IDA-LIKE) peptides and CEPs are all categorized into the posttranslationally modified small peptides (Matsubayashi and Sakagami, 1996; Butenko et al., 2003; Ohyama et al., 2008; Delay et al., 2013). In contrast, peptides like RALFs, EPF (EPIDERMAL PATTERN FACTOR) peptides and LURE are typical Cysteine-rich peptides (Pearce et al., 2001; Hara et al., 2007; Okuda et al., 2009). As for the non-Cys-rich/non-PTM peptides, this group contains systemin peptides and PEPs (Plant Elicitor Peptides) (Tavormina et al., 2015). In Arabidopsis, PEPs are known as danger signals (which will be described in more detail in section 1.4) that are released from the C termini of their precursors (PROPEPs) by proteolysis



and as mediators of basal immune responses protective against invading pathogens (Heil, 2012; Huffaker, 2015; Shen et al., 2019). In any case, regardless of the grouping, plant peptides that fulfill a plethora of functions in signaling pathways need to undergo their respective maturation processes.

In the past few years, an increasing number of ligand-receptor pairs have been reported. Notably, the phenomenon of a large number of ligands being found to be plant peptides has become a focus of attention. For example, within the CLE family, the receptor CLAVATA1 binds to the signaling peptide CLAVATA3 during shoot meristem maturation (Clark et al., 1996; Trotochaud et al., 2000; Ogawa et al., 2008), and also binds to CLE40 peptide during root meristem maintenance (Hobe et al., 2003) and CLE3 peptide during regulation of lateral root formation (Araya et al., 2014). The CLE9 peptide is able to bind to the receptor kinase HAESA-LIKE 1 (HSL1) for the regulation of stomatal lineage cell division and to the BARELY NO MERISTEM (BAM) class receptor kinases for the regulation of periclinal cell division of xylem precursor cells (Qian et al., 2018). CEP peptides bind to receptors CEPR1 and CEPR2 and mediate systemic N-demand signaling (Tabata et al., 2014). The peptides EPF1 and EPF2 have been shown to bind to the ERECTA family LRR-RLKs to regulate stomatal patterning (Shpak et al., 2005; Lee et al., 2012; Torii, 2012). Within the PEP family, PEP1 and PEP2 are found to bind to receptor PEPR1 and PEPR2, contributing to the defense responses in Arabidopsis (Huffaker et al., 2006; Yamaguchi et al., 2010), PEP3 is recognized by PEPR1 receptor that increase salinity stress tolerance in plants (Huffaker and Ryan, 2007; Nakaminami et al., 2018).

There is a growing awareness that receptor kinases are prime candidates for the recognition of various bioactive peptides with signaling functions. Moreover, there is biochemical evidence that the signal peptides interact with leucine-rich repeat (LRR) RLKs that have conserved catalytic kinase domains, and this interaction is expected to phosphorylate serine and threonine residues (Trotochaud et al., 1999; Ni and Clark, 2006; Jun et al., 2008; Stenvik et al., 2008; Butenko et al., 2009). Among the Arabidopsis RLKs, even if we only move the focus onto the 216 LRR-RLKs, there are only a few of them that have been assigned to with functions in peptide signaling. Currently the precise ligands are still unknown for most receptor kinases, and in turn for many biologically active peptides, the receptors remain to be identified (Matsubayashi, 2003). Given the hundreds of cell surface receptors and the large number of small peptides involved in signaling in plants, the vast majority of these putative peptide ligands and their respective receptors require singling out the matching pairs and the confirmation of their physical interactions. Therefore, the identification and characterization of ligand-receptor pairs is of high interest for a more comprehensive understanding of the activation cascade of plant receptor kinases.

#### **1.4 The PROPEP-PEP-PEPR System**

PEPs (PLANT ELICITOR PEPTIDES) were first reported in 2006 (Huffaker et al., 2006), when a 23 aa peptide termed PEP1 and its six homologues were identified in Arabidopsis with the help of the alkalization assay. Soon after the discovery of PEP1, its two receptors were identified, the LRR-RLKs PEPR1 and PEPR2, which were also identified as receptors of PEP2 (Yamaguchi et al., 2006; Yamaguchi et al., 2010). In 2013, an eighth member of PEPs was included in the PEP family (Bartels et al., 2013). The field of PEP research has mainly evolved around its impact on plant immunity (Bartels and Boller, 2015),

and has been intensified when orthologues of PEP have been identified in *Zea mays* and in many important crop species (Huffaker et al., 2011; Huffaker et al., 2013). However, to date, out of the PEP family, only PEP1 has been studied more completely. PEP1 is derived from the C-terminus of the 96 aa precursor protein PROPEP1, and the addition of even low nanomolar concentration of synthetic PEP1 to seedlings or plant parts is able to activate many PTI-related responses, such as mediator alkalization, ethylene, nitric oxide (NO) and ROS production, calcium influx, MAPK activation, cGMP production, increased JA levels, and numerous gene expression changes (Huffaker et al., 2006; Krol et al., 2010; Flury et al., 2013; Ma et al., 2013; Gully et al., 2015; Klauser et al., 2015). Binding of PEP1 to its receptors inhibits root growth by affecting ROS formation and PIN-dependent auxin distribution through interaction with the plasma membrane proton ATPase (Jing et al., 2019; Jing et al., 2020; Shen et al., 2020). The other members of the PEP family have not been adequately studied.

*At*PROPEP1 has 96 amino acids and includes the sequence of *At*PEP1 within its C-terminus, thus was identified as the precursor protein of the *At*PEP1 peptide, and genes encoding *At*PROPEPs have been identified in the Arabidopsis genome (Huffaker et al., 2006). Promoter-GUS analyses of different PROPEPs reveals their different spatial and temporal expression patterns (Bartels et al., 2013). The study points out that the promoter-mediated expression patterns of the PROPEPs fall clearly into two distinct groups: Group one comprises the promoters of PROPEP1, 2, 3, 5 and 8, which shows expression in the roots and slightly in the leaf vasculature, and is inducible by wounding. Group two contains the promoters of PROPEP4 and 7, which are not inducible by wounding and the basal expression is restricted to the root tips. Interestingly, the promoter-mediated expression patterns of PEPR1/2 receptors show a partially overlapping pattern with PROPEP1, 2, 3, 5, and 8, while PROPEP4 and 7 promoter-mediated expression patterns are exclusive to the root tip, where the PEPRs are not expressed.

It is reported that type-II metacaspases (MCs) constitute the proteolytic enzymes that mediate PROPEP processing in Arabidopsis, and in particular, MC4 (Metacaspase 4, AT1G79340 ) is capable of releasing active peptides from the C-terminus after cleavage after arginine or lysine, thereby processing PROPEPs except PEP6 (Shen et al., 2019). The processing of PEPs is induced by calcium signaling and even requires intramolecular proteolytic metacaspase (Hander et al., 2019; Shen et al., 2019). Further requirements for processing of the PEP precursors are not yet known.

PEPR1 has been confirmed as a functional receptor of PEP1 (Yamaguchi et al., 2006; Zhang et al., 2016a) (Song et al., 2017), *At*PEPR2, which shares 76% sequence homology to *At*PEPR1, has been identified as the second receptor of PEP1 in Arabidopsis (Krol et al., 2010; Yamaguchi et al., 2010). *At*PEPR1 carries 26 LRR-motifs and *At*PEPR2 carries 25 LRR-motifs in their extracellular ligand binding domain, they both are transmembrane LRR-RLKs that belong to the class LRR-XI RLKs (Yamaguchi et al., 2006; Yamaguchi et al., 2010; Xi et al., 2019). It has been shown that PEP members do not fully share receptors, for example PEP3 does not bind to the receptor PEPR2 (Nakaminami et al., 2018), while PEPR1 has been shown to be the receptor for PEP1-6 only, and due to the failure to obtain PEP7 in seedlings and leaves in the assay, PEPR1 has not been proved to be the receptor for PEP7 (Yamaguchi et al., 2010). Therefore PEP7 has not been shown to be a ligand for any receptor up to this point.

## 1.5 AE-MS Provides Sensitive Detection of Protein-Protein Interactions under Limited Conditions

The identification of extracellular receptor-ligand pairs in different physiological processes is essential for a more comprehensive understanding of the signaling pathways that govern development and response to stresses. However, despite the importance of ligand-receptor pair, interactions involving plasma membrane proteins are not well described. Challenges exist on many fronts. Unlike the intracellular proteins, membrane proteins are not easily solubilized in aqueous solvents due to their amphiphilic nature and the specific environment in which they reside, therefore makes themselves difficult to be further characterized. For some ligand-receptor pairs, their complex has a very high equilibrium dissociation constant ( $K_d$ ), which indicating a very low affinity. For example the IDA-HAESA pair (Santiago et al., 2016), the signaling peptide IDA binding to its receptor HASEA with a relatively high  $K_d$  of 20  $\mu\text{M}$ . These low affinity interactors can be easily lost when using insufficiently sensitive detection approaches. In addition, the low affinities facilitate the formation of the extremely transient interactions required for dynamic processes regulated by ligands-receptors on the cell surface, making it more challenging to detect their interactions.

The AE-MS (Affinity Enrichment Mass Spectrometry) approach was proposed based on the above challenges. AE-MS has been presented to provide sensitive detection of protein-protein interactions. In contrast to the classical AP-MS (Affinity Purification Mass Spectrometry) approach, AE-MS takes a mild washing step that no longer obsesses over the removal of unspecific binders, but rather retains and utilizes the large unspecific set. The AE-MS approach preserves the weak or transient interactors, and is able to identify the typical background binders by analyzing pull-downs within one experimental series. A stable background profile serves for accurate normalization, and allows the identification of interacting proteins by comparison between samples (Figure 2). AE-MS is highly efficient and easy to operate, and its use of high-resolution mass spectrometry enables more accurate retrieval of protein complexes (Dunham et al., 2012; Keilhauer et al., 2015).

An AE-MS workflow generally consists of four steps as follows:

1. “Bait protein” extraction. In this step, the use of soluble membrane protein recombinant ectodomains is able to solve the problem of membrane protein solubilization. Also, the modified AE-MS by using microsomal fraction will be of great help for studying the protein complex which assembles at the plasma membrane (Xi, unpublished).
2. A single-step immunoprecipitation using anti-tag antibodies coupled with mild washing is performed to enrich the bait protein and specific interactors. The specific enrichment of bait protein as well as the mild washing protect the interacting proteins recruited to the bait protein from disruption, and preserve weak or transient interactions.
3. LC-MS/MS analysis. The peptide mixture from the digested protein complex is subjected into single-shot liquid chromatography tandem mass spectrometry (LC-MS/MS) on an Orbitrap instrument.

4. Data analysis. Data are processed to identify interactors of tagged bait proteins. In this step, the quantitative proteomics software MaxQuant is used for protein identification and quantification, and the resulting label-free quantification (LFQ) intensity matrix is used as the basis for all downstream data analysis.

In plants, receptors on the plasma membrane are induced by ligands and form protein complexes that then undergo signal transduction. These complexes assembled in the plasma membrane region can be subtle, but are essential for the biological function of both the ligands and receptors. AE-MS provides sensitive detection of protein-protein interactions, therefore can be used as a tool for investigating protein complexes. Existing studies have found only a small fraction of the ligand-receptor pairs in plants, for many receptor kinases their putative ligands remain unknown, and for a large number of emerging small peptides, their signaling mechanisms need to be extensively explored. Thus, the AE-MS techniques should be fully utilized to allow us to gain more knowledge in this field.

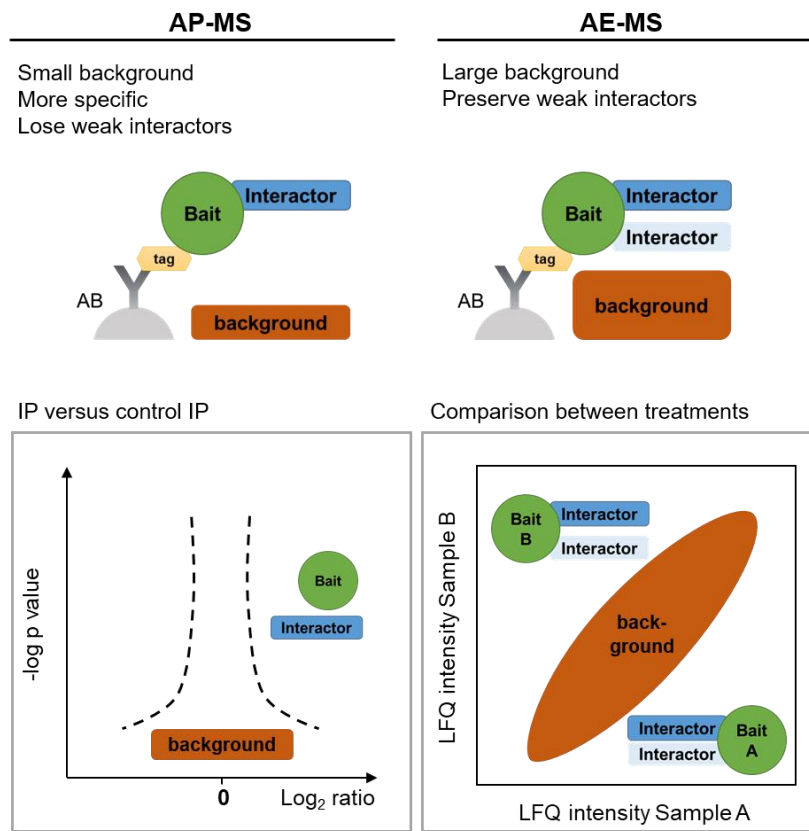


**Figure 2: Comparison of AP-MS and AE-MS, modified from (Walhout et al., 2012; Keilhauer et al., 2015).**

As in Figure, bait is shown in green circle and the interactors are shown in blue, where dark blue indicates strong interactors and light blue indicates weak interactors. Background binders are shown in orange, the size of their area represents the number of background binders. AB: antibody; IP: Immunoprecipitation.

## 1.6 Previous Work on SIRK1 (Sucrose-Induced Receptor Kinase)

Our group has in the past conducted a large-scale phosphoproteomics study in the past in which sucrose was resupplied to sucrose-starved *Arabidopsis* seedlings in a time course manner (Niittyälä et al., 2007). This study provided us with several novel sucrose-induced proteins; one of them showed a significant transient phosphorylation at its serine 744 after sucrose resupply and was selected for follow-up studies. In combination with the fact that this protein belongs to LRR-receptor-like kinase family, we therefore named it SIRK1 (Sucrose-Induced Receptor Kinase). SIRK1 was then subjected into a systematic functional study to determine its role in the context of sucrose stimulus, including mutant analysis, proteomic, physiological, and cell biological experiments (Wu et al., 2013). The substrate proteins of SIRK1 have been successfully identified by phosphoproteomics in combination with the use of mutants. SIRK1, as a membrane-bound receptor kinase, has been found to have direct sucrose-dependent regulatory effects on transporters such as aquaporins and possibly also sucrose exporters. Its sucrose-dependent regulation of the plasma membrane aquaporins (PIP2F) was immediately confirmed in this study. Upon sucrose induction, SIRK1 recruits and phosphorylates PIP2F to form a protein complex that was shown to co-regulate protoplasts water uptake in physiological experiments (Wu et al., 2013). In a subsequent meticulous study of the SIRK1 signaling complex, we identified the co-receptor QSK1 (qiān shǒu, Chinese: 千手 ‘thousand hands’ kinase) (Wu et al., 2019). In response to sucrose stimulation, the C-terminus of QSK1 is phosphorylated by SIRK1 and the two form an active signaling complex. In particular, QSK1 in its phosphorylated state enhances the phosphorylation of PIP2F by SIRK1, therefore QSK1 is characterized as a co-receptor for SIRK1 to co-regulate the aquaporin PIP2F (Figure 3).

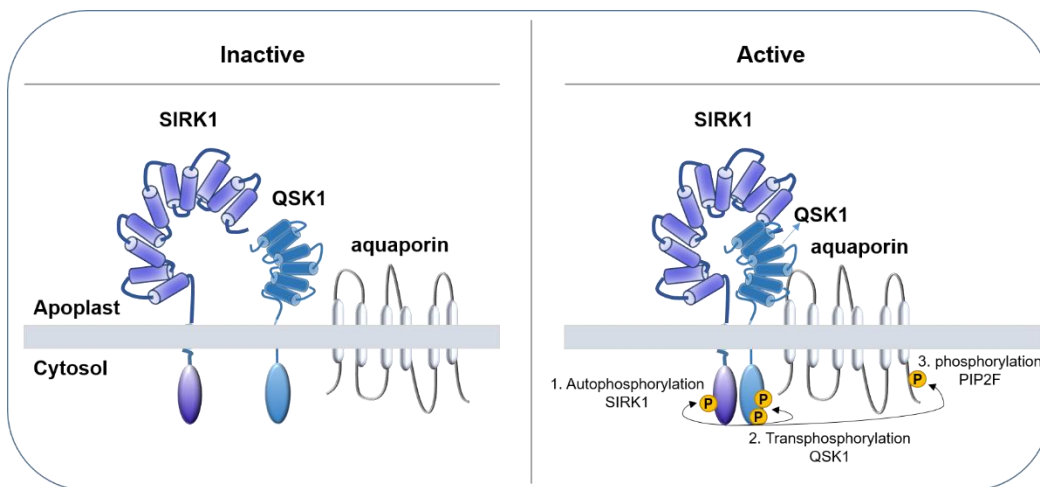


**Figure 3: Scheme of functional model of the SIRK1/QSK1 complex at the plasma membrane, adapted from (Wu et al., 2019).**

SIRK1 in its active state interacts with and transphosphorylates QSK1. The complex of SIRK1 and QSK1 then regulates the activity of aquaporins via phosphorylation. Cylinders represent LRR repeats, SIRK1 has 10 LRR repeats in the extracellular domain and QSK1 has six LRR repeats in the extracellular domain. Aquaporin has six transmembrane spans.

Although we have adequately demonstrated the regulatory role of the signaling complex of SIRK1/QSK1 during activation of aquaporin, phosphoproteome profiling reveals that the phosphorylation status of PIP2F in *sirk1* was opposite to that in *qsk1*, but similar to that in the *sirk1qsk1* mutant (Figure 4A) (Wu et al., 2019). QSK1 alone is not able to phosphorylate the substrate peptide of PIP2F, but the presence of QSK1 enhances the phosphorylation of the PIP2F substrate peptide by SIRK1 (Wu et al., 2019). Furthermore, it has been shown that aquaporin activity is not consistent in *sirk1* and *qsk1*, confirming the different regulatory roles of SIRK1 and QSK1 on aquaporins (Figure 4B). These emergent results may be due to the involvement of QSK1 in multiple signaling pathways or also to the relocalization of QSK1 within the plasma membrane in response to osmotic stress, as has been shown (Grison et al., 2019). At these events, their regulatory effects on aquaporin needs to be explored from a more macroscopic perspective.

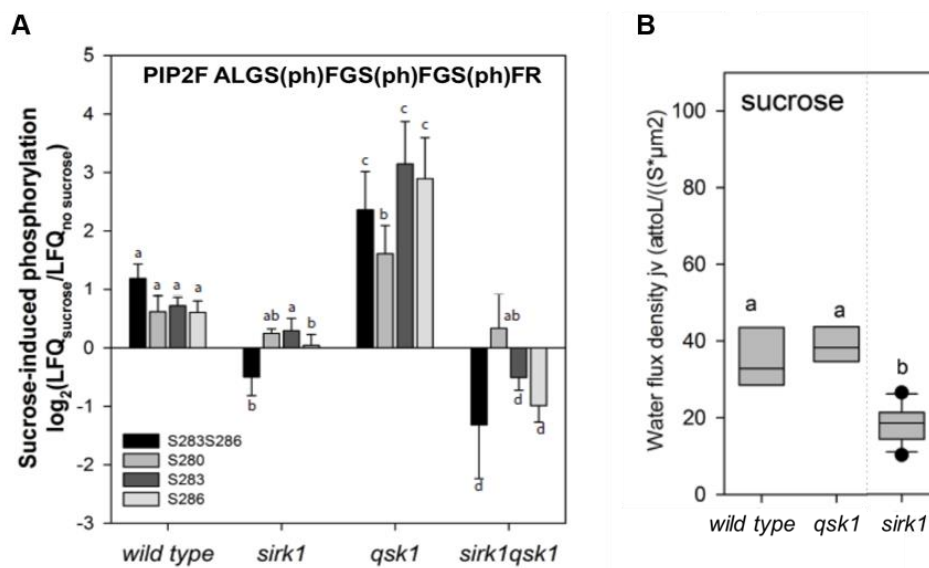


**Figure 4: SIRK1 and QSK1 confer distinct regulatory effects on PIP2F, adapted from (Wu et al., 2019).**

(A) Sucrose-induced phosphorylation of PIP2F in wild type, *sirk1*, *qsk1* and *sirk1 qsk1* double mutant. (B) Sucrose-induced water flux densities in *wild type*, *sirk1* and *qsk1*. Data shown as mean with standard deviation of three replicates. Small letters indicate significant differences ( $p < 0.05$ ; pairwise t-test) for each phosphopeptide between genotypes.

Our previous understanding of SIRK1 is mainly focused on its downstream signaling in response to sucrose induction, and remain clueless about its activation mechanism. SIRK1 is classified in the "ligand-perceiving receptor group" due to its long ECD of 10 LRR, while QSK1 is classified in "co-receptor group" due to its shorter ECD (5 LRR) (Xi et al., 2019). Like the other LRR ligand-perceiving receptors, SIRK1 is considered to have its own ligand. The putative ligand is able to bind to ECD of SIRK1 and activate SIRK1 thereby triggering a series of signaling cascades. However, ligand is not included in the existing model of SIRK1.

## 1.7 Aim of the Research

Based on the unresolved issues within the proposed model of SIKK1, this thesis aims to achieve three main objectives:

*(1) Exploration of the roles of SIKK1 and QSK1 in regulating water uptake in the whole plant by thorough phenotypic analysis under drought and osmotic stress conditions.*

Although QSK1 in its phosphorylated state has a significant enhancing effect on SIKK1, its regulation of PIP2F alone is distinct from that of SIKK1 (Wu et al., 2019). However, it is yet unknown if these cellular processes result in a whole-plant response to drought or osmotic stress. Therefore, drought-stress experiments in soil and on agar plates were carried out using wild type as well as *sirk1* and *qsk1* (*qsk2*), aiming to explore the role of SIKK1 and QSK1 in regulating water uptake at the whole plant level.

*(2) Characterization of a ligand for SIKK1*

With reference to the classic signaling mechanism of other LRR-RLKs (Ullrich and Schlessinger, 1990; He et al., 2000; Chinchilla et al., 2006; Endo et al., 2014; Zhang et al., 2016b), SIKK1 is predicted to expose its putative ligand-binding domain to the extracellular space by sensing ligand to initiate signal at the cell surface. In the efforts to find ligand candidates for SIKK1, a previously conducted ligand-screening assay provides us with the signaling peptide PEP7 as a primary ligand candidate for SIKK1. Given the critical role of ligands in signal transduction for kinase activation, the topic of this section was devoted to a thorough characterization of the function of PEP7 as a ligand candidate. To achieve this, we performed a series of biochemical experiments to verify the recognition of PEP7 by its designated receptor SIKK1 and validate the activation of SIKK1 by PEP7 through the subsequent proteomic (phosphoproteomics) approaches.

*(3) Characterization of the biological function of PEP7-SIKK1.*

It is demonstrated that SIKK1 is involved in the regulation of sucrose-specific osmotic response through direct interaction with and activation of aquaporin PIP2F via phosphorylation (Wu et al., 2013). Besides, other aquaporins also have been found to be regulated by SIKK1 under sucrose induction, acting as phosphorylation substrates that together they control water uptake on protoplasts (Wu et al., 2013; Wu et al., 2019). In addition, the lack of *Sirk1* in Arabidopsis also leads to a sucrose-sensitive primary root phenotype. Therefore, the aim of this section was to characterize the biological function of the PEP7-SIKK1 pair, particularly in modulating water influx into protoplasts and affecting primary root phenotype.

## 2. Material and Methods

### 2.1 Plant Materials and Growth Conditions

*Arabidopsis thaliana* Col-0 accession was used as the wild-type (WT). The homozygous T-DNA insertion mutant *sirk1* (SALK\_125543), *qsk1* (SALK\_019840) and *pep7* (SALK\_025824) were used. In addition, plant materials in the experiment also included double mutant lines (*sirk1pep7* and *sirk1qsk1*, obtained by crossings of the respective single mutants) and over-expression lines (35S::SIRK1-GFP in the background of *sirk1* and *pep7*).

Homozygous T-DNA insertion mutants *sirk1* and double mutant *sirk1qsk1* were confirmed via PCR amplification as reported previously (Wu et al., 2019). Mutants of *pep7* and *sirk1pep7* were confirmed via PCR amplification using T-DNA border primer LBb1.3 (5'-ATTTTGCCGATTTCGGAAC-3') and gene-specific primers (PEP7-RP: 5'-GGAAGGTGCCTAGTTGGTACC-3', PEP7-LP: 5'-GTTTTACAGTTTCAAATTCGG-3'; SIRK1-RP: 5'-TTTCCAGCATTTCACAACTC-3', SIRK1-LP: 5'-CACTAAGCTTGTTGAGGTCGC-3') (Figure S1)

For plant propagation, seeds were germinated and grown under 16/8 day/night (22 °C, 120  $\mu\text{E}/\text{s}\cdot\text{m}^2$ ) in ½ MS medium with 1% sucrose. After seven days, seedlings were transferred into soil (provided by the greenhouse of Plant Physiology and Biotechnology institute in University Hohenheim, Stuttgart, Germany) and were kept in the growth condition of 16/8 day/night (22 °C, 120  $\mu\text{E}/\text{s}\cdot\text{m}^2$ ) to the final maturity.

*Nicotiana benthamiana* plants were maintained in the greenhouse (Plant Physiology and Biotechnology institute in University Hohenheim, Stuttgart, Germany) at 22–24 °C, 120  $\mu\text{E}/\text{s}\cdot\text{m}^2$ , and with 16 h photoperiod for three weeks for final use.

### 2.2 Acquisition of Native Membrane Proteins

#### 2.2.1 Seeds Sterilization and Vernalization

*Arabidopsis* seeds were collected into 2 ml Eppendorf tubes (Eppendorf, Germany) and were incubated by bleaching solution (1.5% NaClO and 3 drops Tween-20 in ddH<sub>2</sub>O) for 12 minutes in a rotator (neoLab, Heidelberg), and then were washed with ddH<sub>2</sub>O (6 times, each washing step takes 5 minutes). The whole procedure of sterilizing seeds was performed at the clean bench (Labogene A/S, Denmark). Surface sterilized seeds were stored at 4° C in darkness for two days for vernalization.

#### 2.2.2 Hydroponic Culture

The plants were cultivated using the hydroponic culture system (Schlesier et al., 2003) for root collection. Approximate 20 mg surface sterilized *Arabidopsis* seeds were placed on the mesh in one glass jar filled with 150 mL ½ MS (Murashige and Skoog, Sigma-Aldrich) medium with 0.5% sucrose and grew on the shaker in the growth chamber (16/8 h day/night, 22 °C and  $110 \pm 10 \mu\text{E s}^{-1} \text{m}^{-2}$ ) for 19 days. Afterwards, the seedlings were starved by replacing the growth medium to a sucrose starvation medium (½ MS without sucrose), and the whole culture vessels were kept in the dark for 48 h for sucrose starvation (Niittylä et al., 2007). The starvation solution was then resupplied with sucrose (to a final concentration of 30 mM) or 1  $\mu\text{M}$



PEP7 (PEPMIC, Suzhou, China) for 5 minutes. Roots were collected and frozen in liquid nitrogen as sucrose starvation (no resupply, control), sucrose treatment (1% sucrose resupply for 5 min), and PEP7 treatment (PEP7 feeding for 5 min), respectively.

### **2.2.3 Microsomal Fraction Isolation**

Microsomal fraction (MF) isolation method was applied as described (Pertl et al., 2001) with minor modification. Plant materials (approximate 1 g roots from hydroponic culture) were broken into pieces with a hammer and then were suspended in appropriate volume of homogenization buffer (330 mM mannitol, 100 mM KCl, 1 mM EDTA and 50 mM Tris-MES pH 7.5, freshly added 5  $\mu\text{L mL}^{-1}$  Protease Inhibitor Cocktail (PIC), 5 mM DTT, protease inhibitors (1 mM Phenylmethylsulfonyl Fluoride (PMSF), 1 mM Benzamidin and 3  $\mu\text{M}$  Leupeptin) and phosphatase inhibitors (25 mM NaF, 1 mM  $\text{Na}_3\text{VO}_4$ ). Homogenate was obtained by a constant potting procedure with glass potter tissue grinder (10 mL glass vessel, Cat.: 89026-382 and 10 mL plain plunger, Cat.: 89026-394, VWR LLC, Radnor, PA). After passing through four layers of Miracloth (Cat.: 475855-1R, Merck KGaA, Darmstadt), the homogenate was centrifuged at  $7,500 \times g$  for 15 min and the supernatant was centrifuged again at  $48,000 \times g$  for 80 min. The remaining microsomal fraction (MF) pellet was then resuspended with membrane buffer (330 mM mannitol, 25 mM Tris-MES, 0.5 mM DTT) and stored at  $-80^\circ\text{C}$  until further processing. All operational steps were performed on ice and the centrifugation step was performed at  $4^\circ\text{C}$ .

## **2.3 Production of Recombinant Protein**

### **2.3.1 Transient Expression of Recombinant SIRK1 in *Nicotiana benthamiana***

*Agrobacterium tumefaciens* GV3101 strains carrying the relevant constructs (GFP-tagged full length SIRK1 and Strep-HA tagged SIRK1-ECD, constructs provided by Dr. Xuna Wu) were grown in liquid LB medium (10 g/L Tryptone, 5 g/L yeast extract and 10 g/L NaCl) supplemented with appropriate antibiotics for 24 h at  $28^\circ\text{C}$ . *Agrobacterium* (strain C58C1) carrying the pBinG1 vector with the P19 gene was also incubated with corresponding antibiotics (Kapila et al., 1997). *Agrobacteria* were collected via  $3,000 \times g$  centrifugation for 10 min and resuspended with resuspension buffer (10 mM Tris-MES pH 7.5, 10 mM  $\text{MgCl}_2$  and 150  $\mu\text{M}$  acetosyringone) to reach final OD 600 (0.5 for GV3101, 0.25 for strain C58C1). Positive single colony of *Agrobacteria* (final OD 600 = 0.5) was mixed with strain C58C1 (final OD 600 = 0.25), and the infiltration solution was prepared with resuspension buffer and incubated for 1-2 h at room temperature. Three-week-old *N. benthamiana* leaves were syringe infiltrated and harvested after 48 h of infiltration. The harvested leaves were flash-frozen in liquid nitrogen and then stored at  $-80^\circ\text{C}$  for protein extraction and purification.

### **2.3.2 Protein Extraction and Strep-Tag Purification**

Leaf material was grounded in liquid nitrogen (Witte et al., 2004) and thawed in extraction buffer (100 mM Tris/HCl pH 8.0, 150 mM NaCl, 1 mM EDTA, 2% w/v PVPP, 0.5% Triton X-100, 1 mM PMSF and 5 mM DTT). The mixture were incubated at  $4^\circ\text{C}$  for 2 h under constant shaking and then the supernatant was obtained as protein extract after centrifugation (14000 rpm, 10 min,  $4^\circ\text{C}$ ).

Flow through assay as the first step of SIRK1-ECD protein purification was performed using Strep-Tactin® column (Cat.no: 2-4013-001, IBA GmbH, Goettingen, Germany). The Strep-Tactin®XT column was firstly equilibrated with 2 CV (column bed volume) wash buffer (100 mM Tris pH 8.0, 150 mM NaCl, 1 mM EDTA), then 10 CV cleared lysate containing SIRK1-ECD protein was added into the column. Finally, the StrepII tagged protein was eluted with elution buffer (50 mM biotin, 100 mM Tris pH 8.0, 150 mM NaCl, 1 mM EDTA).

For further purification of SIRK1-ECD protein, the Macrosep Advance Centrifugal Devices with Omega Membrane 10K (Product ID: MAP010C36, Pall Life Sciences, USA) was used to get rid of the possible biotin contamination in eluate. The eluate from above flow through assay was pipetted into sample reservoir of macrosep advance centrifugal device. During centrifugation, proteins of different molecular weight were separated by omega membrane (3,000 rcf, 80 min, 4 °C), and the target protein (SIRK1-ECD) was retained in sample reservoir while biotin was retained in filtrate receiver.

### **2.3.3 SDS-PAGE and Western Blot**

Protein samples were denatured with SDS loading buffer (diluted from 6 X SDS loading buffer, 12% w/v SDS, 20% v/v Glycerol, 180 mM TRIS/HCl pH 6.8, 600 mM DTT, 0.06% w/v Bromphenol blue) for 10 minutes at 90 °C. Denatured samples were loaded on a prepared SDS polyacrylamide gel as follows:

Separating gel: 375 mM Tris/HCl pH 8, 0.1% (w/v) SDS, 10% (v/v) acrylamide solution (Sigma-Aldrich), 0.03% (w/v) APS, 0.075% (v/v) TEMED;

Stacking gel: 125 mM Tris/HCl pH 6.8, 0.1% (w/v) SDS, 5% (v/v) acrylamide solution (Sigma-Aldrich), 0.03% (w/v) APS, 0.18% (v/v) TEMED.

The whole gel system was obtained from (Biorad). Samples were run on stacking gel in the running buffer (0.2% (w/v) SDS, 25 mM Tris-Glycine, pH 8.6) for about 20 minutes at 70 V. Afterwards voltage has been changed to 120 V for samples running on separating gel for 1 h. The Roti Marker (Roth, Karlsruhe, Germany) and rainbow Marker (Roth, Karlsruhe, Germany) was also loaded together with samples.

At the end of running, for Coomassie Brilliant Blue staining, the gel was immediately stained in the Coomassie solution (0.25% (w/v) Brilliant Blue R 250 (Serva, Heidelberg) for at least 30 minutes on a shaker. then it was de-stained overnight in de-staining buffer (30% methanol, 10% glacial acetic acid) until the protein bands became clearly visible.

Proteins separated by SDS-PAGE were transferred onto either PVDF membrane (Sigma-Aldrich) or different pore size of nitrocellulose membrane (Sigma-Aldrich). For blotting on to the PVDF membrane, the membrane was soaked in pure MeOH and then soaked in transfer buffer (25 mM TRIS, 192 mM Glycine, fill up to 800 ml and store at 4 °C, before use add freshly 20 % MeOH). Instead, the nitrocellulose membrane only had to be soaked in transfer buffer, the other methods were same as above. The filter paper as well as gel were also soaked in transfer buffer. The transfer blot “sandwich” was then assembled (Mahmood and Yang, 2012) and the transfer was performed at 250 mA per blot and 20 V for 1h. The membranes were incubated in the blocking solution (3% (w/v) BSA in PBS-T (80 mM Na<sub>2</sub>HPO<sub>4</sub>, 20 mM NaH<sub>2</sub>PO<sub>4</sub>, 100 mM

NaCl, 0.2% (w/v) Tween-20)) for at least 1 h at room temperature under shaking, after blocking the membranes were washed with PBS buffer for three more times. Afterwards, the antibody diluted in the PBS-T was applied onto the membrane and then were washed with PBS-T again and were stained with AP-detection buffer (100 mM TRIS/HCl pH 9.5, 50 mM MgCl<sub>2</sub>, 100 mM NaCl, 0.165 mg/ml BCIP and 0.33 mg/ml NBT) in the dark. The staining reaction was stopped by ddH<sub>2</sub>O and protein bands became visible.

## **2.4 Protein Concentration Measurement**

### **2.4.1 BCA Assay**

Protein concentration in microsomal fraction was measured using BCA assay (Sorensen and Brodbeck, 1986). To do this, solution A and solution B of the BCA assay kit (Thermo Scientific) were firstly mixed in a 50:1 ratio to obtain the BCA solution. One  $\mu$ l sample was mixed with 19  $\mu$ l ddH<sub>2</sub>O and then mixed with 200  $\mu$ l BCA solution (50 Volume A : 1 Volume B). The mixture was incubated for 10 minutes at room temperature and the absorbance was measured at 562 nm using Tecan Spark® (Männedorf, Switzerland). The protein concentration of BCA assay was determined using a Bovine Serum Albumin (BSA) standard curve. Bovine Serum Albumin (BSA) standard curve was prepared with a range of 1-10  $\mu$ g/ $\mu$ l.

### **2.4.2 Bradford Assay**

The concentration of protein extract that containing 5 mM DTT (or even higher concentration of DTT) was measured using Bradford assay (Bradford, 1976). One  $\mu$ l sample was mixed with 19  $\mu$ l ddH<sub>2</sub>O as well as 200  $\mu$ l 1x Bradford reagent (Roti®-Quant, Roth) in a 96-well transparent microplate. The mixture was incubated for 10 min in the dark at room temperature, and the absorbance was measured at 595 nm. Protein concentration was then determined for three technical replicates using a Bovine Serum Albumin (BSA) standard curve of Bradford assay.

## **2.5 Pull-downs of GFP-tagged SIRK1**

The isolated root microsomal proteins (100  $\mu$ g) were incubated with 15  $\mu$ l GFP-Traps®MA beads (Chromotek, Germany) for two hours on a rotating wheel at 4 °C. After incubation, the slurry was separated with magnet (Chromotek, Germany), the supernatant was discarded and the leftover beads were washed three times with 500  $\mu$ l ice cold wash buffer (10 mM Tris/HCl pH 7.5, 150 mM NaCl and 0.5 mM EDTA). The proteins were either eluted from the beads with 100  $\mu$ l elution buffer (UTU (6 M urea, 2 M thiourea), pH 8) for protein-protein interaction assay, or subjected to washing steps with kinase reaction buffer (50 mM HEPES/KOH, pH 7.4, 10 mM MgCl<sub>2</sub>, 10 mM MnCl<sub>2</sub>, 0.1 mg BSA and 1 mM DTT) for kinase activity assay.

## **2.6 In Vitro SIRK1 Kinase Activity Assay**

An in vitro SIRK1 kinase assay was performed by using unspecific substrate ADP-GLO kit (Promega, Germany). SIRK1-GFP fusion proteins were affinity purified over anti-GFP beads (described as SIRK1-GFP pull down assay). Then the prey protein PEP7 was added into beads for another 1 h incubation at 4 °C. The beads were washed two times with 300  $\mu$ l ice cold kinase reaction buffer (50 mM HEPES/KOH, pH 7.4, 10 mM MgCl<sub>2</sub>, 10 mM MnCl<sub>2</sub>, 0.1 mg BSA and 1 mM DTT), and were re-suspended into 25  $\mu$ l kinase

reaction buffer with ATP and the generic kinase substrate myelin basic protein (50 mM HEPES/KOH, pH 7.4, 10 mM MgCl<sub>2</sub>, 10 mM MnCl<sub>2</sub>, 0.1 mg BSA, 1mM DTT, 100 μM ATP and 0.4 μg μL<sup>-1</sup> myelin basic protein). After one hour reaction, 25 μl ADP-GLO Reagents (Promega, Germany) was added and incubated for 40 minutes to stop the kinase reaction and deplete the unconsumed ATP. Then 50 μl Kinase Detection Reagents were added and incubated for another 40 min to convert ADP to ATP and introduce luciferase to detect ATP. Luminescence as a measure of ATP conversion from ADP was recorded with a luminometer (Tecan M200 Pro).

## 2.7 Detection of Ligand-Receptor Interactions

### 2.7.1 Binding Assays

Co-IP assays were performed to determine the interaction between SIRK1 and PEP7, followed by the identification via mass spectrometry. In this part, the synthetic peptides (PEP7, PEP6 and PEP4), full length SIRK1-GFP protein from MF, and StrepII-HA tagged SIRK1-ECD protein from transient assay in *Nicotiana benthamiana* were used. SIRK1 or PEP7 was first immobilized as bait protein, and putative prey protein was attended artificially in the pull down assay.

*Binding assays of SIRK1 to immobilized PEP7* - The C-terminal HIS-tagged PEP7 was used as bait. 20 μl HisPur™ Ni-NTA Magnetic Beads were equilibrated with equilibration buffer (100 mM sodium phosphate, 600 mM sodium chloride, 0.05% Tween™-20 Detergent, 30 mM imidazole, pH 8.0) and the beads were collected by magnet afterwards. The mixture of 100 μl equilibration buffer and 100 μl ddH<sub>2</sub>O containing 2 μM PEP7-HIS (to the final concentration of 1 μM PEP7-HIS) was incubated with beads for 1h at 4 °C. After incubation, the beads were washed three times with wash buffer (100 mM sodium phosphate, 600 mM sodium chloride, 0.05% Tween™-20 Detergent, 50 mM imidazole, pH 8.0). Full length SIRK1-GFP protein extract from tobacco (50 μg), full length SIRK1 -GFP microsomal fraction from overexpression line (50 μg) as well as the purified protein SIRK1-ECD-HA-StrepII (20 μg, after cut off, described as protein purification section) acting as prey protein was added individually. The whole binding procedure took 20 minutes and the pulled down was eluted with 40 μl elution buffer (100 mM sodium phosphate, 600 mM sodium chloride, 250 mM imidazole, pH 8.0). Ten microgram of the eluate was drained using speed vacuum and re-dissolved by UTU for next trypsin digestion.

*Binding assays of PEP7-HIS to immobilized SIRK1* - Full length SIRK1-GFP protein obtained from membrane fraction as well as SIRK1-ECD-HA-StrepII protein obtained from transient assay in *Nicotiana benthamiana* were used as bait to capture PEP7. For binding assay of SIRK1-GFP to PEP7, 100 μg SIRK1-GFP protein extract was incubated with 12 μl of GFP-Traps® MA beads (Chromotek, Germany) for two hours on a rotating wheel at 4 °C. After incubation, the slurry was separated with magnet, the supernatant was discarded and the leftover beads were washed three times with 500 μl ice cold wash buffer (10 mM Tris/HCl pH 7.5, 150 mM NaCl, 0.5 mM EDTA). Then the prey protein PEP7 (100 μl solution containing 1 μM PEP7) was added into beads for another 1 h incubation at 4 °C. Finally the beads were washed three more times with wash buffer (10 mM Tris/HCl pH 7.5, 150 mM NaCl, 0.5 mM EDTA) and the proteins were eluted with 60 μl UTU (6 M urea, 2 M thiourea, pH 8). For binding assay of SIRK1-ECD-HA-StrepII

to PEP7, 200 µg SIRK1-ECD-HA-StrepII protein extract was incubated with 20 µl of Strep-tag®II beads (IBA GmbH, Goettingen, Germany) for two hours on a rotating wheel at 4 °C. The beads were then collected by centrifugation and washed three times with wash buffer (100 mM HEPES pH8.0, 100 mM NaCl, 0.5 mM EDTA, 0.05% Triton X-100 and 2 mM DTT). PEP7 was added as above and the pulled down was eluted with 100 µl elution buffer (100 mM HEPES pH8.0, 100 mM NaCl, 0.5 mM EDTA, 0.05% Triton X-100, 2 mM DTT and 10 mM biotin) (Witte et al., 2004). Ten microgram of the eluate was drained using speed vacuum and re-dissolved by UTU for next trypsin digestion.

### **2.7.2 Competitive Binding Assay**

A competitive binding assay was further performed to test the binding affinity of SIRK1 and PEP7. All buffer used were same as PEP7-HIS pull down assay. Firstly 100 µl ddH<sub>2</sub>O containing 1 µM PEP7-HIS was immobilized to 20 µl HisPur™ Ni-NTA magnetic beads, then 100 µg of purified protein SIRK1-ECD-HA-StrepII (after flow through assay, described as protein purification section) was bound to PEP7-HIS. Different concentration of PEP7 (100 µl ddH<sub>2</sub>O containing 0 µM, 0.2 µM, 0.5 µM, 1 µM, 1.5 µM, 2 µM, 3 µM) without tag was added to elute the pre-bound SIRK1-ECD. Eluates were collected as “elutes SIRK1-ECD by PEP7”. The leftover that cannot be taken away from beads was then eluted with HIS-beads elution buffer (100 mM sodium phosphate, 600 mM sodium chloride, 250 mM imidazole, pH 8.0). Fractions of all eluates were drained using speed vacuum and re-dissolved by UTU for next trypsin digestion and identification by LC-MS/MS.

### **2.7.3 Microscale Thermophoresis**

The binding of SIRK1 extracellular domain (SIRK1-ECD) with PEP7 was further analyzed by Microscale Thermophoresis (MST). A buffer exchange column was firstly applied to 100 µl purified SIRK1-ECD protein to remove any unfavorable residue (Tris-HCl, DTT). The RED-NHS 2nd generation amine reactive dye (NanoTemper Technologies, Munich, Germany) was used to label the purified SIRK1-ECD (approximately 10 µM) with a 4:1 dye:protein ratio for 30 minutes at room temperature in the dark. Another size exclusion column was employed to remove the excess of dye and produced the solution of labelled SIRK1-ECD. Labelled SIRK1-ECD was adjusted to a final concentration of 20 nM in reaction buffer (50 mM HEPES, pH 7.5, 0.05 % (v/v) Tween 20) and titrated with serial (1:1) dilutions of PEP7 (starting at 0.5 mM), PEP6 or PEP4. The complex was allowed to establish for 10 min at room temperature before the samples were loaded into standard MST capillaries. Their binding was detected by a Monolith NT.115 instrument (NanoTemper Technologies) at 25 °C with 20 % Excitation power and 20 % MST power, and a dose response curve was generated when assay reached the desired requirements.

## **2.8 Sample Preparation for LC-MS/MS**

### **2.8.1 in Solution Trypsin Digestion**

Protein pellets were solubilized in UTU (6 M urea, 2 M thiourea, pH 8). Solubilized proteins were pre-digested with Lys-C (Wako, Japan) for 3 h after being reduced by DTT and alkylated by IAA. The protein mixture was diluted by four volumes of 10 mM TrisHCl, pH 8, before trypsin digestion (Sequencing Grade

Modified trypsin, Promega). The trypsin digestion process took 16 hours at 37°C, after which the reaction was stopped by adding TFA (trifluoroacetic acid) to  $\text{pH} \leq 2$ .

### **2.8.2 Phosphopeptide Enrichment**

Alternatively, for samples for phosphoproteomics studies, dried in-solution digested peptides were resuspended with loading buffer (1 M glycolic acid in 80% acetonitrile (ACN) and 5% TFA) before mixing with  $\text{TiO}_2$  beads (Titansphere, 5  $\mu\text{m}$ , GL Sciences). To do the phosphopeptide enrichment, the  $\text{TiO}_2$  beads were first washed with methanol, then were rinsed with 100  $\mu\text{L}$  elution buffer (1%  $\text{NH}_4\text{OH}$ ) for 10 min vortex to wash away the remaining methanol. Afterwards, the beads were equilibrated with three times 50  $\mu\text{L}$  loading buffer and then incubated with re-solved peptides for 20 min. After incubation, the beads were washed with 100  $\mu\text{L}$  loading buffer for 30 s and three times with 100  $\mu\text{L}$  wash buffer (80% ACN, 1% TFA) for 2 min. Finally the phosphopeptides were eluted with elution buffer with a total volume of 240  $\mu\text{L}$ . Eluates were immediately acidified with 60  $\mu\text{L}$  10% formic acid (Wu et al., 2017). All steps were performed at room temperature (24 °C) and all solution exchanges were done by vortexing and subsequent low-speed centrifugation (2,500  $\times$  g).

### **2.8.3 Peptide Desalting over C18-Stage Tips**

Prior to LC-MS/MS analysis, the peptides were desalted over C18-Stage tips as described (Rappsilber et al., 2003; Szymanski et al., 2013). C18-Stage tips were made by introducing two discs of C18 (Millipore, Schwalbach) to the bottom of a 200  $\mu\text{L}$  pipette tip. The Stage-tips were conditioned with 50  $\mu\text{L}$  of solution B (80% (v/v) acetonitrile and 0.5% (v/v) acetic acid) and equilibrated 2 times with 100  $\mu\text{L}$  solution A (0.5% (v/v) acetic acid). The acidified peptide sample (pH 2) was loaded, and peptides were expected to stick on the C18 membrane. After a brief centrifugation, the tips were washed two times with 100  $\mu\text{L}$  solution A. Peptides were eluted two times with 20  $\mu\text{L}$  solution B, and the collected eluate was concentrated and stored dry at -20°C before loading on mass spectrometer.

## **2.9 LC-MS/MS Analysis of Peptides and Phosphopeptides**

Desalted peptide mixture were analyzed by LC-MS/MS including HPLC-system nanoflow Easy-nLC1000 (Thermo Scientific) and Orbitrap hybrid mass spectrometer (Q-Exactive Plus, Thermo Scientific). Peptides were eluted from a 75  $\mu\text{m}$  x 50 cm analytical C18 column (PepMan, Thermo Scientific) on a linear gradient running from 4% to 64% acetonitrile over 135 min. Proteins were identified based on the information-dependent acquisition of fragmentation spectra for multiple charged peptides. Up to twelve data-dependent MS/MS spectra were acquired in the linear ion trap for each full-scan spectrum acquired at 70,000 full-width half-maximum (FWHM) resolution.

## **2.10 Mass Spectrometric Data Analysis**

### **2.10.1 Peptide and Protein Identification**

MaxQuant (version 1.5.3.8) (Cox and Mann, 2008) was used for protein identification and ion intensity quantitation. Andromeda (Cox et al., 2011) was used to match spectra against the Arabidopsis TAIR10 database (35386 entries). The following parameters were applied: trypsin as cleaving enzyme; minimum

peptide length of six amino acids; maximal two missed cleavages; carbamidomethylation of cysteine was set as a fixed modification; oxidation of methionine as well as phosphorylation of serine, threonine and tyrosine was set as variable modifications. Peptide mass tolerance for the database search was set to 20 ppm on full scans and 0.5 Da for fragment ions. Multiplicity was set to 1. For label-free quantitation, ‘match between runs’ marked with time window 2 min; peptide and protein false discovery rates (FDR) set to 0.01; while site FDR was set to 0.05; common contaminants and reverses (trypsin, keratin, etc.) were excluded. The identified phosphopeptides including their spectra will be available in the phosphorylation site database PhosPhAt (Durek et al., 2010).

### **2.10.2 Label-Free Peptide and Protein Quantitation**

We followed a label-free quantitative approach based on LFQ values as quantitative information obtained from MaxQuant (Cox et al., 2014). For protein identification and quantitation, protein groups information (protein groups.txt) was used, for phosphopeptides the phosphosite data (Phospho (STY)Sites.txt) was used. Data analysis was performed using Perseus software and log<sub>2</sub>-transformation of the raw LFQ-values was used (Tyanova et al., 2016a; Tyanova et al., 2016b).

### **2.10.3 Statistical Analyses and Data Visualization**

MAPMAN was used for protein functional classification (Thimm et al., 2004). SUBA3 was used for subcellular location identification (Tanz et al., 2012). Detailed protein function was manually updated with the support of TAIR (Poole, 2005). Over-representation analysis was done via fisher’s exact test, p values were adjusted using Bonferroni correction. Interactome data from published large-scale data sets were obtained from Arabidopsis Interactome Viewer 2 (Dong et al., 2019) or STRING (Szklarczyk et al., 2015). Other statistical analyses were carried out with Sigma Plot (version 11.0), ORIGIN software (version 2019b) and Excel (Microsoft, 2013).

## **2.11 Phenotype Experiment**

### **2.11.1 Drought Stress in Soil**

Plants were germinated and grown under 16/8 day/night (22 °C, 120 μE/s\*m<sup>2</sup>) in ½ MS (Murashige and Skoog, Sigma-Aldrich) agar plate for 7 days. After 7 days the seedlings were transferred into pots containing exactly 80 g soil and 40 g tap water (provided by the greenhouse of Plant Physiology and Biotechnology institute in University Hohenheim, Stuttgart, Germany). All pots were kept under an LED Panel (Polyklima GmbH, Freising, Germany) in the growth room and were watered with equal volume of water for 3 weeks. After 3 weeks, pots of each genotype were dehydrated until they showed clear signs of dehydration. Throughout the whole procedure, the position of the pots was changed regularly.

### **2.11.2 Osmotic Stress in Plate**

Polyethylene glycol 6000 (PEG-6000, Sigma-Aldrich) was used to adjust osmotic potential (Michel and Kaufmann, 1973; Money, 1989) in agar plates. The PEG-infused plates were made as the previous publications (Van der Weele et al., 2000; Verslues et al., 2006). To make the overlay solution, 550 g PEG-6000 was added per liter in ½ MS medium and mixed medium was poured onto the solidified agar medium.

The volume ratio of agar to PEG overlay solution was kept at 2:3, to achieve the final water potential of approximately -1.0 MPa of the PEG-infused plates. The PEG-infused plates were kept overnight to allow sufficient time for PEG to diffuse into the agar. The overlay solution was poured off completely before usage.

Vernalized seeds were firstly pipetted in ½ MS agar plates with 1% sucrose for 7 days vertical growth. Seedlings with the same growth status were selected and transferred to PEG-infused plates as well as control plates (½ MS agar plates containing 1% sucrose) to continue vertical growth. After 7 more days of growth in different treatments, plates were scanned (Epson Perfection V370) and roots were measured and analyzed by Image-J.

### **2.11.3 Protoplast Swelling Assay**

Surface sterilized seeds after two days vernalization were germinated and grown vertically on sucrose starved medium (½ MS solid medium with 0.02% sucrose). Approximately 30 seedlings were cut into small pieces and then were incubated in 3 ml enzymatic digestion medium (ES-300 M: 300 mM mannitol, 10 mM MES/KOH, pH 5.8, 10 mM CaCl<sub>2</sub>, 10 mM KCl) plus 1% (w/v) cellulase Onozuka R10 (Duchefa, Haarlem, The Netherlands) and 1% (w/v) macerozyme R10 (Duchefa, The Netherlands). After 3 hours of gentle shaking at room temperature in the dark the protoplasts were prepared via a 50 µm nylon mesh filter. Protoplasts were then enriched by centrifugation at 80 g at 4 °C for 10 min, and washed three times with ice-cold ES-300 M without enzymes. The protoplasts were finally resuspended in 150 µL ES-300M buffer and stored in the dark on ice for at least 30 min before an experiment was started.

The protoplast swell assay was minor modified based on the previous publications (Sommer et al., 2007; Wu et al., 2013; Shatil-Cohen et al., 2014). Approximately 40 µL of the protoplast suspension were pipetted into a perfusion chamber that fulfill with ES-300 M. Protoplasts took about 5-10 minutes to settle down and the chamber was perfused with ES-300 M to flush away the no-sticking protoplasts. The “Sticky” protoplasts in the chamber were observed use a 40 x objective lens (Leica).

The video took 5 minutes to capture the dynamic change of the protoplasts with the time interval of 3 seconds. The hypotonic challenge was performed at tenth second of the video by changing hypertonic solution (a total of 300 mM permeability concentration) to hypotonic solution (a total of 150 mM permeability concentration). Perfusion buffer was composed of two parts (Table 1): the osmotic part contains the majority mannitol which jump from 270 mM to 120 mM to conduct the osmotic change; the other portion of the perfusion buffer used as treatments consisted of either 30 mM mannitol as control, 30 mM sucrose for sucrose treatment, or 30 mM mannitol containing 1 µM peptide for peptide treatment.

The diameter of the protoplasts were measured directly by using LAS X (Leica Application Suite X, Leica). The volume and surface area of each protoplast at each time point were calculated. A regression curve was fitted to the dynamic volume change and the maximal slope from the steepest part was obtained from derivative calculation of the curve (Figure 5A). The maximal water flux density that corresponds to aquaporin activity thus was determined by the maximal slope dividing the protoplast surface area at the



corresponding time point (Figure 5B). All the curve fitting analysis and derivative calculation were performed with ORIGIN software.

**Table 1: Overview of the buffers used in the protoplast swelling assays.**

Perfusion buffer	Fixed components of Osmotic solutions	Non-fixed components of Treatment solutions				
		Solute with varying concentrations	Solutes of constant concentration	Control	Sucrose	PEP7
High osmolarity (300mM) solution	270mM Mannitol	10mM MES, pH 5.8 10mM CaCl <sub>2</sub> 10mM KCl	30mM Mannitol	30mM Sucrose	30mM Mannitol containing 1µM PEP7	30mM Mannitol containing 1µM PEPIDE
Low osmolarity (150mM) solution	120mM Mannitol	10mM MES, pH 5.8 10mM CaCl <sub>2</sub> 10mM KCl	30mM Mannitol	30mM Sucrose	30mM Mannitol containing 1µM PEP7	30mM Mannitol containing 1µM PEPIDE

Note: Sucrose and mannitol produce same osmotic pressure (approximately 1.15 mOsmol kg<sup>-1</sup> of 1mM osmolyte), measured with a cryoscopic osmometer (Osmomat 030, Gonotec, Berlin, Germany)

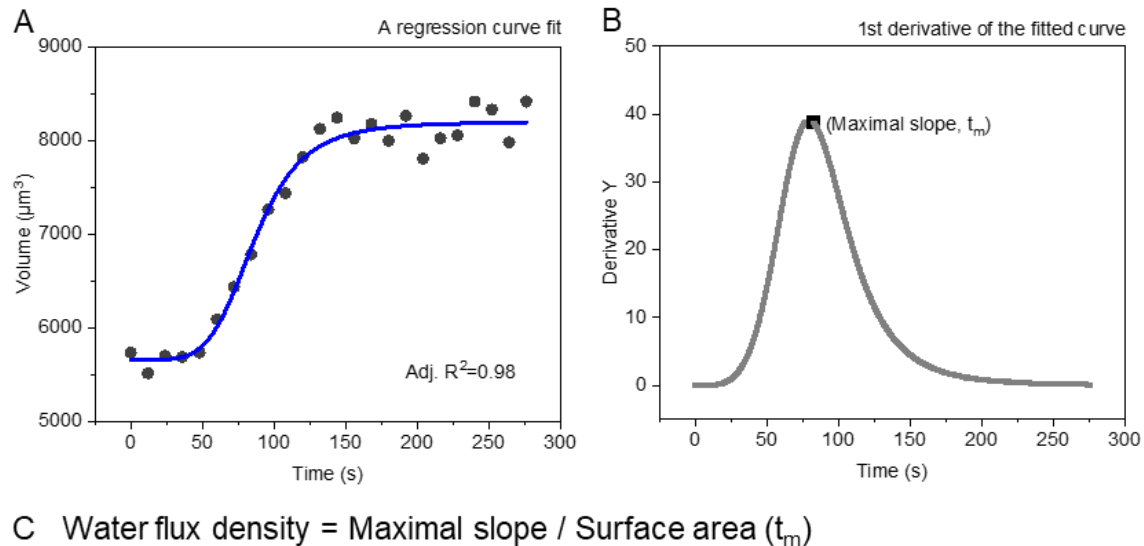


**Figure 5: water flux density calculation.**

(A) The dots in the graph represent the real-time volume of protoplasts at each time point, and the change in volume was fitted to a regression curve; (B) The maximum value of the derivative of the curve in Figure A is used as the maximum slope of the curve, the time point at which the maximum slope occurs means that the protoplast has the maximum water flux at this time; (C) The water flux density is obtained by dividing the maximum slope by the surface area of the protoplast at this moment.

#### **2.11.4 Plate Assay for Primary Root Elongation**

Surface sterilized seeds after two days vernalization were germinated and grown vertically on sucrose starved medium (½ MS solid medium with 0.02% sucrose), sucrose supply medium (½ MS solid medium with 1% sucrose) or PEP7 supply medium sucrose starved medium with 1 µM PEP7). Plates were scanned (Epson Perfection V370) after 5 days germination and the primary root length was measured by Image-J.

### 3. Results

#### 3.1 SIRK1 and QSK1 Co-responded to Abiotic Osmotic Stress at the Whole Plant Level

Although SIRK1 and QSK1 act as sucrose-stimulated receptor/co-receptor, the phenotypic analysis of *Sirk1* and *Qsk1* loss-of-function mutants at the cellular level are not identical (as introduced in section 1.6). This relationship raises the question of whether this cellular-level phenotype result in a whole plant response to osmotic stress, and whether SIRK1 and QSK1 could be primary candidates to explain the molecular basis of the response. In order to know the property of SIRK1 and QSK1 in regulating water maintenance at the whole plant level, a drought-stress experiment in soil and (simulated drought-stress) on agar plates was carried out using wild type as well as *Sirk1* and *Qsk1* knock-out mutants.

##### 3.1.1 The *sirk1qsk1* Double Mutant Showed the Most Superior Survival Ability in Response to Drought Stress in Soil

Soil drying experiments were conducted to assess the plant survival. Lines with simultaneous planting had exactly the same growing conditions. After a certain period of growth, water in the pots was withheld for a fixed period for the purpose of dehydration. As shown in the Figure 6, only the double mutant *sirk1qsk1* survived after ten days dehydration. The *sirk1* mutant and the *qsk1* mutant behaved similarly to the wild type in response to drought stress, both did not survive after the ten-day dehydration and failed to be rescued by rehydration (rehydration results are not shown in the figure). This result indicated that SIRK1 or QSK1 alone did not show significant effects at the whole plant level in response to drought stress, however, when *Sirk1* and *Qsk1* were both knocked out, the *sirk1qsk1* mutant showed the strongest drought resistance, indicated that SIRK1 and QSK1 co-respond to abiotic osmotic stress at the whole-plant level. This result was coordinated with previous finding on regulation of protoplast permeability by SIRK1 and QSK1 (Wu et al., 2019).

In soil drying situations, plant water loss originates from protoplasts as well as cell wall (Oertli, 1985; Verslues et al., 2006), whereas our previous exploration of SIRK1 and QSK1 was limited to the cellular level, with only the observation of protoplasts water influx. The plant's responses to unfavorable conditions requires differential cell wall synthesis and remodeling besides direct regulation of transport processes (Moore et al., 2008; Tenhaken, 2015). Therefore the phenotypic analysis of *sirk1* and *qsk1* may not fully be generalized at the whole-plant level versus the cellular level. However, it was certain, SIRK1 and QSK1 were indeed the primary candidates that were involved in the plant response to drought stress.

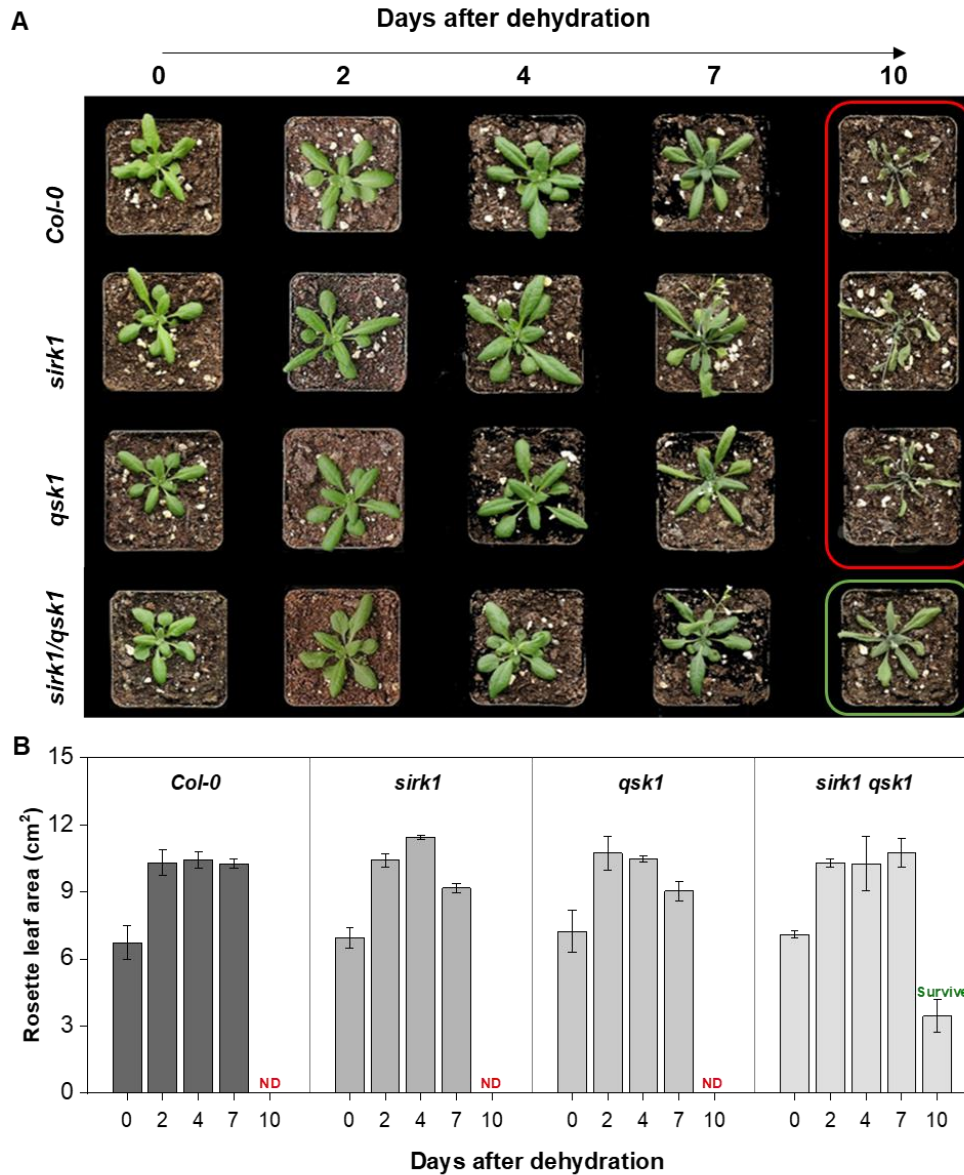


**Figure 6: Phenotypes comparison of *sirK1*, *qsk1*, *sirK1qsk1* and wild type plant under drought conditions in soil.**

(A) and (B): For the drought stress treatment, the photographs were taken after withholding water for 0 d, 2 d, 4 d, 7 d and 10 d, respectively. After 10 days of dehydration, only the *sirK1qsk1* mutant survived (indicated in the green box), while all plants of other genotypes died (indicated in the red box) and could not be rescued by rehydration. The experiments were repeated two times with similar results.

### 3.1.2 The Roots of *sirK1qsk1* Double Mutant Showed a Strong Osmotic Stress Tolerance Capacity in Response to Osmotic Stress in Plates

To observe the root morphology, we implemented simulated drought conditions using PEG-6000. The high molecular weight PEG-6000 is unable to penetrate the pores of the plant cell wall, thus well simulating the loss of water from the soil: when soil water content decreases, water is withdrawn from the cell wall as well as protoplasts, resulting a process in which both the cell wall and protoplasts shrink (Verslues et al., 2006).

Under osmotic stress conditions generated by PEG, plant roots by absorbing more water, therefore, we were able to determine the drought tolerance of the plants by observing the root morphology of the different genotypes.

For comparison with the wild type, we first measured the total root length (including primary and lateral roots) of each lines. Changes in root length under PEG condition and control condition for each genotype were normalized (Figure 7A). Compared to the wild type, *sirk1* had significantly higher resistance to osmotic stress, while *qsk1* exhibited slightly higher resistance than wild type which was not statistically significantly. The double mutant *sirkqsk1* showed the most superior osmotic stress resistance in this experiment, indicating that it had the strongest tolerance in response to the PEG-6000 treatment (Figure 7B). Obviously, root osmotic stress response demonstrated that SIRK1 and QSK1 work in the same signaling pathway. Combined with the above experiments on plant survival in soil, we considered that in Arabidopsis, SIRK1 and QSK1 co-controlled plant water permeability at the whole-plant level in response to osmotic stress. The results from both plant survival experiments and root morphology experiments were consistent with our existing SIRK1/QSK1 model, and illustrated the stabilization and enhancement of SIRK1 by QSK1.

**A** Calculation of normalized osmotic stress tolerance of mutants based on wild type:

$$\text{Log}_2 \left( \frac{\text{Mutant (Root length}_{\text{PEG}} - \text{Root length}_{\text{Con}}) / \text{Root length}_{\text{Con}}}{\text{Col-0 (Root length}_{\text{PEG}} - \text{Root length}_{\text{Con}}) / \text{Root length}_{\text{Con}}} \right)$$

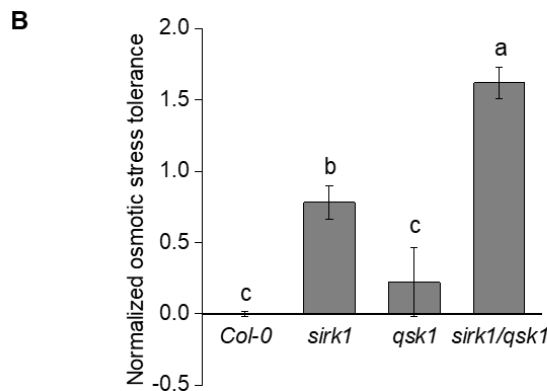


**Figure 7: Root phenotypes of Col-0, *sirk1*, *qsk1*, and *sirk1qsk1* under osmotic stress (generated by PEG) and normal condition (Con) on agar plates.**

(A) Calculation of the ability to resist osmotic stress in different genotypes. On PEG-infused plates, roots grew more vigorously in order to absorb water, and their relative growth differences from normal conditions would respond to resistance to osmotic stress. The root phenotypes of all mutants were normalized to the wild type. (B) Comparison of the ability of different genotypes to resist osmotic stress. The wild type was normalized to 0 and mutants with values higher than 0 were considered to have greater resistance to osmotic stress than the wild type. Small letters indicate significant differences ( $p < 0.05$ ) as determined by oneway ANOVA with Holm-Sidak correction.

## 3.2 Characterization of PEP7 as a Ligand Candidate

### 3.2.1 Identification of SIRK1 Ligand Candidates

In order to identify the ligand of SIRK1, we implemented a large-scale ligand screening assay. In the ligand-screening assay, plant apoplast peptides were isolated and fractionated. Each fraction was measured for its ability to activate SIRK1. Proteins in fractions that favored increased SIRK1 activity were analyzed by mass spectrometry. The apoplast proteins were obtained from wild type liquid seedling cultures grown under optimal nutrition conditions and all protein components greater than 1 kDa were excluded by ultrafiltration. SIRK1-GFP was enriched from root tissue of hydroponic cultures after two days of sucrose starvation, and it was used along with fractionated apoplast proteins for kinase activity assays (Figure 8A). SIRK1-GFP enriched from sucrose stimulated hydroponic cultures were used as a positive control for induction of SIRK1 kinase activity (Figure 8B). Exposure of sucrose alone to SIRK1-GFP enriched from sucrose starved plants was not able to induce SIRK1 activity (Figure 8B). SIRK1 activity was most strongly induced after exposure of the SIRK1-GFP enrichment to protein fraction F2 and to a lesser extent in protein fraction F1, whereas exposure of SIRK1-GFP to protein fraction F3 resulted in the lowest kinase activity (Figure 8B). Thus, proteins with high peptide counts present in fractions F1 and F2 but not in fraction F3 were identified as candidate proteins. Before mass spectrometric analysis, each fraction was again run over a molecular weight cutoff filter of 30kDa. An aliquot of each fraction was analyzed by mass spectrometry without prior digestion, in case peptide candidate proteins did not yield suitable tryptic peptides. Out of the final identified proteins, in the tryptic samples 30 proteins were predicted to be secreted proteins, and 14 of these met the requirements of high abundance in fractions F1 and F2, but not in fraction F3 (Figure 8C). Two of these candidate proteins were also identified in the non-tryptic samples, namely RALF1 (AT1G02900) and PEP7 (AT5G09978). All tryptic and non-tryptic peptides identified for RALF1 and PEP7 covered the C-terminal parts of the respective propeptides, which constitutes the biologically active RALF1 or PEP7, respectively. Also other RALF peptides were identified in the fractions F1, F2 and F3, but RALF22, RALF32 and RALF33 did not strictly meet the criteria set for putative ligands. Thus far, ligand candidates were narrowed down to a few small peptides.

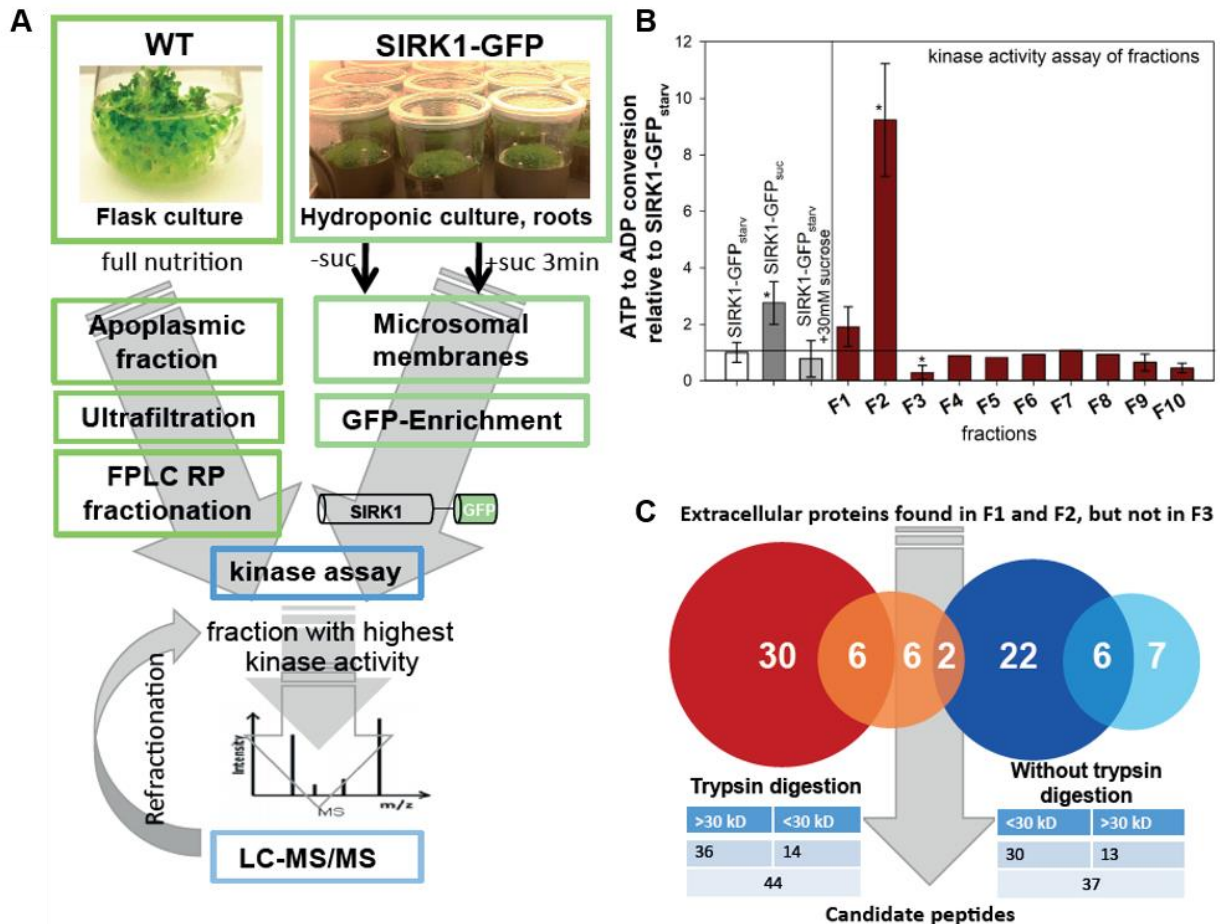


**Figure 8: Screen for peptide ligands, data collected from Stefanie König's master's thesis.**

(A) Workflow involving apoplast protein fractions exposed to SIRK1-GFP from hydroponic culture with and without sucrose stimulation. (B) Kinase activity of SIRK1-GFP exposed to different fractions of apoplast proteins. Asterisks indicate significant differences to SIRK1-GFP isolated from sucrose starved cultures (SIRK1-GFP<sub>starv</sub>). For fractions F4 to F8 only one fraction was analyzed, all other fractions were tested in three independent replicates. (C) Summary of the number of proteins with predicted extracellular location identified in Fractions F1 and F2, but not F3. Figure developed based on Master Thesis Stefanie König.

### 3.2.2 PEP7 Induced Kinase Activity of SIRK1 in a Concentration-Dependent Manner

We first used synthetic peptides PEP7 and RALF1 to assay their ability to activate SIRK1-GFP preparations (Figure 9A). In this assay, equal amounts of SIRK1-GFP were immobilized on anti-GFP beads and then separately exposed to different concentrations of PEP7 (0  $\mu$ M, 0.01  $\mu$ M, 0.05  $\mu$ M, 0.1  $\mu$ M, 0.5  $\mu$ M, 1  $\mu$ M and 2  $\mu$ M) or RALF1 (0  $\mu$ M, 0.1  $\mu$ M, 0.2  $\mu$ M, 0.5  $\mu$ M, 1  $\mu$ M and 2  $\mu$ M), respectively, to test their ability to induce SIRK1 kinase activity. At the initial concentration of PEP7 (10 nM), there was a significant jump in the kinase activity of SIRK1-GFP, indicating the sensitivity of SIRK1 kinase activity to PEP7. At a PEP7 concentration of approximately 1  $\mu$ M, the kinase activity of SIRK1 reached saturation. The kinase activity of SIRK1-GFP increased with increasing PEP7 concentrations and was not altered by the addition of RALF1. We also used synthetic peptides of RALF22, RALF32, and RALF33 at different concentrations to test for their ability to induce the kinase activity in SIRK1-GFP preparations (Figure 9B). Non-related peptides IDA and CLE were used as negative controls, which resulted in significantly lower kinase activity

than measured for SIRK1-GFP enrichments from sucrose-starved roots. Kinase activities were also low when SIRK1-GFP was exposed with RALF22, RALF32 and RALF33, and no concentration-dependent kinase activities were observed when RALF peptides were supplied to SIRK1-GFP. Therefore, each of the small peptides filtered out by the ligand screening test was examined, of which only PEP7 showed an inducible effect on SIRK1 activity in a concentration dependent manner.

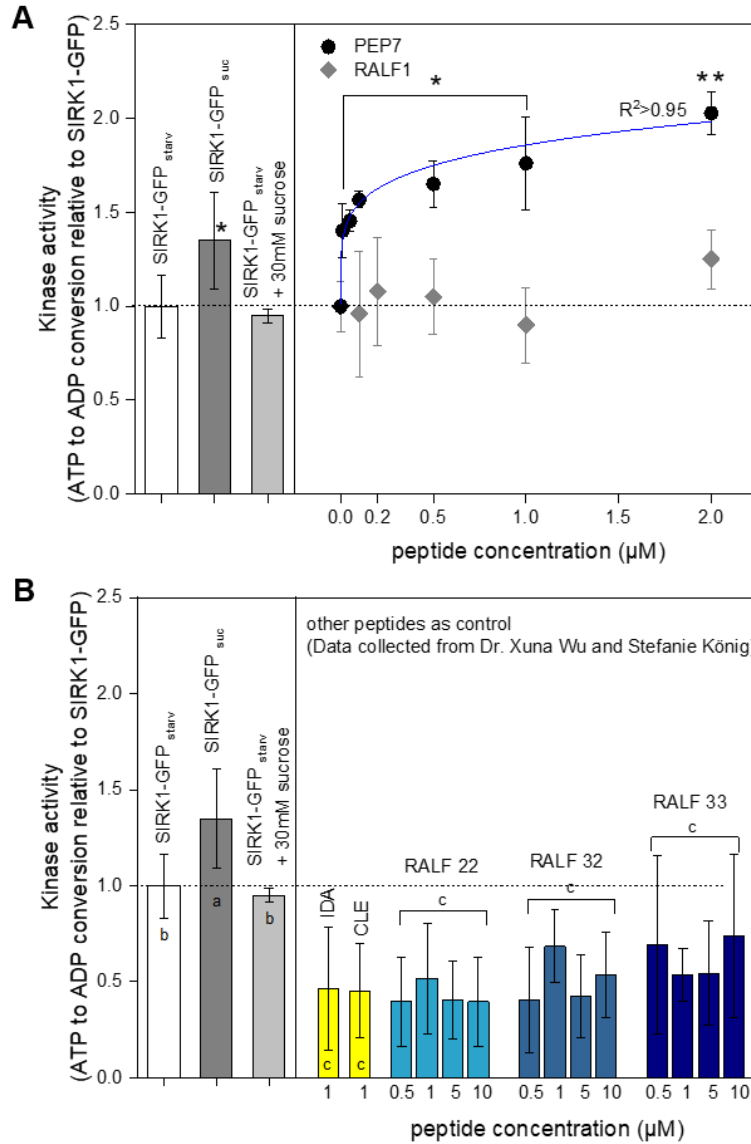


**Figure 9: Kinase activity of SIRK1-GFP induced by different signaling peptides.**

(A) Kinase activity assay for SIRK1-GFP enriched from sucrose-starved roots by exposure to different concentrations of PEP7 or RALF1. (B) Kinase activity assay for SIRK1-GFP enriched from sucrose-starved roots by exposure to different unrelated signaling peptides, IDA and CLE were used as negative controls, RALF peptides were supplied at different concentrations. Data shown as mean with standard deviation of three replicates. Asterisks indicate significant differences to SIRK1-GFP under sucrose starvation (white bar). Small letters indicate significant differences ( $p < 0.05$ ) as determined by oneway ANOVA with Holm-Sidak correction.



### **3.3 PEP7 Bound to SIRK1 Ectodomain**

After the above characterization of PEP7, we finalized PEP7 as a ligand candidate for SIRK1 in the follow-up study. This section specifically tested the binding of PEP7 and SIRK1.

#### **3.3.1 In Vitro Inverse Binding Assay Enables Detection of PEP7-SIRK1 Interactions**

##### **3.3.1.1 Prey Protein PEP7 could be Captured by Immobilized SIRK1**

To test if PEP7 can directly bind to SIRK1, we applied a series of co-immunoprecipitation experiments. Full length SIRK1-GFP as well as extracellular domain SIRK1ECD-StrepII were immobilized and behaved as baits in the first binding assay. Immobilized SIRK1 was exposed to 1 $\mu$ M PEP7, several washing steps were performed afterwards and the binding of putative ligand to SIRK1 was detected by mass spectrometry. PEP7 was detectable and quantifiable from the generated data, suggesting that PEP7 can directly bind to SIRK1 (Figure 10A), and in particular to the extracellular domain of SIRK1 (SIRK1-ECD) (Figure 10B).

##### **3.3.1.2 Immobilized PEP7-HIS could pull down SIRK1 As well As SIRK1-ECD**

To confirm these findings, we implemented an inverse co-immunoprecipitation experiment. Synthetic PEP7-HIS was immobilized and exposed to SIRK1-GFP enrichments (50  $\mu$ g) from sucrose starved roots, or 20  $\mu$ g of SIRK1-ECD purified from transient expression in *Nicotiana benthamiana*, or root microsomal membrane fractions (50  $\mu$ g) which were expected to contain native SIRK1 (Figure 10C). Again, all versions of SIRK1 (full length SIRK1-GFP, extracellular domain of SIRK1, and native SIRK1) were captured by immobilized PEP7.

Indeed, the in vitro inverse binding assays enabled the detection of PEP7-SIRK1 binding, PEP7 was found to bind to the extracellular domain of SIRK1, further confirming PEP7 as a ligand for SIRK1.

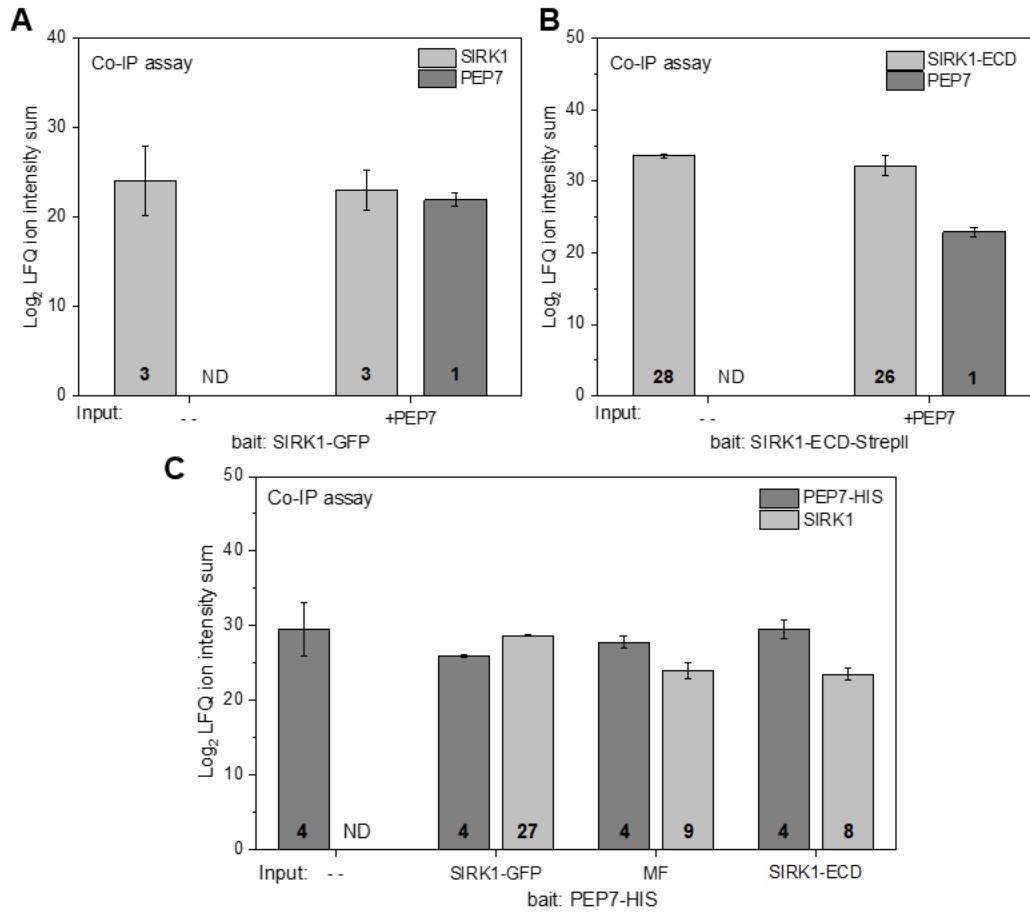


**Figure 10: Binding assays of PEP7 to immobilized SIRK1.**

Normalized ion intensity (LFQ values) of SIRK1 and PEP7 in Co-IP assays. (A) SIRK1 and PEP7 in Co-IP assays with SIRK1-GFP with or without the supply of PEP7. (B) SIRK1-ECD-StrepII and PEP7 in Co-IP assays with SIRK1-ECD-StrepII with or without the supply of PEP7. (C) SIRK1 and PEP7 in Co-IP assays with PEP7 with or without the supply of SIRK1. Averages of at least three biological replicates are displayed with standard deviations. Numbers in bar charts indicate the number of peptides identified.

### 3.3.2 Pre-bound SIRK1-PEP7 Complex could be Competitively Released by Free PEP7

After the above co-immunoprecipitation experiments demonstrating that PEP7 binds to the extracellular domain of SIRK1, we then tested if PEP7-SIRK1 binding can be competitively eluted with excess PEP7. To do this, PEP7-HIS was firstly fixed to beads and captured equal amount of SIRK1-ECD extract (obtained from transient expression of recombinant SIRK1-ECD in *Nicotiana benthamiana*). By detecting all fractions that generated from the competitive binding assay, a release of SIRK1-ECD from the PEP7-HIS beads with increasing concentrations of free PEP7 was observed (Figure 11). Pre-bound SIRK1-ECD was eluted with increasing concentrations of free PEP7. As PEP6 was used as a control, there was no SIRK1-ECD that was released by excess PEP6 (Figure 11). Free PEP7 disassembled the bound PEP7-HIS/SIRK1ECD complex and eluted SIRK1-ECD in a concentration-dependent manner. Saturation was reached when the concentration of PEP7 was higher than 1  $\mu$ M.

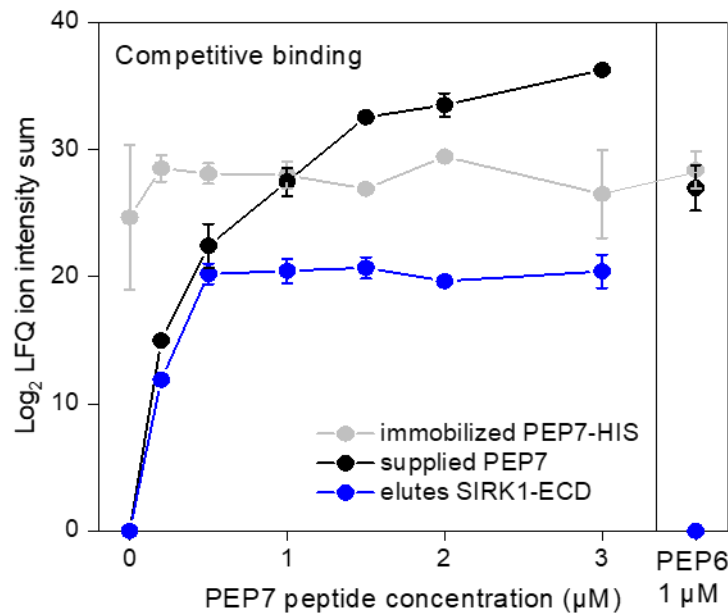


**Figure 11: Competitive binding assays.**

Competitive elution of SIRK1-ECD from pre-bound complexes with immobilized PEP7-HIS with different concentrations of PEP7. PEP6 was used as a control. In all panels, averages of at least three biological replicates are displayed with standard deviations.

### 3.3.3 Microscale Thermophoresis Uncovered the Ligand-Receptor Binding of PEP7 to SIRK1

Based on the binding results, microscale thermophoresis experiments (MST) were performed to demonstrate the dose-response curve of PEP7 binding to the extracellular domain of SIRK1. Firstly, SIRK1-ECD was carefully purified (Figure 12A). Purified SIRK1-ECD was analyzed by SDS-PAGE as well as mass spectrometry before subjecting it to the MST assay. The protein gel electropherogram gave a clear single band after purification (Figure 12B). Besides, purified SIRK1-ECD protein was subjected to trypsin digestion, and the digest peptides were identified and quantified. There were only 14 peptides that were quantified by LFQ. Nine of the fourteen peptides belonged to SIRK1, and their summed LFQ intensity was approximately 6-fold higher than the summed LFQ intensity of all the other peptides (Figure 12C). All identified SIRK1 peptides covered only the extracellular domain of SIRK1 (Figure 12D). Taken together, the purification of SIRK1-ECD protein was considered to be eligible for fluorescent labeling to perform MST assays.

PEP7 was used as a putative ligand as a binding partner to SIRK1-ECD in the MST assay. At the same time two other members of the PEP family, PEP4 and PEP6, were also included in the assay as controls. We used FNorm (normalized fluorescence) as an output value to get an intuitive observation of the binding of the three different small peptides to SIRK1-ECD. For each trace, the FNorm value for the Dose Response Curve is calculated by dividing  $F_{\text{hot}}$  by  $F_{\text{cold}}$ .  $F_{\text{hot}}$  corresponds to the fluorescence value measured in the heated state, while  $F_{\text{cold}}$  is the fluorescence value measured in the cold state before the IR laser is turned on (Jerabek-Willemsen et al., 2014). Ligand-dependent changes in normalized fluorescence FNorm can directly reflect ligand-induced changes in thermophoresis and be used to determine the binding constants (Entzian and Schubert, 2016).

After several pre-experiments, we performed serial dilutions using an initial concentration of 500 nM of the small peptides. A significantly sigmoidal binding curve of PEP7 and SIRK1-ECD was achieved with a high signal-to-noise ratio (12.5), allowing the calculation of a binding constant ( $K_d$  value) of 19  $\mu\text{M}$  (Figure 13). However, by exposure of PEP4 and PEP6 with the SIRK1-ECD, no sigmoidal dose-response curve appeared and the signal-to-noise ratio was too low to calculate  $K_d$  values. The microscale thermophoresis demonstrated the ligand-receptor binding event of PEP7/SIRK1ECD without the help of other domains of SIRK1 or its co-receptor QSK1 (Wu et al., 2019). Microscale thermophoresis, as a well-established means of detecting protein interactions (Wienken et al., 2010; Jerabek-Willemsen et al., 2011; Seidel et al., 2013; Jerabek-Willemsen et al., 2014), provided plausible evidence that PEP7 bound to SIRK1-ECD as a ligand. The fact that binding of PEP6 and PEP4 to SIRK1-ECD could not be confirmed also highly suggests that exclusivity PEP7 may be considered as a ligand to SIRK1. These results further affirm the plausibility of PEP7 being screened out as the correct ligand by large-scale ligand screening assays. Thus far, experimental evidences from the biochemical binding assays, competitive binding test and microscale thermophoresis, pointed to PEP7 bound to the extracellular domain of SIRK1.

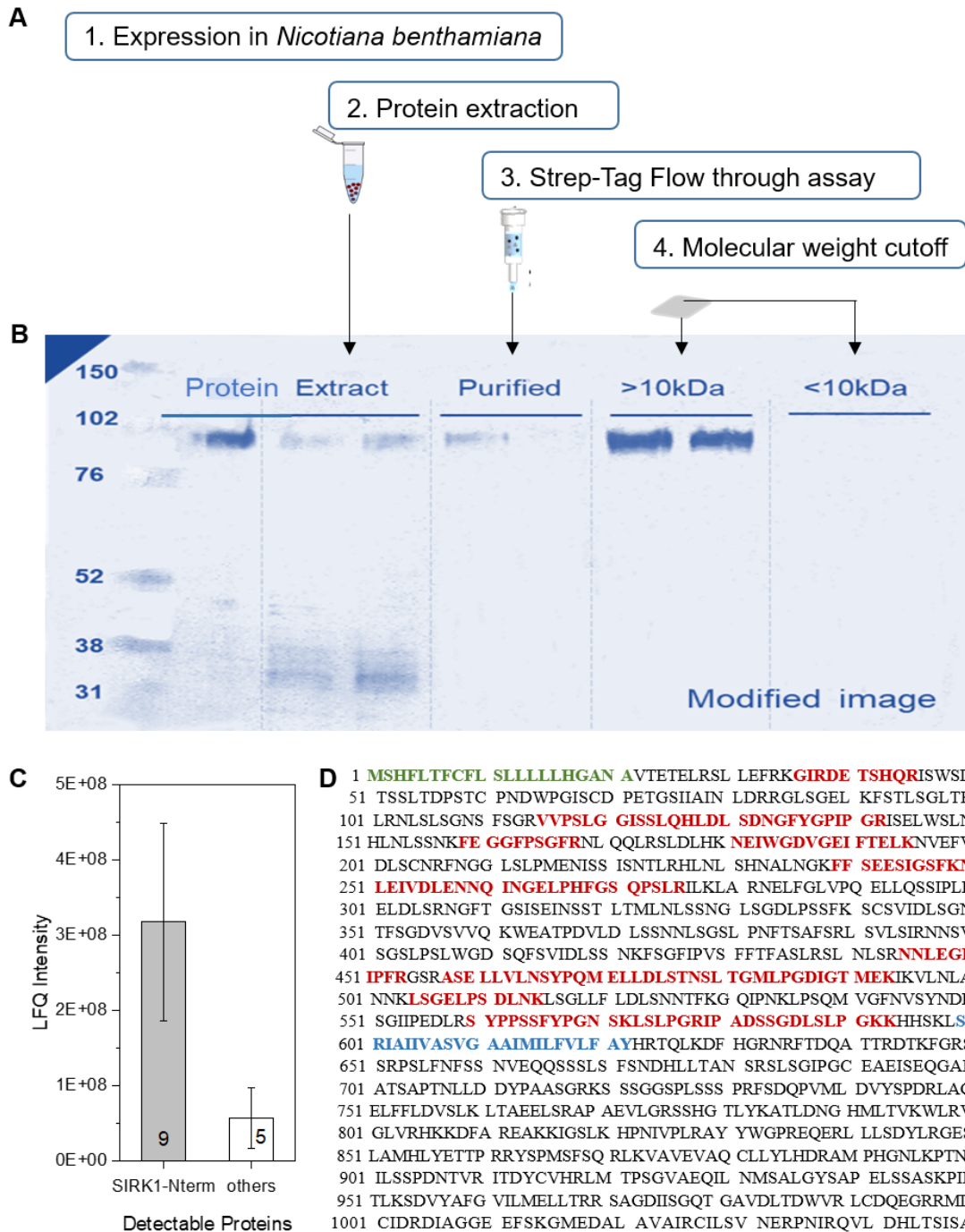


**Figure 12: Purification and identification of SIRK1-ECD.**

(A) Purification steps of SIRK1-ECD. (B) SDS-PAGE analysis of fractions after purifications. (C) LFQ intensity comparison of tryptic digest peptides from final purified SIRK1-ECD. (D) Tryptic digest peptides mass fingerprint analysis of purified SIRK1-ECD. The sequence of full length SIRK1 is shown with signal peptide in green and the transmembrane domain in blue. All identified peptides from the sample were shown in red.

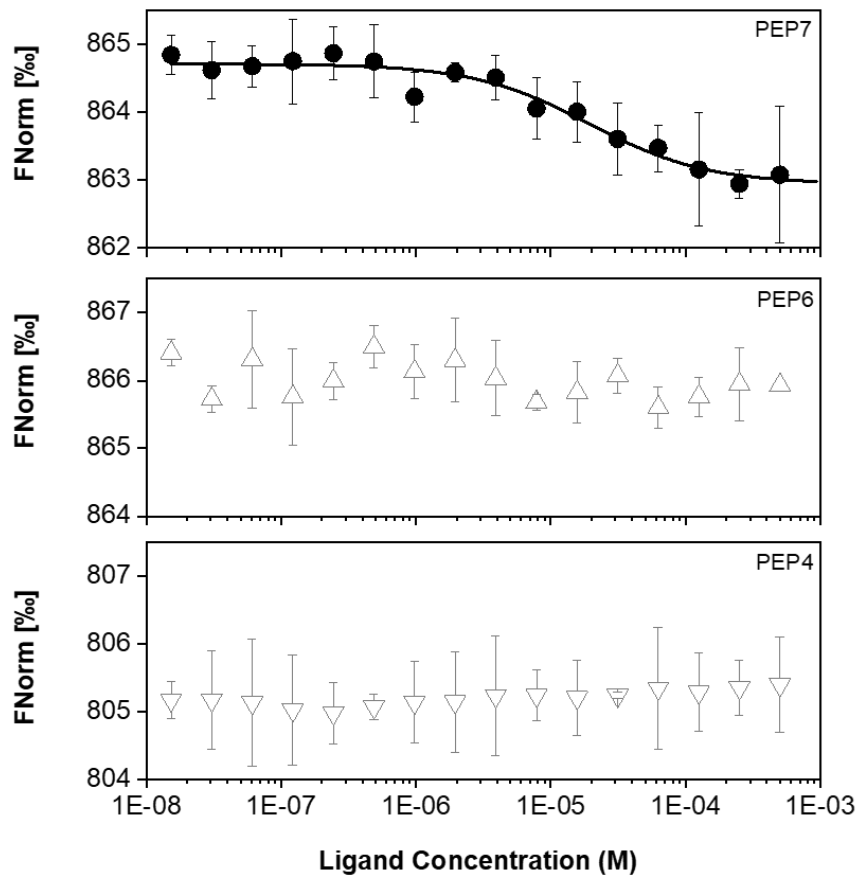


**Figure 13: Microscale thermophoresis assay.**

Microscale thermophoresis experiment with the extracellular domain of SIRK1 (SIRK1-ECD) and PEP7 or PEP6 as putative ligands. A signal to noise ratio of 12.5 was reached of PEP7-SIRK1-ECD binding, and only 1.4 for PEP6-SIRK1-ECD. Each dot represents an average of at least three independent measurements. Fitting of the dose-response curve was performed by the instrument software.

### **3.4 PEP7 was Capable of Activating the SIRK1 Signaling Cascades**

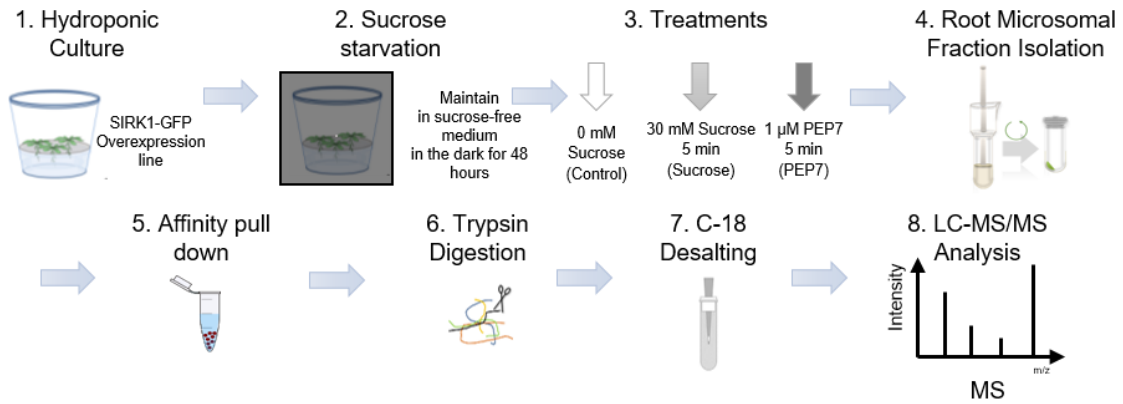
In the next step, we explored how PEP7 activates the signaling cascade of SIRK1. This section specifically tested the activation of SIRK1 downstream signaling by PEP7. The (phospho) proteomics approaches were performed. “PEP7 feeding” was applied in combination with affinity pull-down assays and phosphoproteomics assays.

#### **3.4.1 Experimental Design and Workflow**

In order to study the PEP7-induced SIRK1 signaling complex formation, over-expression line (35S::SIRK1-GFP in the background of *sirk1*) was grown in hydroponic culture. A total of three treatments were performed after sucrose starvation: no sucrose resupply (sucrose starvation treatment, control), 30 mM sucrose resupply for 5 min (sucrose) and 1  $\mu$ M PEP7 supply for 5 min (PEP7). Roots were harvested and the microsomal fraction was isolated. The SIRK1 signaling complex was enriched from microsomal preparation by GFP affinity pull-down. Samples were subjected to trypsin digestion followed by mass spectrometry analysis (Figure 14A).

For phosphoproteomics studies, wild-type, *sirk1*, *pep7* and *sirk1pep7* were grown in hydroponic culture. The same sucrose starvation and the three treatments described above were applied to the seedlings. Afterwards, the harvested root microsomal fractions were first subjected to a trypsin digestion step, followed by a phosphopeptide enrichment step, and finally the enriched phosphopeptides were analyzed by mass spectrometry (Figure 14B).

### A SIRK1 complex formation:



### B Phosphoproteomics:

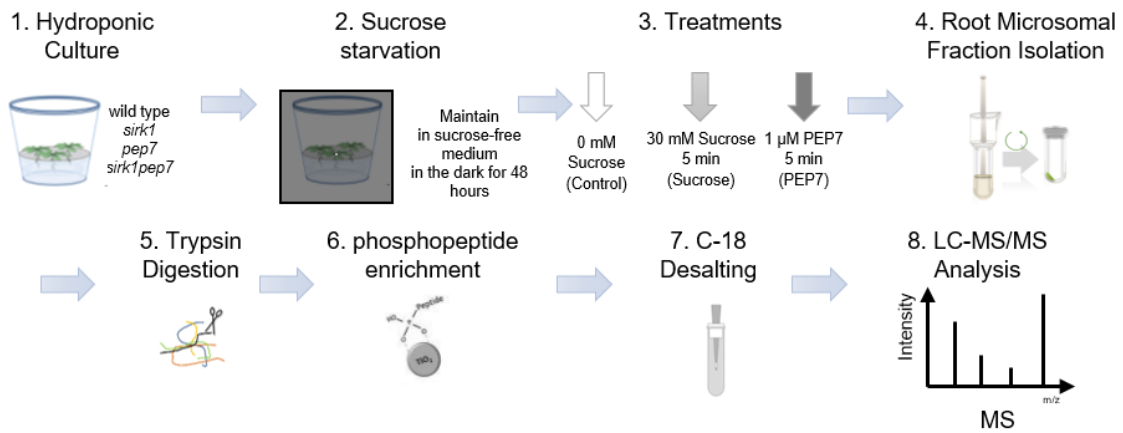


**Figure 14: Proteomics (phosphoproteomics) experimental design and workflow.**

Schematic representation of (phospho) proteomic study workflow. (A) Overexpression line of SIRK1-GFP in the *sirk1* background was used. Plant growth, sucrose and PEP7 treatments, microsomal preparation and SIRK1-GFP pull down. Protein samples were then digested with Trypsin and analyzed by HPLC system nanoflow Easy-nLC (Thermo Scientific) and Orbitrap hybrid mass spectrometer. (B) Wild-type, *sirk1*, *pep7* and *sirk1pep7* were used. Microsomal fraction were directly subjected to trypsin digestion. The cleaved peptides were subjected into phosphopeptide enrichment step. The rest of the workflow is the same as in A.



### 3.4.2 PEP7 Induced SIRK1 Signaling Complex Formation

SIRK1-GFP overexpression lines were used in affinity pull down assays to investigate the interactome of SIRK1 induced by sucrose or PEP7. Under each treatment, protein abundances were firstly normalized to the protein abundance of the bait protein SIRK1-GFP (Figure 15A). The abundances of the majority of identified proteins were lower than the abundance of bait protein SIRK1 after normalization. This result was consistent with the general pattern of pull-down experiments when using overexpression lines. Compared to control, sucrose and PEP7 triggered similar patterns of overall higher protein abundances.

For comparison of different experiments, we then calculated the  $\log_2$ -fold changes in protein abundance under treatment with sucrose or PEP7 versus the untreated control (Figure 15B). All the  $\log_2$ -fold changes were again normalized by the overall median of the two data sets (0.9, figure not shown). The individual medians of two dataset were then calculated (median of 0.1463 for sucrose/control comparison, and median of -0.0848 for PEP7/control comparison) for further data processing. There was a large overlap of proteins found with treatment induced  $\log_2$ -fold changes upon sucrose and PEP7 (Figure 15C). The  $\log_2$  fold changes in prey protein abundance were closely correlated under sucrose induction and PEP7 induction (Figure 15D). Proteins with  $\log_2$  fold changes higher than the individual medians (median of 0.1463 for sucrose/control comparison, and median of -0.0848 for PEP7/control comparison) were considered to be recruited as interactor with SIRK1 upon both treatments.

Given the previously demonstrated regulatory role of SIRK1 on other receptor kinases and aquaporins, we specifically observed the correlation analysis of receptor kinases (Figure 15E) as well as water aquaporins (Figure 15F) in sucrose and PEP7 induction. Among the receptor kinases, the known co-receptor QSK1 and its homolog QSK2 were found to be among the recruited interaction partners to SIRK1 (Figure 15E). Furthermore, seven of the nine identified aquaporins were found to be recruited by SIRK1, particularly PIP2F (Figure 15F), which was confirmed to be involved in the SIRK1/QSK1 signaling complex in our previous study.

Based on overview results and further detailed analysis of SIRK1 substrates, we observed that PEP7 induced a similar recruitment pattern of interactors to SIRK1 as did sucrose treatment (Figure 15A, B, C and D). Our results particularly showed the PEP7 induced recruitment of SIRK1 to aquaporins and co-receptor QSK1 (Figure 15F). In summary, affinity pull-down assays showed that PEP7 induced the formation of the SIRK1 signaling complex in the manner similar to that of external sucrose supply.

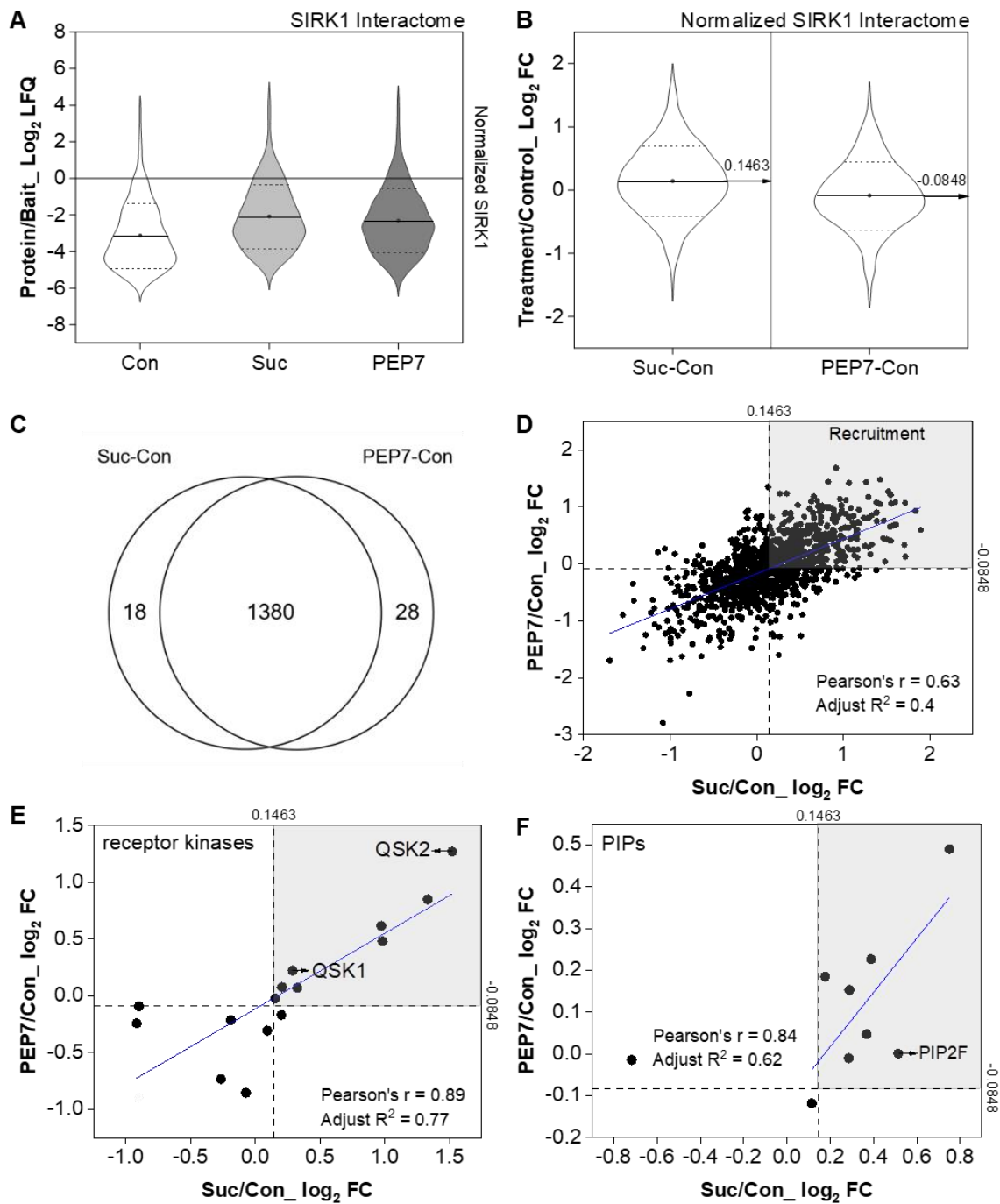


**Figure 15: Interactome of SIRK1 induced by PEP7 and Sucrose.**

(A) Normalized protein distribution based on bait. (B) Distribution of treatment/control comparisons, normalized by median values. The two median values within each comparison are shown in the violin plot, respectively. (C) Venn diagram of two comparisons. (D) Correlation analysis of all protein comparisons under two treatments. Proteins with values greater than the median were considered to be recruited by SIRK1 under both treatments. (E) Correlation analysis of only receptor kinases and (F) Correlation analysis of only PIPs under two treatments.

### 3.4.3 PEP7 Induced Phosphorylation of SIRK1 Substrates

The studies on SIRK1 signaling pathway initially reveals its role in controlling aquaporin activity via phosphorylation in response to external sucrose stimulation (Wu et al., 2013). Further research presented the functional model of SIRK1 and its co-receptor QSK1 that involves trans-phosphorylation of QSK1 and phosphorylation of the aquaporins by SIRK1 (Wu et al., 2019). Based on the SIRK1/QSK1 model, and under consideration that PEP7 could act as a ligand to SIRK1, we hypothesize that the binding of PEP7 to SIRK1 could prompt SIRK1 to phosphorylate its substrates QSK1 and aquaporins. To test this, we thus conducted the phosphorylation study of SIRK1 substrates in response to external PEP7 supply as well as sucrose. By comparing their phosphorylation patterns under two treatments we aimed to uncover how PEP7 affects the phosphorylation status of SIRK1 substrates, especially aquaporins.

In the final phosphoproteomic dataset, serines (Ser/S) with single phosphorylation sites accounted for 57%, serines with double phosphorylation sites for 28%, and serines with triple phosphorylation sites for 5%. Threonine (Thr/T) phosphorylation sites accounted for a total of 10%, while a very small proportion of tyrosine (Tyr/Y) was also found (Figure 16A).

The phosphopeptides of QSK1, its homolog QSK2, and PIPs were chosen to be presented, the corresponding phosphorylation site intensities were quantified and normalized (Figure 16B). The phosphorylation status of QSK1/QSK2 induced by PEP7 was consistent with our hypothesis of PEP7 inducing coreceptor transphosphorylation and aquaporin phosphorylation through activation of SIRK1. In the wild type, PEP7 treatment resulted in increased phosphorylation of QSK1/QSK2, as did sucrose. In the receptor mutant *sirk1*, QSK1/QSK2 showed a stronger reduction in phosphorylation in response to external PEP7 rather than external sucrose supply. In the *pep7* mutant, sucrose failed to induce phosphorylation of QSK1/QSK2, however, the supply of PEP7 was able to restore the phosphorylation. In the double mutant *sirk1pep7*, neither sucrose nor PEP7 induced increased phosphorylation of QSK1/QSK2.

The phosphorylation patterns of PIPs under PEP7 treatment were essentially the same as that of QSK1/QSK2 (Figure 16B). In wild type, PEP7 treatment resulted in increased phosphorylation of aquaporins as did sucrose. In the receptor mutant *sirk1*, external sucrose supply resulted in reduced phosphorylation of some PIPs (PIP2A, PIP2E and PIP2F), and external PEP7 supply resulted in an even stronger reduction of their phosphorylation; while some other PIPs (PIP3A and PIP3B) exhibited reduced phosphorylation only upon PEP7 supply. In the ligand mutant *pep7*, sucrose was not able to induce SIRK1 to phosphorylate aquaporins, while PEP7 supply partially restored the phosphorylation of aquaporins. In the double mutant *sirk1pep7*, neither sucrose nor PEP7 induced the increased in phosphorylation of aquaporins.

To obtain a more detailed understanding of PEP7 effect on SIRK1 in terms of regulation of aquaporins, we checked the status of each phosphopeptide within PIPs between different genotypes. According to the literature, S280 of PIP2A, S279 of PIP2E, S280 of PIP2F and S273 of PIP3A are conserved with the pore gating S274 of SoPIP2A (Törnroth-Horsefield et al., 2006), while S283 of PIP2A, S282 of PIP2E, S283 of PIP2F and S276 of PIP3A are conserved with S283 of PIP2A controlling plasma membrane localization

(Prak et al., 2008) (Figure 16C). Thereby, phosphorylation of these sites is associated with higher activity or preferred residence in the plasma membrane, whereas dephosphorylation is associated with pore closing and removal from the plasma membrane.

These involved phosphorylation sites were quantified (Figure 16D). Most of identified sites were the pore gating phosphorylation sites except the phosphorylation site S282 of PIP2E. As shown, in wild type, phosphorylation sites connected with pore gating displayed high levels for all PIPs, whereas in the mutants the phosphorylation sites connected with pore gating were generally lower. However, the application of external PEP7 significantly increased the abundance of aquaporin phosphopeptides in the *pep7* mutant, especially PIP2F, whose phosphorylation sites connected to the pore gating were largely restored to the level consistent with the wild type. The rescue of phosphorylation sites connected to pore gating by PEP7 was dependent on the presence of SIRK1, as in *Sirk1* knockout mutants (*sirk1* and *sirk1pep7*), neither the supply of PEP7 nor the supply of sucrose resulted in an increase of aquaporin phosphorylation.

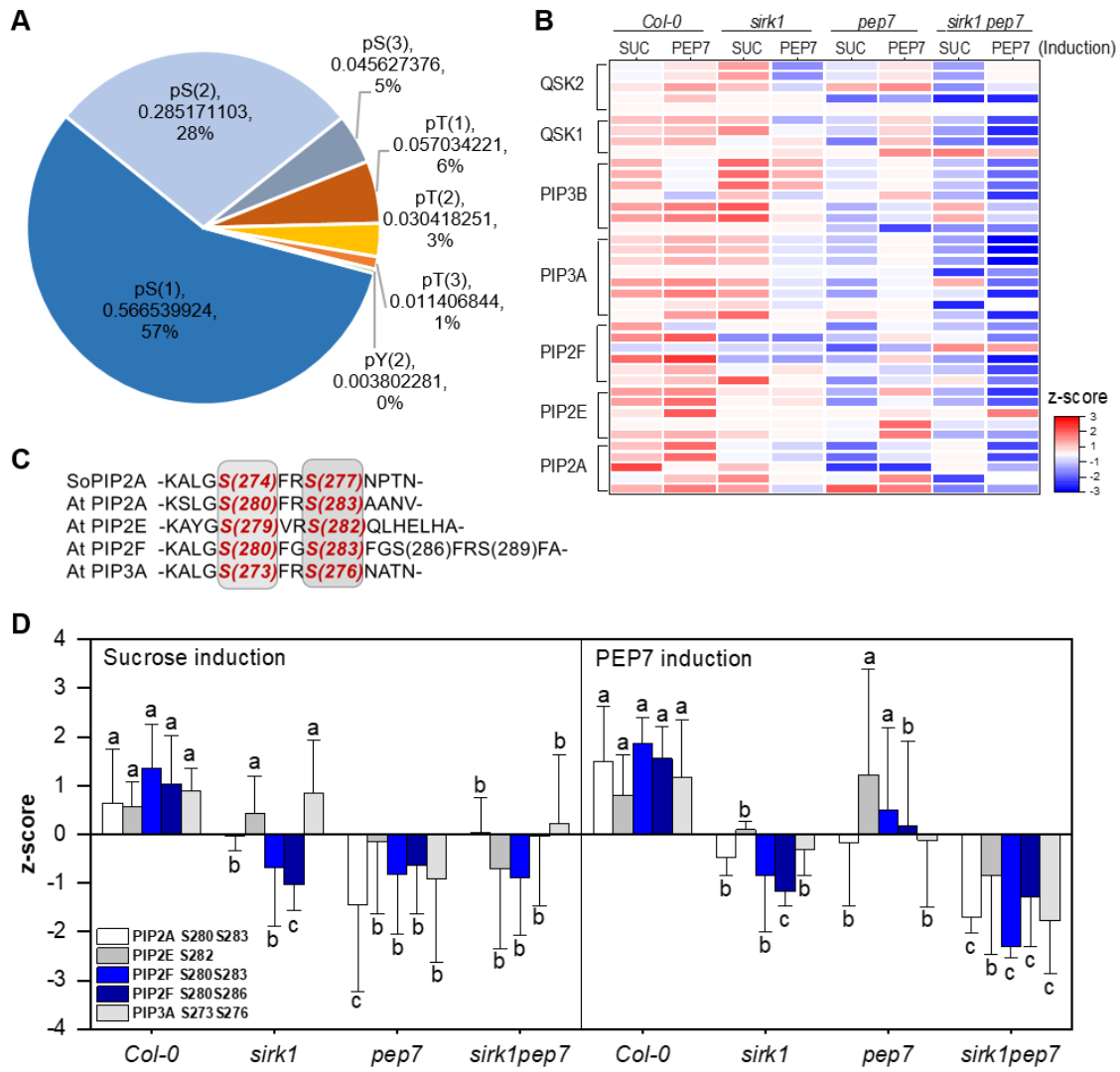


**Figure 16: PEP7-induced alterations of phosphorylation of SIRK1 substrates.**

(A) Distribution of phosphorylated residues in each peptide detected in phosphopeptide profiling experiment. The lowercase letter p represents phosphorylation, the capital letters S, T, and Y represent serines (Ser/S), threonines (Thr/T) and tyrosines (Tyr/Y), and the number in parentheses represents the number of phosphorylation sites detected on a phosphopeptide. (B) Heatmap of means of z-scored phosphosite intensities of different phosphopeptides identified for known members of the SIRK1 signaling pathway. Each row represents one phosphopeptide. (C) Sequence alignment of C-terminal phosphorylated plant aquaporins. Grey area indicate the conserved residues that can be phosphorylated. (D) z-scored phosphorylation levels of conserved residues of PIPs that induced by sucrose and PEP7. All phosphorylation sites are marked in the figure (localization probability > 0.75), where the phosphorylation sites that corresponding to the pore gating are marked in blue.

### 3.5 PEP7 Affected Water Influx to Protoplasts via SIRK1

Aquaporins were found to be interaction partners of SIRK1 and substrates phosphorylated by SIRK1 upon treatment with PEP7 in above profiling experiments. The regulatory role of SIRK1 on aquaporins led us to explore whether PEP7 can further affect the aquaporin activities via SIRK1. Sucrose as an osmotic agent has been shown to fail to induce water influx into protoplasts specifically in *sirk1* mutants (Wu et al., 2013), indicating the role of SIRK1 in modulating water flux across the plasma membrane. Thus, here we wanted to explore whether PEP7 could have an effect on aquaporin activities through SIRK1.

We performed protoplast swelling assays with wild type, *sirk1*, *pep7* and the *sirk1pep7* double mutant to test if supply of PEP7 was also able to induce water influx and whether this was dependent on the presence of SIRK1 receptor kinase. The results are presented in two parts:

1. We observed the real-time volume change of protoplast during the swelling, comparing the state of the same protoplast before (left) and after (right) swelling process (Figure 17). As shown, mannitol as a control, caused similar swelling of protoplasts in all mutants (*sirk1*, *pep7* and *sirk1pep7*) as in the wild type, all resulted in a swelling rate of approximately 1.5 in protoplast volumes at the end state. In the wild type, the effect of sucrose-induced protoplast swelling was essentially similar to that of mannitol, while the application of PEP7 caused the most violent volume expansion of the protoplasts, with a nearly 2-fold increase in volume compared to the initial state, and illustrated the role of PEP7 in influencing water influx to the protoplasts. In the *sirk1* mutant, sucrose and PEP7 largely failed to induce water influx into the protoplasts when the osmotic potential changed. In both *pep7* mutant and *sirk1pep7* mutant, sucrose resulted in a smaller protoplast volume expansion, similar to that in *sirk1* mutant. Interestingly, in the *pep7* mutant, the ability of protoplasts to swell upon external supply of PEP7 were restored to similar level with mannitol treatment. However, in the *sirk1pep7* mutant, the protoplast swelling capacity remained low upon the external supply of PEP7, the protoplast volume swelling status was similar to that of sucrose treatment.

2. We calculated the water flux density for each genotype of protoplasts under different treatments, the values were able to directly reflect the aquaporin activity on the plasma membrane (Figure 18). In the wild type, mannitol and sucrose induced water influx (Figure 17, 18A), whereas external supply of PEP7 significantly increased water influx compared with that observed in the presence of mannitol or sucrose only. In the *sirk1* mutant, as expected, mannitol induced water influx, but the presence of sucrose did not. The supply of PEP7 to the *sirk1* mutant also resulted in a low rate of water influx (Figure 17, 18A), similar to the rate of influx observed with sucrose treatment. In the *pep7* mutant, mannitol induced water influx, but sucrose supply resulted in low water influx, similar to the *sirk1* mutant. Strikingly, the external supply of PEP7 to the *pep7* mutant restored water influx to an inflow rate that was indistinguishable from that of the wild type (Figure 17, 18A). In the *sirk1pep7* double mutant, neither the external supply of sucrose nor PEP7 resulted in high water influx rates. Thus, when SIRK receptor was absent (as in the *sirk1* and *sirk1pep7*), neither sucrose, nor PEP7 were able to activate aquaporins. When the ligand PEP7 was absent, as in the *pep7* mutant, external supply of ligand was able to restore signaling only in the presence of SIRK1. In addition, we included PEP4 and PEP6 treatments to the protoplast swelling experiments, tested whether they had similar effects as PEP7 in directing water influx into the protoplasts together with SIRK1. Under

either PEP4 or PEP6 treatment, the protoplast expansion of all genotypes was not significantly different from the effect caused by mannitol. It indicated that PEP4 or PEP6 did not affect the aquaporin activity on the plasma membrane, and did not work in conjunction with SIRK1 (Figure 18B).

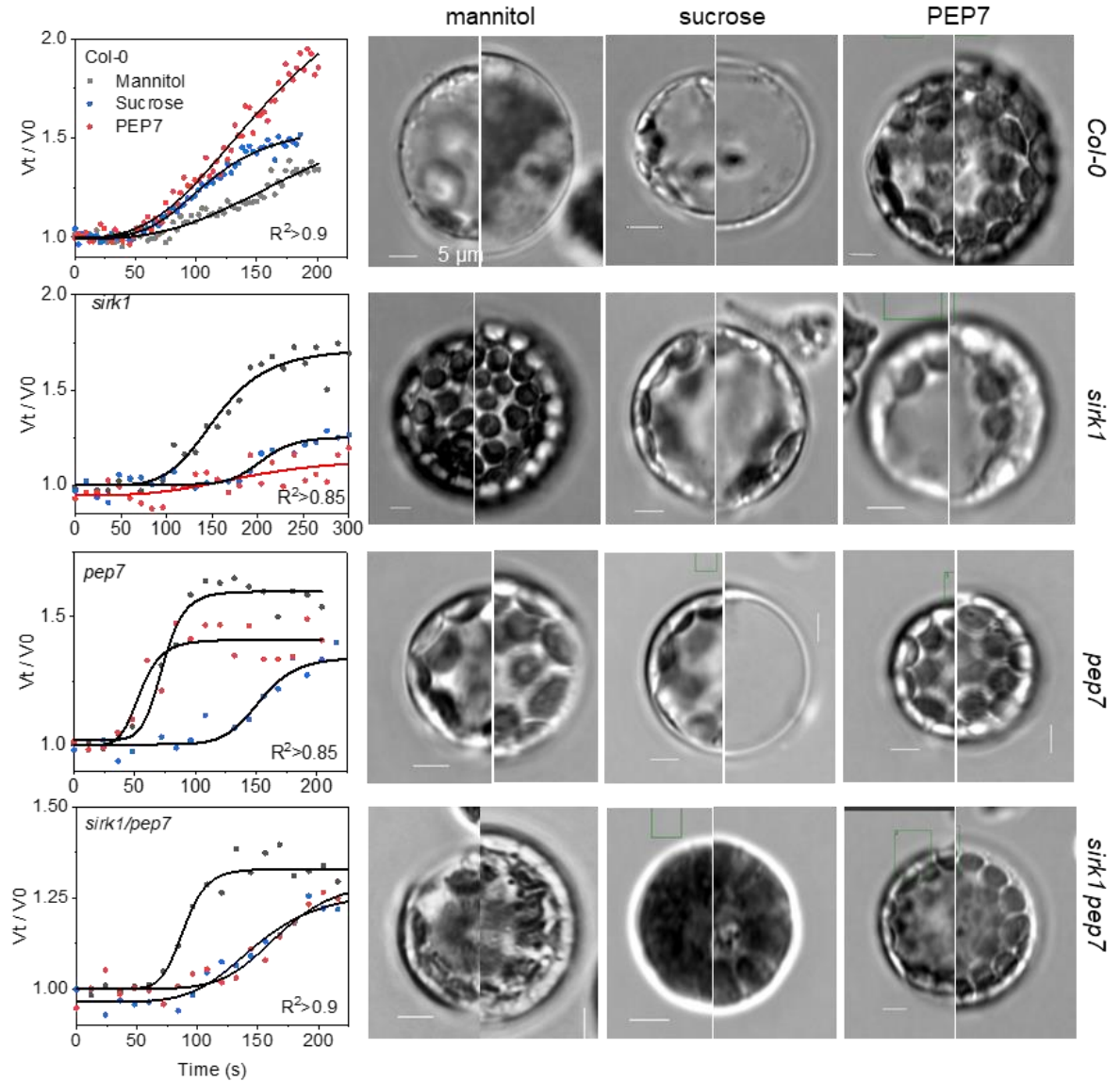


**Figure 17: Volume change of protoplasts over time.**

Volume change of protoplasts over time induced by mannitol only, in presence of sucrose or in presence of PEP7 and representative images of protoplasts at high and low osmolarity conditions. Scale bar 5  $\mu$ m.

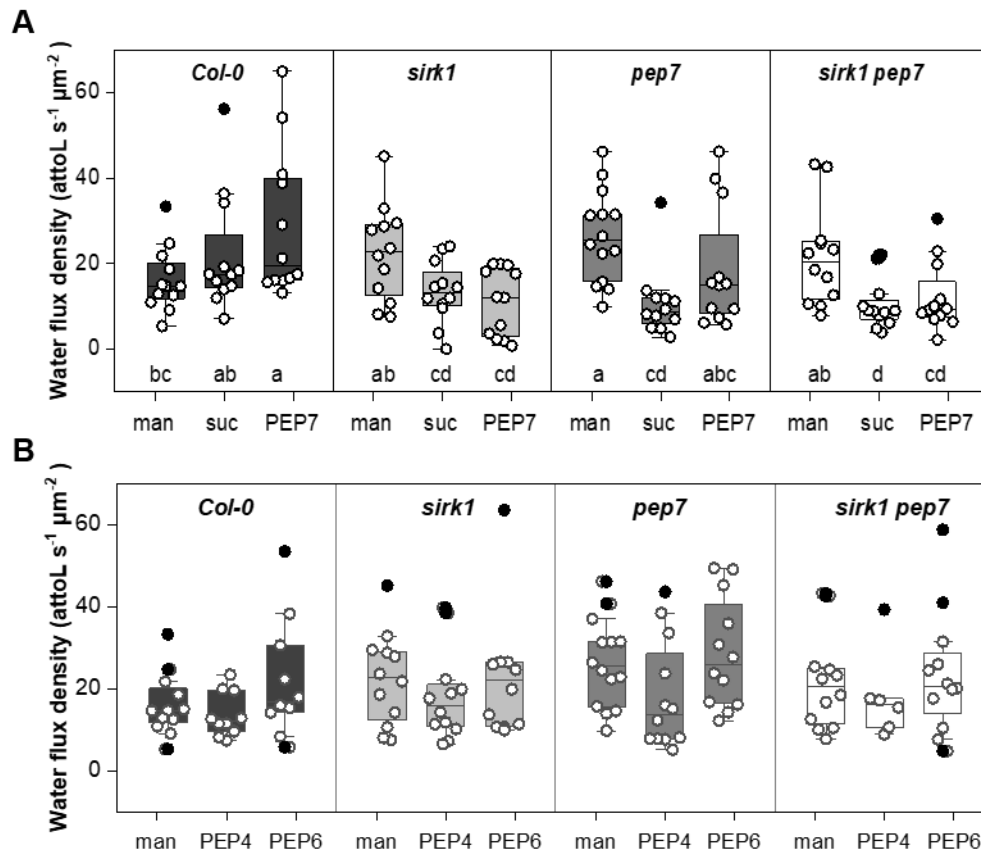


**Figure 18: Water influx density of protoplasts induced by osmotic changes.**

(A) Water influx density of protoplasts induced by osmotic changes through mannitol, sucrose or PEP7 in wild type (*col-0*), *sirk1*, *pep7* and the double mutant *sirk1 pep7*. (B) Water influx density of protoplasts induced by osmotic changes through mannitol, PEP4 or PEP6 in wild type (*col-0*), *sirk1*, *pep7* and the double mutant *sirk1 pep7*. Boxplots show the median and upper/lower 25th percentile. White dots represent individual measurements. Small letters indicate significant differences ( $p < 0.05$ ) as determined by oneway ANOVA with Holm-Sidak correction.



### 3.6 PEP7/SIRK1 Signaling Pathway Affected Root Growth

Next, we explored the whole-plant effects of the PEP7/SIRK1 signaling pathway. Root growth relies on sucrose supply as a source of carbon and water transport (Péret et al., 2012), implying that the root growth of *Sirk1* knockout mutants may be influenced by the sucrose content in the growth conditions. Also based on the whole plant drought experiments (section 3.1), an involvement of SIRK1 in water loss of the plants was supported. Therefore, we set up a series of growth environments with different sucrose contents to test the root growth of the *Sirk1* knockout mutants. Meanwhile, the knockout mutants of *Pep7* and *Qsk1* were also involved in the experiments. In addition, we also explored the effect of PEP7 on SIRK1 at the whole-plant level by external PEP7.

Indeed, after 5 days of growth under low external sucrose supply (0.02%), the root growth of the *sirk1* mutant was impaired, the primary roots of *sirk1* were significantly shorter than those of the wild type. When both the receptor (SIRK1) and co-receptor (QSK1) were knocked out (in the double mutant *sirk1qsk1*), this short root phenotype was enhanced as expected (Figure 19A, D). On agar plates with a high (1%) external sucrose supply, there was no significant difference in root length for *sirk1* as well as *sirk1qsk1* compared to the wild type (Figure 19B, D). The short root phenotype of *sirk1* and *sirk1qsk1* under low sucrose conditions was rescued by high sucrose condition (Figure 19B, D) as well as by SIRK1 overexpression (Wang, unpublished). Thus, the presence of sucrose was a necessary and sufficient condition to rescue the short root phenotype of *sirk1* and *sirk1qsk1*, and the root growth phenotype of *sirk1* mutant was dependent on SIRK1 expression and activity.

Under low external sucrose supply (0.02%), the *Pep7* knockout mutants (*pep7* and *sirk1pep7*) had short root phenotypes similar to that of the *sirk1* mutant (Figure 19A, D). High external sucrose supply similarly rescued the short root phenotype of *sirk1pep7* (Figure 19A, D). Interestingly, the root growth of the *pep7* mutant was slightly greater than that of the wild type under high external sucrose supply (Figure 19B, D).

Supply of external PEP7 (1  $\mu$ M) to agar plates resulted in a slight increase in root growth in the wild type compared with control conditions (Figure 19C, D). In the *sirk1* mutant, external supply of PEP7 did not affect its short root phenotype. Similarly in *sirk1qsk1*, external supply of PEP7 had no effect. In the *pep7* mutant, external PEP7 supply restored the primary root length to the same level as in the wild-type (Figure 19C, D), but this was not observed in the *sirk1pep7* mutant, which also lacks the receptor. This root growth enhancement by external PEP7 supply was not observed in the receptor-deficient mutants *sirk1*, *sirk1qsk1* and *sirk1pep7*. These results suggested that the presence of the SIRK1 was required in PEP7 signaling.

In summary, SIRK1 expression and activity would severely affect root growth in Arabidopsis, and the PEP7-induced root growth phenotype was mediated through SIRK1 signaling. Therefore, at the whole plant level, the PEP7/SIRK1 signaling complex could affect root growth.

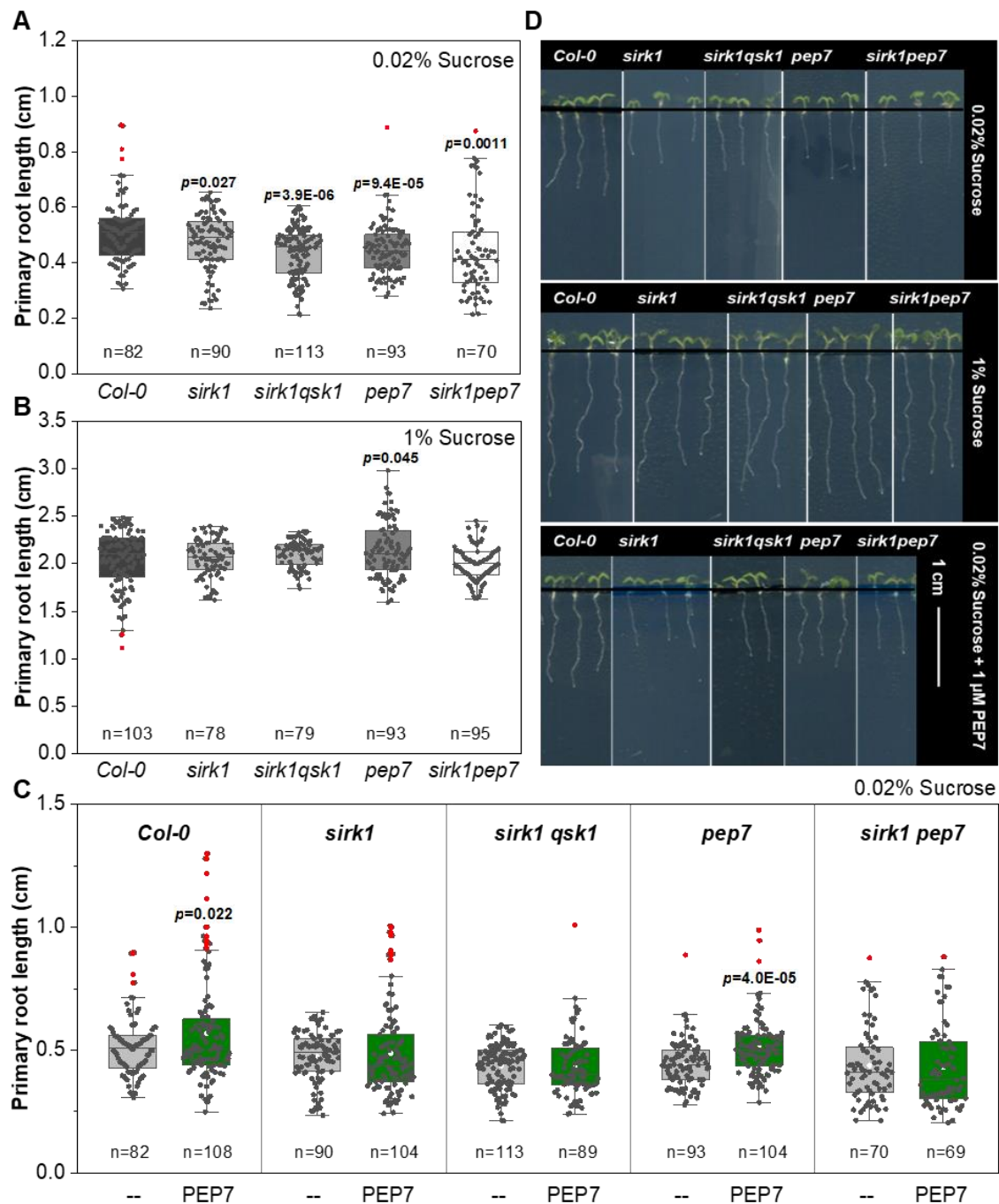


**Figure 19: Root growth phenotype.**

Wild type (Col-0), *sirkl1*, *pep7*, and *sirkl1qsk1* and *sirkl1pep7* double mutants grown on agar plates of (A) low external sucrose and (B) high external sucrose. (C) The effect of PEP7 supply (1  $\mu$ M) to roots was tested for the four genotypes at low external sucrose. (D) Scanned images of roots. Boxplots represent values of individual plants, numbers of plants analyzed are noted below each box. In panels A and B, p-values indicate significant differences to wild type. In panel C, p-values indicate significant differences of the PEP7-treatment to control treatment within each genotype.

## 4. Discussion

The ligand-receptor system in plants plays an unparalleled role in signal transduction, cell physiological regulation and stress response, and the search for a pairing system has become a research focus in recent years. In the present study, we sought to confirm our search for a ligand candidate, PEP7, to form a ligand-receptor system with the receptor SIRK1 and to explore the biological function of this system. First, the two members were singled out, and the recognition of them was tested using a series of biochemical experiments including affinity pull-down, immunoprecipitation and microscale thermophoresis. Subsequently, proteomic (phosphoproteomic) approaches were performed to reveal the induction of the PEP7 (as ligand) to the SIRK1 (as receptor) signaling complex. Mutants of the ligand-receptor system were then subjected to physiological experiments to verify their biological function.

### 4.1 PEP7 as a Specific Member of the Danger Signal Peptide Family

Very little is known about PEP7 within the PEP-family. Members of PEP family are commonly recognized as damage-associated molecular patterns (DAMPs) that represent endogenous signals for stress and wounding (Boller and Felix, 2009). PEPR1 has been shown to be a receptor for PEP1-6, but no result suggests that it is also a receptor for PEP7, while PEPR2 has so far been identified only as a receptor for PEP1 and PEP2 (Krol et al., 2010; Yamaguchi et al., 2010). Promoter-GUS analyses of different PROPEPs reveals expression of PROPEP7 in the root elongation zone and lateral root primordial, and does not share any gene expression patterns with the receptors PEPR1 and PEPR2 (Bartels et al., 2013). Although the propeptides of PEP4 and PEP7 are similarly expressed in the root tip (Bartels et al., 2013), the sequences of PEP4 and PEP7 mature peptides are very different (Zhang et al., 2016a). Based on the sequence of the active peptide, PEP7 does not show a strong similarity to any of the family members.

PEP1 perception by its receptors inhibits root growth by affecting ROS formation and PIN-dependent auxin distribution (Jing et al., 2019; Jing et al., 2020; Shen et al., 2020). PEP3 is recognized by the PEPR1 receptor that enables increased salinity stress tolerance in plants (Nakaminami et al., 2018). Besides, PEP3 was found to be associated with dark-induced leaf senescence and this response is inhibited by the supply of sucrose (Gully et al., 2015). Thus, members of the PEP family also appear to be involved in signaling functions other than biotic stress responses and have been shown to be released in response to changes in plant-centered metabolism. In a recent study, single-cell RNA sequencing of root cells clustered PEP7 with marker genes of mature root hairs and PEP6 with marker genes of endocortex, while other members of the PEP-family or the respective receptors were not found (Ryu et al., 2019).

The exclusivity and unknown nature of PEP7 in its family makes its study more challenging. PEP7 exhibits very different characteristics from the other members of PEP family in terms of amino acid sequence, expression pattern, and function prediction. The uniqueness of PEP7 offers the possibility of its involvement in other signaling pathways than plant defense and is consistent with our hypothesis that it may be a ligand for SIRK1. In turn, our studies on the ligand-receptor system of PEP7 and SIRK1 suggests a role of the PEP family beyond biotic stress responses.

## 4.2 Linkage between Sucrose and PEP7

The SIRK1 signaling pathway previously was reported to be activated under sucrose resupply condition (Wu et al., 2013; Wu et al., 2019). Current research revealed the SIRK1-dependent signaling pathway can be activated by PEP7, however, the present study did not establish a systematic inquiry of the link between sucrose stimulation and PEP7 appearance. Therefore, the relationship between PEP7 and sucrose is in need for discussion.

### 4.2.1 Sucrose Supply Induces the Secretion and Accumulation of PEP7

Polypeptides can be highly enriched by TFA extraction (Pearce et al., 2001). In the study on screening of SIRK1 ligand candidates (section 3.2.1), our group successfully obtained apoplast peptides by using the TFA extraction method, confirming the efficiency of this method. Also by TFA extraction, we obtained peptides from sucrose-treated roots and examined the levels of PEP7 therein. Compared to sucrose starvation conditions, PEP7 levels in roots increased significantly after 3-5 min of sucrose repletion (Xi, unpublished). In addition, another study in our lab has demonstrated that PEP7 was secreted to the apoplast specifically at sucrose resupply. This secretion was not observed when nitrate was resupplied to nitrate-starved seedlings (Figure 20). Therefore, sucrose supply induces the secretion and accumulation of the mature PEP7 *in planta*.

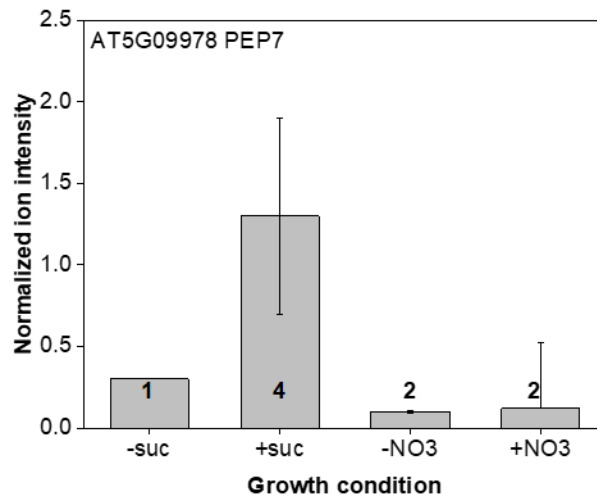


**Figure 20: Normalized ion intensity of PEP7 in apoplast fractions under different nutrient supply.**

PEP7 secretion was specifically observed at sucrose resupply. Averages of at least three biological replicates are displayed with standard deviations, numbers indicate the number of peptides identified.

### 4.2.2 Sucrose Affects Gene Expression Level and Phosphorylation Status of PROPEP7

The mature peptide PEP7 is derived from its precursor PROPEP7 (Huffaker et al., 2006). Mining of the published transcriptome data (Shulze et al., 2019) revealed that the gene expression level of PROPEP7 was significantly increased with sucrose supply. In single-cell sequencing studies of root cells, the gene expression of PROPEP7 (clustered with cortical marker genes) was found to be induced by sucrose supply, whereas the expressions of PROPEP6 and PROPEP4 (both clustered with endothelial marker genes) were

not induced by sucrose, and other PEP family members were not identified under sucrose-altered conditions (Shulse et al., 2019). This indicates that sucrose could influence PEP7 generation at the level of gene expression.

Meanwhile, observation of another set of phosphoproteomic data from our lab revealed that PROPEP7 in roots can be phosphorylated in the presence of external and internal sucrose (Figure 21) (Xi, unpublished). In this phosphoproteomic data set, it was observed that plant internal sucrose concentrations (especially in roots) were closely correlated with PROPEP7 phosphorylation. In this experiment, plant materials from sucrose-related mutants (including wild-type, *sirk1* mutant, sucrose export mutant *sweet11/12* (Chen et al., 2012), and starch biosynthesis mutant *pgm* (Caspar et al., 1985)) were harvested at the end of the day (higher sucrose concentration) and at the end of the night (lower sucrose concentration), resulting in the variation plant internal sucrose concentrations. We observed that in roots (but not in shoots), internal sucrose concentration showed a significant negative correlation with the phosphorylation of PROPEP7 at the N-terminus of threonine T37 (Figure 21). Under the assumption that the phosphorylation of precursor PROPEP7 could be involved in the production of mature PEP7, we hypothesize that sucrose is able to specifically induce the maturation of PEP7 from its precursor PROPEP7. In that way the root internal sucrose concentration may be closely related to the production of PEP7. Furthermore, these findings suggest a unique mechanism in peptide maturation, which apparently involves the phosphorylation of precursors.

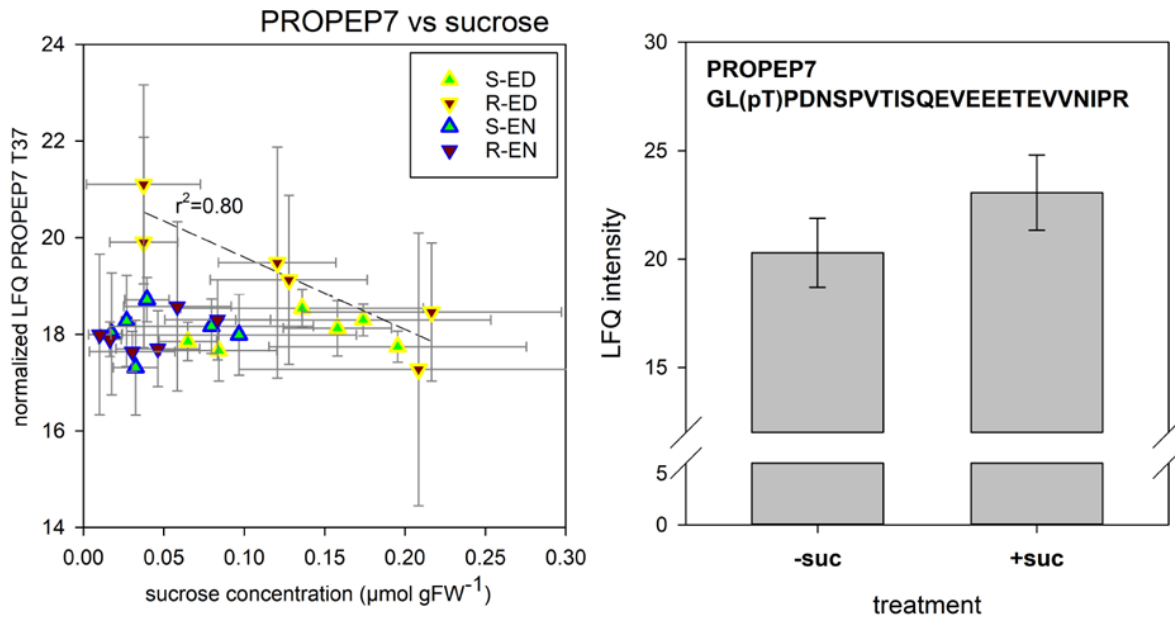


**Figure 21: Phosphorylation of PROPEP7 in context of internal and external sucrose.**

(A) LFQ intensity values of PROPEP7 phosphopeptide in relationship with sucrose concentration in shoots (S) and roots (R) at the end of day (ED) and end of night (EN). Within each tissue and each time point, individual data points represent wild type, *sirk1* mutant, *pgm* mutant, *sweet11/12* mutant, *sirk1 pgm*, as well as *sirk1 sweet11/12*. (B) Abundance of PROPEP7 phosphopeptide in wild type roots without and with external sucrose supply. Symbols and bars represent mean with standard deviation of six or three replicates in panels A, and B respectively.

### 4.2.3 Processing of PEP7

Another unsettled question is how PROPEP7 is processed into PEP7. Recently, it was reported that Ca<sup>2+</sup>-dependent type-II metacaspases (MCs) constitute the proteolytic enzymes that mediate PROPEP processing in Arabidopsis (Shen et al., 2019), and in particular, MC4 (Metacaspase 4, AT1G79340 ) is capable of releasing active peptides from the C-terminus after cleavage after arginine or lysine, thereby processing PROPEPs including PROPEP7. Another study suggests that the processing of PEPs is induced by calcium signaling (Hander et al., 2019) and even requires intramolecular proteolytic metacaspase. In any case, even though MC4 has been shown to process PROPEPs, including PROPEP7, existing studies have focused on a detailed understanding of the release of only PEP1 by MC4. The requirement for further processing of PEP7 precursors requires additional studies and more extensive data describing propeptide phosphorylation. Unfortunately, MC4 was not found in our data and therefore could not be further speculated and discussed in this study.

### 4.2.4 Possible Feedback Regulation of PEP7/SIRK1 Signaling

As mentioned above, PROPEP7 in roots can be phosphorylated in the context of external and internal sucrose, and the internal sucrose concentration in the roots may be closely related to the production of PEP7. Another clue also illustrates the effect of root internal sucrose concentration on PEP7. In the experiment exploring the effect of PEP7 on SIRK1 kinase activity (section 3.2.2), we additionally used SIRK1-GFP proteins obtained from roots harboring various internal sucrose concentrations (instead of sucrose-starved roots), exposed them to PEP7 and observed the effect of PEP7 on SIRK1 kinase activities. As shown in Figure 22, the effect of PEP7 on SIRK1 kinase activity showed opposite trends at low internal sucrose concentration and high internal sucrose concentration. Under high sucrose condition, increasing PEP7 concentrations (before it reached saturation, Figure 9A) instead showed a trend of inhibition of SIRK1 activity. Internalization of SIRK1 has been shown to occur during long-term sucrose induction (Wu et al., 2013), therefore, an explanation for the inhibitory effect of PEP7 on SIRK1 kinase activity at high sucrose concentration is the possible internalization of SIRK1 induced by high concentrations of sucrose *in vivo*. Combined with the aforementioned negative correlation between PROPEP7 phosphorylation and sucrose concentration, it may also function as a feedback regulatory mechanism for high sucrose concentration-induced SIRK1.

The very limited data only suggest that root internal sucrose concentration is perhaps closely related to the production and/or maturation of PEP7. To date, we still know very little about the linkage between sucrose stimulation and PEP7 secretion. Many unanswered questions still await us: what is the role of PROPEP7 phosphorylation and could PROPEP7 phosphorylation provide a new perspective to decipher the mechanism of PEP7 maturation? Besides inducing PROPEP7 phosphorylation, what is the involvement of sucrose in PEP7 secretion? And how exactly does plant internal sucrose concentration related to PEP7 pathway? ...

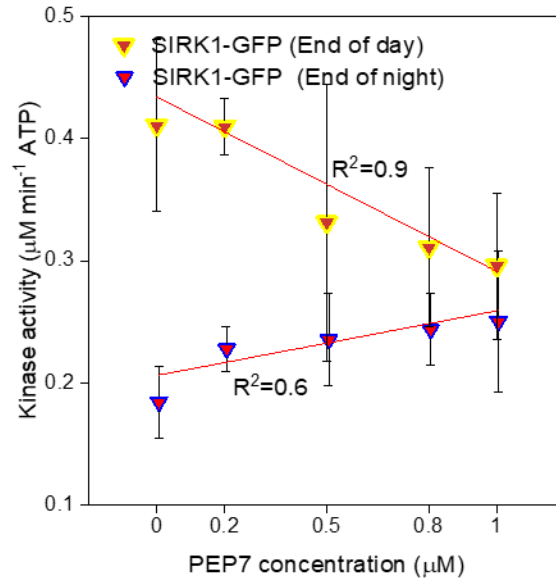


**Figure 22: PEP7 inducible SIRK1 kinase activity in relationship with the concentration of PEP7 at different internal sucrose concentrations.**

PEP7 inducible SIRK1 kinase activity in relationship with the concentration of PEP7 at the end of day (ED, corresponding to high sucrose levels) and end of night (EN, corresponding to low sucrose levels). Data shown as mean with standard deviation of three replicates.

### 4.3 Receptor-Ligand Binding

In our study, we determined the dissociation constant of the PEP7/SIRK1 ectodomain (SIRK1-ECD) complex by microscale thermophoresis, as 19 µM, which is high compared with the  $K_d$  values of other ligand-receptor pairs, implying a low binding affinity of PEP7 to SRK1-ECD. However, the saturation of activation of SIRK1 by external PEP7 was reached at far lower concentrations than 19 µM (Figure 9A). When reviewing the  $K_d$  values of other ligand-receptor pairs, it is found that most of the  $K_d$  values detected by different assays are much lower. For example, the  $K_d$  for the binding of brassinolide to its receptor BRI1 was determined as 15 nM by immunoprecipitation (Wang et al., 2001). Scatchard plot suggested a  $K_d$  of 17 nM for the binding of CLAVATA3 to its receptor CLAVATA1 (Ogawa et al., 2008), a  $K_d$  of 33 nM was revealed for the binding of CLE41/44 to its receptor PXY by the use of isothermal titration calorimetry (Zhang et al., 2016b), and a  $K_d$  of about 1 µM for the binding of RALF to FERONIA was measured by microscale thermophoresis (Xiao et al., 2019). A particular example is the ligand-receptor pair of IDA and HAESA, where in the absence of the co-receptor SERK1, isothermal titration calorimetry detected a  $K_d$  value of 20 µM for receptor binding (Santiago et al., 2016). In contrast, in the presence of SERK1, the binding affinity of IDA-sensing HAESA increased approximately 60-fold (at which point the  $K_d$  value was 0.35 µM), indicating that the co-receptor SERK1 is involved in the specific recognition of the peptide ligand. Higher  $K_d$  values, as in the case of IDA, were obtained under conditions where the co-receptor (SERK1) was not present and was not part of the interaction. In that regard, the  $K_d$  value obtained here for the binding

of PEP7 to the receptor SIRK1-ECD is within the expected range, if the co-receptor QSK1 is required for high-affinity binding.

In fact, one important function of the co-receptor is to stabilize the interaction of the receptor with the ligand. The co-receptor ectodomain acts as a complementary shaped component that holds the ligand in place by interacting with the receptor (Santiago et al., 2013; Sun et al., 2013; Zhang et al., 2016a; Zhang et al., 2016b). The published results have already demonstrated the stabilizing signaling effect of the co-receptor QSK1 on the receptor SIRK1 (Wu et al., 2019). Thus, it is not surprising that lower binding affinity was found in our study when co-receptor was not present. Another point to note is that in our microscale thermophoresis binding assays, the receptor we used was only the isolated extracellular domain of SIRK1. Other results from our group have already specified the important role of the juxtamembrane domain and kinase domain of SIRK1 in its recruitment to co-receptor QSK1, which indicated the possible stable structure complex requirement (Xi, unpublished). Therefore, the use of SIRK1 with only the isolated ectodomain in the microscale thermophoresis assay may also result in low affinity for PEP7-SIRK1. In summary, the binding mechanism of PEP7-SIRK1 needs to be investigated in more detail, and the addition of co-receptor QSK1 in binding assays would be the next step in determining the  $K_d$  of the PEP7-SIRK1 system.

#### **4.4 The Possible Role(s) of the PEP7-SIRK1/QSK1-PIPs System in Plant Drought Tolerance**

According to our study, PEP7 was proven to be involved with signaling functions in abiotic stress responses. Our results revealed the regulatory function of PEP7-SIRK1 on aquaporins, established the novel signaling transduction system consisting of PEP7-SIRK1-PIPs, and verified the role of this system in regulating protoplasts water uptake by physiological approaches. This system directly regulates plant cells water uptake in the presence of sucrose, and this cellular-level physiological process also extends to affect plant morphogenesis. This was illustrated by our phenotypic experiments on primary root elongation.

Phenotypic experiments using mutants in soil provide evidence for a role of SIRK1 and QSK1 in plant responses to drought stress (section 3.1). The water-regulatory properties of SIRK1 and QSK1 at the whole-plant level may derive from their regulation of aquaporins at the cellular level. However, because the environmental conditions to which the whole plant was subjected were far more complex than cellular experiments, more studies on the plant-level responses of the SIRK1 signaling complex to abiotic stresses may be needed. First, we should incorporate PEP7 into the SIRK1 signaling complex and use respective mutants (*sirk1*, *pep7*, *qsk1*, *sirk1qsk*, *sirk1pep7* and *sirk1qsk1pep7*) in performing whole-plant level drought assays (only mutants of SIRK1 and its co-receptor QSK1 were involved in our experiments). In addition, the simulation of drought conditions should be more refined, for example, by using different molecular weights of PEG to create conditions that more precisely lead to water loss from different components of the cell.

When it comes to plant adversity physiology, such as drought and osmotic stress, we should have a broader view beyond focusing only on PEP7-SIRK1/QSK1-PIPs in Arabidopsis. Indeed, the PEP family is present in multiple plant species including crop plants (Huffaker et al., 2011; Huffaker et al., 2013; Trivilin et al.,



2014), and their activation status is predicted to be potentially involved in multifaceted roles (Lori et al., 2015). Sucrose, as a photosynthetic source product and metabolite of plants (Lemoine, 2000; Zimmermann and Milburn, 2012; Lemoine et al., 2013), is disrupted in its internal equilibrium in plants when they are exposed to drought stress (Saibo et al., 2009; Pinheiro and Chaves, 2011). For example, when wheat is subjected to moderate (non-lethal) drought stress, higher levels of metabolites, including sucrose, will accumulate in the body (Marček et al., 2019).

In the context of drought, many RLKs have been shown to be involved in plant drought resistance processes at different levels. For example, the LRR-RLK gene FON1 in rice phosphorylates a key component of the ABA signaling pathway, activating ABA signaling and initiating drought stress responses (Feng et al., 2014). The Arabidopsis homolog of the wheat LRK10 gene, LRK10L1.2, acts as a positive regulator of the drought response by closing stomata (Lim et al., 2015). OsSIK1 overexpression in rice inhibits stomatal development, reduces stomatal density in rice leaves, and promotes drought tolerance by reducing water loss (Ouyang et al., 2010). OsSIK2 improves drought tolerance by detoxification of reactive oxygen species (ROS) (Chen et al., 2013). Novel strategy has been proposed to optimize plant responses to drought stress by manipulating the activity of the RLK pathway and to support translational studies from model species (e.g. Arabidopsis) to economically useful crops (Marshall et al., 2012). Therefore, the role of PEP7-SIRK1/QSK1-PIPs system guided by sucrose content in crop stress resistance deserves extensive investigation.

## 5. Conclusions and Perspective

In conclusion, we herein identify PEP7, a member of the Plant Elicitor Peptide (PEP) family, as a ligand for the receptor kinase SIRK1. It forms a ligand-receptor pair with SIRK1 and affects water uptake in plant cells by regulating aquaporins.

1. We demonstrate that the mature peptide PEP7 is able to bind to the extra-membrane domain of SIRK1. The binding is consistent with a typical ligand-(LRR) receptor binding profile, and in the natural state the binding may require the involvement of the co-receptor QSK1.
2. We reveal the induction of PEP7 on the formation of signaling complexes involving SIRK1, QSK1, and aquaporins as substrates. PEP7 induces SIRK1 kinase activity, and induces aquaporin phosphorylation via SIRK1.
3. We found that PEP7 regulates protoplast water influx activity through SIRK1 and affects root growth. The lack of response of knockout mutants of receptor SIRK1 (*sirk1* and *sirk1pep7*) to external PEP7 treatment supports this conclusion.

Our results propose a novel small peptide (as ligand)-receptor pair and explore its biological functions. Small peptide-receptor systems in plants are of great interest, and the exploration of unknown members of such systems will help us to gain insight into plant growth, development and stress resistance mechanisms.

## 6. Supplementary Data

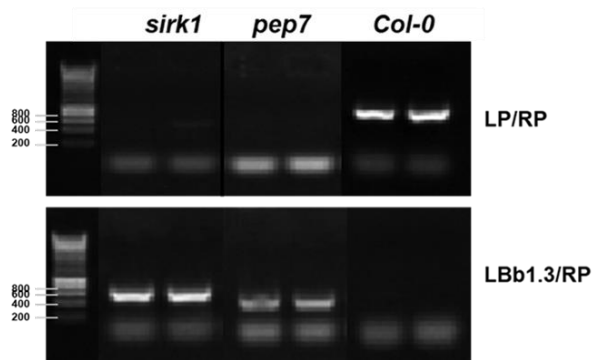


**Figure S1: Identification of double mutant of *sirk1pep7* as a result of crossing single mutants *sirk1* (SALK\_125543) and *pep7* (SALK\_025824).**

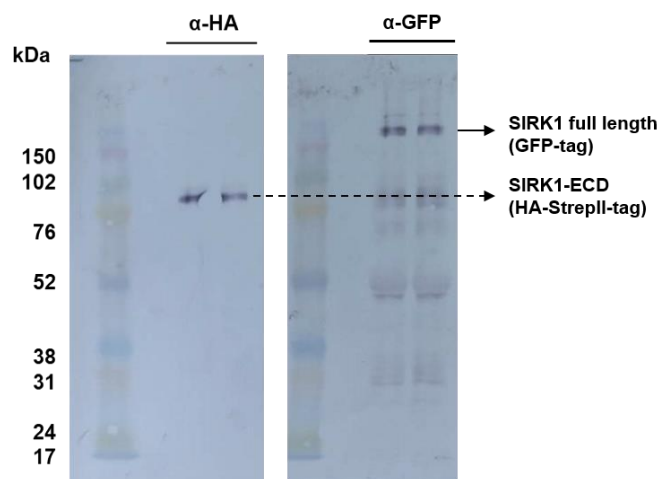


**Figure S2: Expression of SIRK1 was detected by western blotting.**

Western blotting was used to detect the expression of SIRK1. SIRK1-ECD protein was extracted and purified from transient expression in *Nicotiana benthamiana* and SIRK1-GFP protein was enriched from microsomal fraction.

**Table S1: Synthetic peptides used in the experiment.**

AGI	Name	Peptide sequence
AT5G09980	PEP4	GLPGKKNVLKKSRESSGKPGGTNKKPF
AT2G22000	PEP6	ITAVLRRRPRPPYSSGRPGQNN
AT5G09978	PEP7	VSGNVAARKGKQQTSSGKGGGTN
	PEP7-HIS	VSGNVAARKGKQQTSSGKGGGTNHHHHHH

**Table S2: Interaction partners recruited by SIRK1 under different treatments.**

Function	AGI	log <sub>2</sub> fold (suc vs control)	log <sub>2</sub> fold (PEP7 vs control)	suba	Function	AGI	log <sub>2</sub> fold (suc vs control)	log <sub>2</sub> fold (PEP7 vs control)	suba	
Photosynthesis	AT1G55490	1.4865	1.4457	P	lipid metabolism	AT4G33120	1.0607	1.5037	C,G	
	AT2G28000	1.5583	2.0824	P		AT4G36750	1.0667	0.8815	PM	
	AT3G60750	1.7614	1.8818	P		AT5G58800	1.0835	1.3029	C	
major CHO metabolism	AT4G29130	1.5685	1.1949	M		AT4G35790	1.1442	0.8678	PM	
	AT2G31390	1.7267	2.3396	C		AT1G24360	1.1722	0.869	P	
	AT5G20830	2.796	1.4938	C		AT5G42890	1.1875	1.1799	PX	
minor CHO metabolism	AT5G57655	1.1356	1.2825	ER		AT3G05420	1.3089	1.2574	C	
	AT1G70290	1.5207	0.8469	V,PM		AT1G80460	1.3959	1.0076	C	
	AT5G20250	2.2857	1.978	P		AT3G05970	1.4808	0.8175	PX	
glycolysis	AT5G56630	1.274	0.9187	C		AT3G15730	1.7167	1.5786	C	
	AT1G79550	1.3053	1.1374	C	AT3G06860	1.725	1.1327	PX		
	AT3G55440	1.311	1.4237	C	AT4G29010	1.8447	1.2908	PX		
	AT2G36530	1.644	1.7275	C	AT5G35360	1.8795	1.9272	P		
	AT1G20950	1.895	0.8164	C	AT1G48600	2.0801	1.8465	C		
	AT5G56350	1.9206	1.0309	C	AT4G26690	2.1926	2.0713	PM		
	AT3G14940	2.0904	0.8256	C	N- metabolism	AT5G07440	1.5187	0.9896	M	
	AT2G36580	2.7339	1.8299	C,PM		amino acid metabolism	AT2G31810	1.0794	1.0153	P
fermentation	AT1G54100	2.37	1.66	C	AT4G34200		1.1083	0.8184	P	
	OPP	AT1G12230	1.1584	1.1211	P		AT1G18500	1.1778	1.1761	P
		AT5G13420	1.5537	1.792	P		AT4G35630	1.3593	1.233	P
AT5G13110		1.6384	1.1036	P	AT1G14810		1.3645	1.0752	P	
TCA / org transformation	AT1G04410	1.1572	1.2778	PM	AT2G22250		1.4148	1.1329	P	
	AT3G13930	1.1644	1.3247	M	AT4G24830		1.45	1.7282	P	
	AT3G17240	1.2161	1.4281	M	AT4G13940		1.5122	1.0992	C	
	AT1G70410	1.2614	1.4569	C	AT5G04740		1.5315	1.5366	P	
	AT3G27380	1.5104	1.8686	M	AT2G36880		1.5591	0.9301	C	
	AT4G35260	1.7853	1.7105	M	AT1G64660	1.8738	1.7869	C		
	AT5G03290	2.4475	2.1096	M	AT2G33150	1.8859	1.85	PX		
mitochondrial electron transport / ATP synthesis	AT3G52730	1.0751	1.7193	M	AT5G19550	1.9294	1.7751	C		
	AT4G28510	1.2213	1.6342	M	metal handling	AT3G56240	1.1769	0.8745	C	
	AT5G05370	1.293	1.788	M		AT4G14030	1.4073	1.4877	C	
	ATMG00640	1.773	1.3435	M		AT5G23990	2.6163	1.9689	PM	
ATMG00480	2.326	1.9465	M	secondary metabolism	AT1G74020	1.1629	1.3225	V		
cell wall	AT3G10740	1.1299	1.0224		EX	AT5G47950	1.2516	1.5045	C	
	AT5G20950	1.304	0.9753		EX	AT2G25450	1.3544	1.2905	C	
	AT1G11580	1.3801	1.3749		EX	AT4G34050	1.5418	1.5739	C	
	AT1G63000	1.4325	1.4817		C	AT4G33360	1.5456	0.939	ER	
	AT3G48530	1.4813	1.2909	C	AT5G54160	1.8152	1.6482	C		
AT2G04780	1.5639	1.7082	EX,PM	misc	AT1G02920	1.0481	1.102	C		
hormone metabolism	AT3G11930	1.0952	0.986		C,N	AT1G66270	1.0766	1.1947	ER	
	AT2G22475	1.5473	1.5497		C	AT1G10290	1.0774	0.8345	PM	
	AT4G27450	1.6555	1.2871		C	AT5G64100	1.1126	0.9596	EX	
	AT3G22850	1.6831	1.2888		C	AT2G30860	1.1158	1.3214	C	
	AT3G15450	1.7359	1.8977		C	AT3G32980	1.1594	1.4959	EX	
	AT5G59530	1.8389	1.0741		C	AT2G30870	1.168	2.1318	C	
	AT5G43830	1.9312	2.0168		C	AT4G02520	1.1949	1.4855	C	
	AT1G52070	2.3641	1.3466		EX	AT4G38540	1.2594	0.9164	C	

Function	AGI	log <sub>2</sub> fold (suc vs control)	log <sub>2</sub> fold (PEP7 vs control)	suba	Function	AGI	log <sub>2</sub> fold (suc vs control)	log <sub>2</sub> fold (PEP7 vs control)	suba
stress	AT2G21620	1.1589	1.5088	C	misc	AT2G18980	1.3372	1.1567	EX
	AT2G01530	1.2009	1.2185	C		AT1G05250	1.3513	1.1024	EX
	AT3G17020	1.2574	1.2299	C,PM		AT4G30170	1.3547	1.06	EX
	AT5G56010	1.2907	1.3449	C		AT5G44380	1.3649	1.077	EX
	AT5G06320	1.3048	1.2351	PM		AT1G14830	1.3774	0.9117	C
	AT1G70850	1.331	1.0607	C		AT5G17820	1.4167	0.8953	EX
	AT4G24280	1.4436	1.4729	P		AT5G63840	1.4942	1.567	ER
	AT1G54410	1.4969	0.9523	C		AT2G14120	1.6324	1.0297	C
	AT3G53990	1.4994	1.514	C,PM		AT4G26010	1.6903	1.4255	EX
	AT1G09560	1.5169	1.496	EX		AT1G80410	1.7063	0.9742	N
	AT5G54430	1.609	1.9046	C		AT2G44790	1.9668	2.3215	PM
	AT1G30360	1.825	0.9365	PM		AT3G29250	1.9869	1.877	EX
	AT1G79930	1.9213	1.5406	C		AT1G78850	2.0133	1.3674	EX
redox	AT3G06050	1.1119	1.1579	M	nucleotide metabolism	AT3G54470	1.1645	0.958	C
	AT5G48810	1.2888	1.1675	ER		AT4G29690	1.6493	0.8288	V,PM
	AT3G54960	1.294	1.7089	ER		AT4G09320	1.8156	2.5849	C
	AT1G21750	1.3064	1.3028	ER	C1- metabolism	AT3G59970	1.3185	1.2558	C
	AT1G07890	1.3223	1.446	C		AT4G13930	2.1535	1.2146	C
	AT5G63030	1.6181	1.3177	C	cell	AT5G65020	1.1881	1.1979	C,PM
	AT1G45145	1.7828	1.5027	C		AT2G38750	2.0662	1.6339	C,PM
RNA	AT5G16840	1.1722	1.1495	C		AT3G61260	1.2512	1.161	PM
	AT3G49430	1.1735	0.9747	N		AT3G09740	1.3013	0.9896	PM
	AT2G45820	1.1987	1.2658	PM		AT3G11820	1.3473	1.0505	PM
	AT2G33340	1.323	1.1562	N		AT4G21450	1.4049	1.2375	PM
	AT5G58470	1.5811	1.1258	N		AT2G33120	1.4368	1.4281	PM
	AT3G13300	1.615	1.392	C	AT5G12370	1.5136	0.9256	PM	
	AT5G07350	1.6633	1.2421	N	AT3G52400	1.6143	1.4955	PM	
	AT5G61780	1.8036	1.357	N	AT4G23460	2.2133	1.0682	PM	
	AT1G76880	1.8212	1.2304	N	AT1G50010	1.0569	0.8809	C	
	AT4G17720	2.327	2.3784	C	AT5G09810	1.0589	1.1056	C	
DNA	AT3G42170	1.0631	1.0345	N	AT5G59880	1.2454	2.1339	C	
	AT5G59970	1.4131	1.0378	N	AT5G62700	1.2567	0.8719	C	
	AT5G63190	1.5116	0.9476	C	AT3G18780	1.3115	1.1745	C	
	AT5G10980	1.5421	0.9489	N	AT5G44340	1.38	1.0475	C	
	AT3G53110	1.5743	1.5813	C,N	AT3G53750	1.4077	0.8927	C	
	AT4G34490	1.6193	1.9125	C	AT4G30160	1.4135	1.3153	C	
	AT1G20960	1.6756	0.9868	N	AT1G20010	1.4291	1.1251	C	
development	AT5G66170	1.2231	1.777	C	AT4G20890	1.5024	1.2589	C	
	AT2G23810	1.2734	1.6675	PM	AT4G34450	1.6027	0.8237	C	
	AT2G44060	1.3123	1.1604	C	AT4G31480	1.6297	0.8312	C,G	
	AT2G41475	1.3342	1.3703	EX	AT1G35720	1.64	1.0707	PX	
	AT2G34040	1.3742	1.9314	C	AT3G09840	1.6444	1.415	C	
	AT4G21150	1.386	0.8221	PM	AT3G57890	1.7192	1.8803	C	
	AT2G19520	1.5989	1.1571	N	AT5G03540	1.7518	1.4348	C	
	AT2G17840	1.6288	0.9471	C	AT4G10840	1.8101	1.633	C	
	AT2G46140	1.6395	1.6225	C	AT1G23900	1.9483	1.1864	G	
	AT3G13870	1.6604	0.9452	ER,G	AT4G32150	2.2851	1.7999	V	

Function	AGI	log <sub>2</sub> fold (suc vs control)	log <sub>2</sub> fold (PEP7 vs control)	suba	Function	AGI	log <sub>2</sub> fold (suc vs control)	log <sub>2</sub> fold (PEP7 vs control)	suba
protein	AT3G06720	1.5916	1.2029	N	protein	AT1G72370	1.9803	1.3361	C
	AT3G23990	1.5992	2.0037	M		AT3G53020	2.0167	1.1527	C
	AT1G03230	1.6047	1.1851	EX		AT3G24830	2.0262	1.0455	C
	AT3G04920	1.6269	0.8236	C		AT2G32730	2.0525	1.4523	C,N
	AT1G78680	1.6327	1.2972	V		AT5G02870	2.0602	1.0083	C
	AT1G60780	1.635	1.154	C		AT5G09900	2.1397	1.7057	C,N
	AT1G09620	1.6408	1.2128	C		AT5G03850	2.1637	2.3322	C
	AT5G26710	1.6456	1.0833	C		AT3G53870	2.1926	1.1947	C
	AT4G19006	1.6459	1.8395	C,N		AT3G47370	2.2297	1.2392	C
	AT2G39390	1.6464	0.9219	C		AT1G03220	2.2863	1.6514	EX
	AT4G00100	1.6607	1.1099	C		AT2G44120	2.3828	0.9392	C
	AT3G25520	1.6752	0.8613	C		AT3G05560	2.4045	1.3331	C
	AT5G14670	1.6789	1.1803	C		AT5G16130	2.4405	1.5486	C
	AT2G19730	1.695	1.2452	C		AT5G53480	2.4482	1.3063	C,P,N
	AT5G05780	1.7079	1.2027	C,N		AT5G59850	2.4859	1.5788	C
	AT5G43010	1.7132	1.551	C,N		AT5G56710	2.5008	1.981	C
	AT5G59090	1.7176	1.3481	EX		AT2G23140	1.0471	1.2916	C
	AT2G34480	1.7887	1.3491	C		AT3G25800	1.05	1.5552	C
	AT3G02200	1.7894	1.2452	C,N		AT4G39200	1.0798	1.4297	C,N
	AT3G57290	1.7909	1.8507	C		AT1G10840	1.0859	1.1508	C
	AT5G27700	1.7964	1.6481	C		AT1G11910	1.095	1.1445	V
	AT1G33140	1.819	1.2123	C		AT5G27470	1.0981	0.9227	C
	AT1G67680	1.8372	1.18	N		AT3G46740	1.1005	1.0551	P
	AT2G30050	1.8635	2.0367	C,N		AT2G20630	1.1694	1.0972	C
	AT4G04460	1.8686	1.3966	V		AT4G38630	1.1822	1.0132	C
	AT1G57860	1.8721	0.9886	C		AT5G52650	1.1833	0.8866	C
	AT1G20200	1.8759	1.1249	C,N		AT4G20110	1.1933	0.8421	V
	AT2G31610	1.8969	1.1002	C		AT1G75950	1.1947	1.079	C
	AT3G62120	1.901	1.3526	C		AT3G56490	1.2178	1.0792	PX
	AT2G41840	1.9155	0.9385	C		AT4G20360	1.2357	1.7943	P
	AT1G29150	1.9615	1.5382	C,N		AT2G17980	1.2407	1.2677	PM
	AT4G24820	1.9626	1.7303	C,N		AT4G39090	1.2514	1.0063	V,N
	AT1G04270	1.9701	1.1497	C		AT1G79340	1.2618	1.038	C
	AT3G05590	2.6078	1.2315	C		AT3G19390	1.4221	0.8924	V,EX
	AT5G41520	1.2659	0.9949	C		AT4G20410	1.427	1.4088	PM
	AT3G13920	1.2846	1.2957	C		AT3G53890	1.4551	1.2653	C
	AT4G34555	1.2873	0.8511	C,N		AT2G14720	1.461	0.9433	V
	AT5G23540	1.2892	1.2883	C,N		AT2G37270	1.4666	0.9035	C
	AT1G12310	1.2936	1.2373	C		AT1G09270	1.5092	1.0475	N
	AT1G34750	1.3213	1.5013	C,PM		AT5G20890	1.515	1.1023	C
	AT5G67560	1.3239	1.0773	V,G		AT3G62250	1.521	1.4686	C
	AT4G16143	1.3371	0.9471	N		AT2G36070	1.5235	1.0987	M
	AT1G30690	1.3469	1.3108	C		AT1G25490	1.5465	1.5094	PM
	AT4G09800	1.3511	0.8595	C		AT3G58500	1.5481	1.092	C
	AT1G64520	1.352	1.5377	C,N		AT4G16190	1.5632	1.3648	V
	AT3G11710	1.3845	0.9267	C		AT3G56150	1.5676	0.9303	C,N
	AT3G03960	1.4007	1.0884	C		AT5G57870	1.579	1.3457	C,N
	AT3G18190	1.4025	1.0448	C		AT3G19760	1.5852	1.398	N

Function	AGI	log <sub>2</sub> fold (suc vs control)	log <sub>2</sub> fold (PEP7 vs control)	suba	Function	AGI	log <sub>2</sub> fold (suc vs control)	log <sub>2</sub> fold (PEP7 vs control)	suba	
signaling	AT3G20410	1.2154	1.0059	PM	transport	AT5G43350	2.6187	1.0245	PM	
	AT4G04720	1.4993	1.057	PM		AT1G75220	1.1756	0.8171	PM	
	AT3G57530	1.6154	0.8245	PM		AT1G11260	1.6124	1.183	PM	
	AT5G03520	1.5472	0.8293	PM		not assigned	AT3G12050	1.0472	1.2353	C
	AT2G44610	1.1572	0.8722	G			AT4G22310	1.0533	0.9964	M
	AT5G64260	1.1786	0.9254	EX			AT1G24310	1.0668	1.0651	N
	AT3G51550	2.2316	1.7501	PM			AT5G11680	1.1567	1.0327	PM
	AT3G14840	1.8829	1.3798	PM			AT5G10860	1.1945	0.8706	M
	AT3G02880	1.1885	1.1224	PM			AT4G21105	1.2001	1.5987	M
	AT5G16590	2.422	2.1715	PM			AT2G21160	1.2108	1.0187	ER
	AT5G65430	1.2823	1.4734	N			AT5G63910	1.2329	1.7831	V
	AT3G21630	1.2241	0.9701	PM			AT3G44100	1.2337	1.0268	EX
	AT3G54840	1.2936	1.0626	ER			AT5G41950	1.2735	1.0403	N
	AT4G17170	1.312	1.1422	ER			AT4G16450	1.31	1.2024	M
	AT4G38470	1.3414	0.8791	C			AT1G69340	1.3892	1.0517	C
	AT5G49760	1.1059	0.9766	PM			AT5G62740	1.4024	0.8685	PM
	AT3G28450	1.8744	1.5154	PM			AT3G11780	1.4093	1.1974	EX
	AT1G35670	1.3568	1.4447	C			AT3G01290	1.4447	1.039	PM
	AT3G24550	1.0543	0.8768	PM			AT2G01540	1.4728	1.4216	C
	AT1G18070	1.4079	1.597	C			AT2G47960	1.4985	1.4291	C
	AT2G21880	1.4896	0.837	C			AT2G17440	1.5082	1.0495	PM
	AT3G17410	1.5136	1.2937	C			AT5G51570	1.5242	1.0644	G
	AT3G57330	1.535	0.8694	V			AT2G43780	1.5296	1.9941	M
	AT5G38480	1.6256	1.8157	C			AT3G47200	1.5711	1.1495	C,PM
	AT1G35160	1.6551	1.922	C			AT4G38350	1.5781	0.9958	V
	AT5G16760	1.66	1.2788	C			AT5G23890	1.5926	0.9436	P
	AT4G35860	1.9731	1.7159	G			AT3G21140	1.7052	1.8942	P
	AT5G46070	2.0657	1.4269	C,N			AT1G71820	1.7329	0.8278	PM
	AT3G43300	2.0679	1.1513	C			AT2G39420	1.7821	1.6842	C
	transport	AT3G54540	1.2955	0.8693			C	AT4G24800	1.792	1.7695
AT3G08580		1.3095	1.1029	M	AT2G01690		1.8228	0.8379	C,N	
AT3G28715		1.3139	1.2709	V	AT5G54870		1.8379	1.7263	EX	
AT1G59870		2.0593	1.3356	PM	AT1G64090		1.9556	1.5239	ER	
AT2G47000		2.5103	1.5908	PM	AT5G39590	2.0104	1.6289	C		
AT3G26520		1.4523	1.1189	V	AT1G15130	2.0199	1.7463	N		
AT2G37180		1.0763	1.0849	PM	AT1G18270	2.059	1.501	PM,PX		
AT3G61430		1.188	1.0527	PM	AT5G19820	2.0851	1.6175	C		
AT1G64200		1.603	1.4501	V	AT5G26260	2.1905	1.7048	EX		
AT2G45960		1.2881	1.1265	PM	AT3G63460	2.4544	1.9596	C		
AT4G23400		1.6504	1.39	PM						
AT3G28710		1.6408	1.6498	V						
AT1G01620		1.1847	0.8893	PM						
AT2G37170		1.2676	0.9469	PM						
AT5G60660		1.4136	0.9003	PM						
AT1G19910		1.7983	1.4667	V						
AT5G59520		1.7253	1.3368	PM						
AT2G18960		1.3997	0.9233	PM						
AT5G57350		1.6564	0.8943	PM						

Note: SUBA annotation (C: cytosol; ER: endoplasmic reticulum; EX: extracellular; G: golgi; M: mitochondrion; N: nucleus; P: plastid; PM: plasma membrane; PX: peroxisome; V: vacuole).

**Table S3: List of identified phosphopeptides.**

Locus	Phospho (STY) Probabilities	Description/Name	Multiplicity	Amino acid
AT5G01530	NLAGDVIGT(0.817)RT(0.183)EAADAK		1	T
ATCG00020	T(1)AILERR	psbA	1	T
ATCG00270	T(1)IALGKFTK		1	T
ATCG00560	T(0.997)QS(0.003)NPNEQSVELNR		1	T
ATCG00570	T(0.996)IDRT(0.004)YPIFTVR		1	T
ATCG00710	AT(1)QT(1)VEDSSRSGPR		1	T
ATCG00710	AT(1)QT(1)VEDSSRSGPR		1	T
ATCG00710	AT(1)QT(1)VEDSSRSGPR		2	T
ATCG00710	AT(1)QT(1)VEDSSRSGPR		2	T
AT5G20280	INS(0.997)AES(0.003)MELWASQQK		1	S
AT1G74910	VS(0.083)S(0.917)FEALQPATR	At1g74910	1	S
AT1G35580	SVLDT(0.812)PLS(0.62)S(0.568)AR	CINV1	2	T
AT1G71710	S(0.002)YS(0.998)DPPS(1)PGR		2	S
AT1G71710	S(0.002)Y(0.001)S(0.997)DPPS(1)PGR		2	S
AT1G07110	S(0.001)LS(0.988)AS(0.009)S(0.001)FLIDTK	FKFBP	1	S
AT4G15530	GGMT(0.975)S(0.025)HAAVVAR		1	T
AT3G07330	S(0.096)S(0.096)S(0.763)DS(0.042)GLT(0.002)ELSK	CSLC6	1	S
AT1G53840	MDSVNS(1)FKGYGK	PME1	1	S
AT2G18730	MDS(1)PVSKTDASK	DGK3	1	S
AT4G11850	EVPVGT(0.001)VS(0.098)VY(0.002)NS(0.899)PR	PLDGAMMA1	1	S
AT1G37130	S(0.009)VS(0.943)T(0.048)PFMNTTAK		1	S
AT5G43830	VDS(0.945)S(0.055)QNWAGHI	At5g43830	1	S
AT3G10980	FGLGS(0.152)S(0.848)PK	F9F8.20	1	S
AT1G11310	SVENYPS(0.096)S(0.906)PS(0.998)PR	MLO2	1	S
AT2G17480	LGGDGS(0.003)AS(0.833)PT(0.118)AS(0.023)T(0.023)VR		1	S
AT1G11310	SVENYPS(0.096)S(0.906)PS(0.998)PR	MLO2	2	S
AT1G11310	SVENYPS(0.096)S(0.906)PS(0.998)PR	MLO2	2	S
AT2G26890	ILEIS(0.012)LNNVS(0.898)S(0.09)DDLNR	GRV2	1	S
AT3G08710	VTSIIDSVPES(1)PQRP	TRX9	1	S
AT2G38280	T(0.406)GS(0.594)FVRPIS(1)PK	AMPD	2	S
AT1G59610	QLS(1)IHDNR	DRP2B	1	S
AT1G59610	QSLs(0.997)EGS(0.003)LDK	DRP2B	1	S
AT1G59610	AT(0.193)S(0.806)PQPDGSSSTGGSLK	DRP2B	1	S
AT1G16610	RGRS(1)PPPPSK	SR45	1	S
AT1G16610	VS(0.031)S(0.969)PPKPVSAAPK	SR45	1	S
AT1G16610	GRS(0.999)PS(0.136)S(0.865)PPPRR	SR45	2	S
AT1G16610	GRS(0.999)PS(0.136)S(0.865)PPPRR	SR45	2	S
AT1G33990	TLS(1)DPFSNGK	MES14	1	S
AT1G51510	ANIESEAVDFEPEEDDLMDEEGTAIDGADVS(1)PR	Y14	1	S
AT1G80930	VIADKPS(1)DEEDDRQR	F23A5.29	1	S
AT5G04430	MESTESYAAGS(1)PEELAKR	BTR1	1	S
AT3G13570	GYNS(1)PPAKR	SCL30A	1	S
AT3G55460	GRS(1)PPPPPPR	SCL30	1	S
AT4G31580	ARS(1)PPPPR	RSZ22	1	S
AT5G52040	VAS(1)PENGAVR	RS41	1	S
AT2G37340	DRS(1)PVLDDDEGS(1)PKIIDGS(1)PPPS(1)PK	RS2Z33	2	S
AT2G37340	DRS(1)PVLDDDEGS(1)PKIIDGS(1)PPPS(1)PK	RS2Z33	2	S
AT2G37340	IIDGS(1)PPPS(1)PK	RS2Z33	2	S
AT2G37340	IIDGS(1)PPPS(1)PK	RS2Z33	2	S

Locus	Phospho (STY) Probabilities	Description/Name	Multiplicity	Amino acid
AT4G31580	RRS(1)PS(1)PPPAR	RSZ22	2	S
AT4G31580	RRS(1)PS(1)PPPAR	RSZ22	2	S
AT2G37340	DRS(1)PVLDDDEGS(1)PKIIDGS(1)PPPS(1)PK	RS2Z33	3	S
AT2G37340	DRS(1)PVLDDDEGS(1)PKIIDGS(1)PPPS(1)PK	RS2Z33	3	S
AT2G37340	IIDGS(1)PPPS(1)PK	RS2Z33	3	S
AT2G37340	IIDGS(1)PPPS(1)PK	RS2Z33	3	S
AT2G27100	S(0.292)GRT(0.333)S(0.38)EPNS(0.995)EDEAAGV GKR	SE	2	S
AT5G28040	AS(0.033)DQRDT(0.033)DFS(0.052)AES(0.882)PDL EEDGGGGGGGR	At5g28040	1	S
AT4G39680	SDS(0.012)S(0.107)VS(0.88)EDGPKER	At4g39680	1	S
AT5G07350	IGIWQYGDIES(1)DDEDTGPAR	Tudor1	1	S
AT1G77180	AS(0.083)GS(0.917)PPVPVMHS(0.95)PPRPVT(0.05) VK	SKIP	2	S
AT1G77180	AS(0.091)GS(0.909)PPVPVMHS(0.99)PPRPVT(0.01) VK	SKIP	2	S
AT3G60600	VTYVAPRPPS(0.999)PVHEGS(0.145)EEGS(0.512) S(0.344)PR	PVA11	2	S
AT3G60600	VT(0.001)YVAPRPPS(0.999)PVHEGS(0.998)EEGS (0.582)S(0.42)PR	PVA11	2	S
AT3G60600	VTYVAPRPPS(0.999)PVHEGS(0.145)EEGS(0.512) S(0.344)PR	PVA11	3	S
AT3G60600	VT(0.001)YVAPRPPS(0.999)PVHEGS(0.998)EEGS (0.582)S(0.42)PR	PVA11	3	S
AT1G64790	ALLEGGS(1)DDEGASTEAGQR	ILA	1	S
AT3G19420	VMAADASVFSFGDEDDFES(1)D		1	S
AT2G01470	IIMDPEKS(0.997)EDDDES(0.002)SSSSSSSR	STL2P	1	S
AT3G51800	S(0.986)S(0.986)DDERDEKELS(0.024)LT(0.003)S(0. 001)PEVVTK	EBP1	1	S
AT3G51800	S(0.986)S(0.986)DDERDEKELS(0.024)LT(0.003)S(0. 001)PEVVTK	EBP1	1	S
AT3G51800	S(0.986)S(0.986)DDERDEKELS(0.024)LT(0.003)S(0. 001)PEVVTK	EBP1	2	S
AT3G51800	S(0.986)S(0.986)DDERDEKELS(0.024)LT(0.003)S(0. 001)PEVVTK	EBP1	2	S
AT2G38140	IKIDIDESLFS(1)N		1	S
AT1G07320	YGVDAVEEEDDDEDET(1)EGS(1)EEA		1	S
AT1G07320	YGVDAVEEEDDDEDET(1)EEEA		1	T
AT1G07320	YGVDAVEEEDDDEDET(1)EGS(1)EEA		2	S
AT1G07320	YGVDAVEEEDDDEDET(1)EGS(1)EEA		2	T
AT1G15930	S(1)GDEAAPVVPPVPAEPAIPEDMDLMTALEL TLR	RPS12A	1	S
AT2G32060	S(1)GDEAVAAPVVPPVAEAAVIPEDMDVSTALE LTVR	RPS12C	1	S
AT5G08180	GS(0.998)DT(0.002)EAEKSIQK		1	S
AT3G06700	KHNVKAGENAS(1)AEE	RPL29A	1	S
AT3G09200	VEEKEES(1)DEEDYGGDFGLFDEE	RPP0B	1	S
AT3G11250	KEES(1)DEEDYEGGDFGLFDEE	RPP0C	1	S
AT1G01100	KKDEPAEES(1)DGDLGFLFD		1	S
AT4G00810	KDEPAEES(1)DGDLGFLFD	RPP1B	1	S
AT2G27720	KEEKEES(1)DDDMGFLFE		1	S
AT5G57290	KKEES(1)EEEEGDFGFLFD		1	S
AT1G26630	S(1)DDEHHFEASESGASK	ELF5A-2	1	S
AT1G69410	S(1)DDEHHFESSDAGASK	ELF5A-3	1	S
AT5G27640	DGEVS(1)DVEEDEYEAK		1	S
AT3G56150	Y(0.005)LQS(0.997)GS(0.997)EDDDDTDTKR	TIF3C1	2	S
AT3G56150	Y(0.005)LQS(0.997)GS(0.997)EDDDDTDTKR	TIF3C1	2	S
AT5G47880	Y(0.064)QLDMT(0.111)AFDS(0.825)EDGEALDDD S(1)E		2	S



Locus	Phospho (STY) Probabilities	Description/Name	Multiplicity	Amino acid
AT5G47880	Y(0.151)QLDMT(0.095)AFDS(0.754)EDGEALDDD S(1)E		2	S
AT2G45140	VVYVAPRPPS(0.897)PVREGS(0.445)EEGS(0.341) S(0.316)PR	PVA12	2	S
AT1G72160	SMIPQNLGS(0.998)FKEES(0.001)SK	PATL3	1	S
AT5G62810	S(0.161)AS(0.836)PPAAPADS(0.002)S(0.001)APPH PK	PEX14	1	S
AT1G68070	SRPGDLEAAQATNQDS(1)EDEDNDER	T23K23.8	1	S
AT1G68070	SSPES(0.988)PS(0.011)GSDSSTPLLR	T23K23.8	1	S
AT5G67385	T(0.006)S(0.006)S(0.005)S(0.005)T(0.002)IS(0.003)T( 0.009)NPS(0.198)S(0.75)PIS(0.011)T(0.003)ASTGKP PLPR		1	S
AT4G35470	S(0.002)DS(0.998)QSSLNFSER	PIRL4	1	S
AT1G05150	EMRDNDVPVS(0.063)Y(0.009)S(0.876)GS(0.051)G GPTK		1	S
AT1G19870	VEPEES(0.863)ES(0.137)DDVHVRK	IQD32	1	S
AT1G74690	SGGMLET(0.001)QNVGPEEIS(0.999)DDEIELPEG K	IQD31	1	S
AT2G32450	DNNVPVS(0.975)Y(0.003)S(0.018)GNGIPT(0.004)K		1	S
AT2G32450	EMRDNNVPVS(0.067)Y(0.023)S(0.831)GNGIPT(0.0 79)K		1	S
AT2G43680	S(0.039)LS(0.961)PKPFDR	IQD14	1	S
AT4G29900	S(0.135)GQFNNS(0.794)PRGEDKDVEAGT(0.031)S (0.02)S(0.02)FT(0.001)EYEDSPFDIASTK	ACA10	1	S
AT5G03040	QS(0.002)S(0.021)S(0.113)S(0.864)PPPALAPR	iqd2	1	S
AT5G37710	S(0.131)NS(0.869)GEFVLNDNVVPER	At5g37710	1	S
AT5G62390	EIAEGVTQIVQMLET(1)EEE	BAG7	1	T
AT2G43680	T(0.037)LS(0.963)PKPPS(1)PR	IQD14	2	S
AT2G43680	T(0.037)LS(0.963)PKPPS(1)PR	IQD14	2	S
AT2G03150	TVDVKQET(0.121)GS(0.867)PDT(0.012)K	emb1579	1	S
AT2G43130	S(1)DDDERGEEYLFK	RABA5C	1	S
AT3G22942	MEAGSSNS(0.02)S(0.977)GQLS(0.003)GR	GG2	1	S
AT3G17840	VFDLEDLLRAS(1)AEVLGK	RLK902	1	S
AT2G27060	IQNS(1)PDNPTSR	At2g27060	1	S
AT3G02880	LIEEVSHSS(0.001)GS(0.999)PNPVS(1)D	QSK1	1	S
AT3G02880	LIEEVSHSS(0.002)GS(0.998)PNPVS(1)D	QSK1	1	S
AT5G16590	SFGEFDLGLLKAS(1)AEVLGK	QSK2	1	S
AT3G17840	SYVNEYS(0.904)PS(0.096)AVK	RLK902	1	S
AT5G16590	LIEEVSRSPPAS(1)PGPLS(1)D	QSK2	1	S
AT5G16590	LIEEVSRSPPAS(1)PGPLS(1)D	QSK2	1	S
AT3G02880	LIEEVSHSS(0.001)GS(0.999)PNPVS(1)D	QSK1	2	S
AT3G02880	LIEEVSHSS(0.002)GS(0.998)PNPVS(1)D	QSK1	2	S
AT3G08680	AS(0.135)S(0.865)PEMIRS(0.198)S(0.166)DS(0.635) PV		2	S
AT3G08680	AS(0.461)S(0.539)PEMIRS(0.057)S(0.05)DS(0.893)P V		2	S
AT5G16590	LIEEVSRSPPAS(1)PGPLS(1)D	QSK2	2	S
AT5G16590	LIEEVSRSPPAS(1)PGPLS(1)D	QSK2	2	S
AT4G35310	NSLNIS(1)MRDA	CPK5	1	S
AT3G45780	S(0.085)S(0.085)GEMS(0.83)DGDVPGGR		1	S
AT5G41260	S(1)NPDVTGLDEEGRGESNDLPQFR		1	S
AT3G17420	SNAT(0.009)T(0.896)LPVT(0.048)QS(0.048)PR		1	T
AT3G08510	EVPS(1)FIQR	PLC2	1	S
AT3G13530	LAS(0.034)IS(0.966)GGLDQAPR	M3KE1	1	S
AT2G43790	VT(0.182)S(0.162)ES(0.162)DFMT(0.503)EY(0.986) VVT(0.005)R		2	Y
AT1G42550	S(0.822)GES(0.178)VDESENYLSDLGK		1	S

Locus	Phospho (STY) Probabilities	Description/Name	Multiplicity	Amino acid
AT5G20490	QQALAIS(0.776)PT(0.112)S(0.112)R	XI-K	1	S
AT2G45200	FTQGGYVDT(0.024)GS(0.835)PT(0.141)VGSGR		1	S
AT3G11820	AS(0.002)S(0.996)FIRGGT(0.002)DQLQTAR	SYP121	1	S
AT4G21450	YLAQQQGEGADS(1)V	PVA42	1	S
AT5G13850	LEEQKIDLDKPEVEDDDNDEDD(1)EDDDEAE GHDGEAGGR		1	S
AT3G63400	NFS(1)PGDVS(1)DREAK	CYP63	2	S
AT3G63400	NFS(1)PGDVS(1)DREAK	CYP63	2	S
AT3G63400	S(0.023)FRS(0.976)PS(0.959)PS(0.041)GVPK	CYP63	2	S
AT3G63400	S(0.17)FRS(0.846)PS(0.972)PS(0.012)GVPKR	CYP63	2	S
AT3G20550	GG(1)EEPVEEDSVAR	DDL	1	S
AT1G32400	AANTPAEYDS(1)DDEYLAPR		1	S
AT2G19520	MES(0.005)DEAAAVS(0.989)PQAT(0.004)T(0.001) PSGGTGASGPK	MSI4	1	S
AT4G11270	AAS(0.947)LS(0.017)T(0.017)S(0.017)KPSSSQEK	At4g11270	1	S
AT5G14120	REDQEPGLQT(1)PDLILS(1)EVEDEKPK	At5g14120	2	S
AT5G14120	REDQEPGLQT(1)PDLILS(1)EVEDEKPK	At5g14120	2	T
AT1G57990	QTTAEGSANPEPDQILS(1)PRR	PUP18	1	S
AT3G01390	MES(0.953)NRGQGS(0.047)IQQLLAAEVEAQHIV NAAR	VHA-G1	1	S
AT5G62670	GLDIETIQAYT(1)V		1	T
AT5G03280	SLSGEGGS(0.981)GT(0.288)GS(0.7)LS(0.031)R	EIN2	1	S
AT5G03280	SLSGEGGS(0.001)GT(0.052)GS(0.894)LS(0.052)R	EIN2	1	S
AT5G20650	S(0.066)S(0.066)S(0.866)GVS(0.003)APLIPK	COPT5	1	S
AT5G03280	SLSGEGGS(0.981)GT(0.288)GS(0.7)LS(0.031)R	EIN2	2	S
AT5G03280	SLSGEGGS(0.001)GT(0.052)GS(0.894)LS(0.052)R	EIN2	2	S
AT5G64410	ATADEFS(1)DEDTSPIEEVR	OPT4	1	S
AT5G27150	GFVFPVPGS(0.941)PT(0.057)ERNPPDLS(0.003)KA		1	S
AT4G23640	SIS(1)EANIAGSSR	POT3	1	S
AT5G09400	S(0.001)LES(0.994)DGNDDS(0.502)DS(0.502)EEDF PGSR		2	S
AT5G09400	SLES DGNDDS(1)DS(1)EEDFPGSR		2	S
AT5G09400	SLES DGNDDS(1)DS(1)EEDFPGSR		2	S
AT4G33530	ALES(1)DGDHNDT(1)DS(0.995)EDDT(0.004)T(0.00 1)LSR	POT13	3	S
AT4G33530	ALES(1)DGDHNDT(1)DS(0.999)EDDT(0.001)TLR	POT13	3	S
AT4G33530	ALES(1)DGDHNDT(1)DS(0.999)EDDT(0.001)TLR	POT13	3	T
AT1G17840	NGTQNTTVAPDGLTQS(0.014)PS(0.986)LR		1	S
AT1G59870	S(0.001)LS(0.97)T(0.03)ADGNR	ABCG36	1	S
AT2G39480	GFQEPS(0.119)S(0.881)PK	ABCB6	1	S
AT3G62700	SIS(1)IESPRQPK	ABCC14	1	S
AT3G62700	SIS(1)IESPRQPK	ABCC14	2	S
AT3G62700	S(0.001)IS(0.999)IES(1)PRQPK	ABCC14	2	S
AT2G39970	DQT(0.006)AAPES(0.826)PS(0.14)S(0.026)NAEALV AVEPRPYGT(0.001)FNT(0.001)IR		1	S
AT1G11260	FVEDGEY(0.004)GNALEM GKNS(0.941)NQAGT(0. 055)K	STP1	1	S
AT1G19450	S(1)FRDDNTEEGR		1	S
AT1G75220	S(1)FRDDNEEARNDLR		1	S
AT5G17010	S(0.001)S(0.002)GEIS(0.997)PEREPLIK		1	S
AT5G57110	TSLKKS(0.925)S(0.075)PGR	ACA8	1	S
AT5G57110	TSLKKS(0.128)S(0.872)PGR	ACA8	1	S
AT4G13510	RVEPRS(0.98)PS(0.755)PS(0.237)GANT(0.013)T(0.0 12)PT(0.003)PV	AMT1-1	2	S
AT4G13510	RVEPRS(0.978)PS(0.879)PS(0.149)GANT(0.45)T(0.4 82)PT(0.061)PV	AMT1-1	2	S

Locus	Phospho (STY) Probabilities	Description/Name	Multiplicity	Amino acid
AT5G43370	SLEELSGEAEVS(1)HDEK		1	S
AT3G58730	GIS(1)INAAR	VHA-D	1	S
AT4G30190	GLDIETPS(0.001)HYT(0.999)V	AHA2	1	T
AT2G16850	ALAS(1)FRS(1)NPT(1)N	PIP3B	1	S
AT3G53420	AS(0.019)GS(0.096)KS(0.885)LGS(1)FR	PIP2A	1	S
AT3G53420	SLGS(1)FRS(1)AANV	PIP2A	1	S
AT2G39010	S(1)QLHELHA	PIP2E	1	S
AT2G39010	TKDELTA(0.006)EEES(0.976)LS(0.019)GKDYLDPVPV	PIP2E	1	S
AT4G35100	ALGS(1)FRS(1)NAT(1)N	PIP3A	1	S
AT4G35100	ALGS(1)FRS(1)NAT(1)N	PIP3A	1	S
AT5G60660	ALGS(1)FGS(0.999)FGS(0.001)FR	PIP2F	1	S
AT5G60660	ALGS(1)FGS(0.002)FGS(0.998)FR	PIP2F	1	S
AT2G16850	ALAS(1)FRS(1)NPT(1)N	PIP3B	2	S
AT2G16850	ALAS(1)FRS(1)NPT(1)N	PIP3B	2	S
AT3G53420	AS(0.055)GS(0.055)KS(0.893)LGS(0.997)FR	PIP2A	2	S
AT3G53420	AS(0.019)GS(0.096)KS(0.885)LGS(1)FR	PIP2A	2	S
AT3G53420	SLGS(1)FRS(1)AANV	PIP2A	2	S
AT2G39010	S(1)QLHELHA	PIP2E	2	S
AT2G39010	TKDELTA(0.006)EEES(0.976)LS(0.019)GKDYLDPVPV	PIP2E	2	S
AT4G35100	ALGS(1)FRS(1)NAT(1)N	PIP3A	2	S
AT4G35100	ALGS(1)FRS(1)NAT(1)N	PIP3A	2	S
AT5G60660	ALGS(1)FGS(0.998)FGS(0.002)FR	PIP2F	2	S
AT5G60660	ALGS(1)FGS(0.999)FGS(0.001)FR	PIP2F	2	S
AT5G60660	ALGS(1)FGS(0.002)FGS(0.998)FR	PIP2F	2	S
AT5G60660	ALGS(0.873)FGS(0.127)FGS(0.012)FRS(0.989)FA	PIP2F	2	S
AT2G16850	ALAS(1)FRS(1)NPT(1)N	PIP3B	2	T
AT2G39010	T(0.006)KDELTA(0.994)EEES(0.954)LS(0.044)GKDY (0.001)LDPPPVK	PIP2E	2	T
AT4G35100	ALGS(1)FRS(1)NAT(1)N	PIP3A	2	T
AT2G16850	ALAS(1)FRS(1)NPT(1)N	PIP3B	3	S
AT2G16850	ALAS(1)FRS(1)NPT(1)N	PIP3B	3	S
AT4G35100	ALGS(1)FRS(1)NAT(1)N	PIP3A	3	S
AT4G35100	ALGS(1)FRS(1)NAT(1)N	PIP3A	3	S
AT2G16850	ALAS(1)FRS(1)NPT(1)N	PIP3B	3	T
AT4G35100	ALGS(1)FRS(1)NAT(1)N	PIP3A	3	T
AT3G48740	LGT(0.001)VS(0.059)S(0.925)PEPIS(0.016)VVR	SWEET11	1	S
AT5G23660	LGTLT(0.115)S(0.885)PEPVAITVVR		1	S
AT1G06890	ESEKDPLIAAENG(0.033)GVLS(0.967)DGGGGV QK		1	S
AT1G16860	KVS(1)GPLDSSGLMK		1	S
AT1G78880	QNS(1)GPIPLPTGLITSGPIT(0.219)S(0.724)GPLN S(0.044)S(0.012)GAPR	F9K20.7	1	S
AT2G07360	T(0.001)S(0.001)S(0.998)ISAGPGR	At2g07360	1	S
AT3G06550	ALLIEDGGGLQS(0.006)AS(0.994)PR		1	S
AT3G14120	MSQLELQEELS(0.097)S(0.903)P	NUP107	1	S
AT5G65687	S(0.005)NEVS(0.995)EDDEVEEDKLES(0.001)K		1	S
AT1G52200	GRVTPSEEDSNNGLPVQPGT(1)PNQR	PCR8	1	T
AT4G15610	GYET(0.025)KS(0.088)T(0.876)LDT(0.012)ER		1	T
AT1G78880	QNS(1)GPIPLPTGLITSGPIT(0.219)S(0.724)GPLN S(0.044)S(0.012)GAPR	F9K20.7	2	S
AT3G05090	GG(1)FLAGNLS(1)FNR	LRS1	2	S
AT3G05090	GG(1)FLAGNLS(1)FNR	LRS1	2	S

Locus	Phospho (STY) Probabilities	Description/Name	Multiplicity	Amino acid
AT3G06170	AGSS(0.001)TTFLS(0.999)PPS(0.562)S(0.438)PR	At3g06170	2	S
AT5G50640	S(0.063)LS(0.932)FS(0.029)GHS(0.976)FQGR		2	S
AT5G50640	S(0.141)LS(0.856)FS(0.007)GHS(0.996)FQGR		2	S
AT1G10140	IEEEEEETEEGS(1)VNP	At1g10140	1	S
AT1G15400	VS(1)PAVDPPS(1)PR		1	S
AT1G52220	AS(0.853)GES(0.127)S(0.02)DSSTDLDVVSTIQNV WDK		1	S
AT1G52780	VMS(0.995)ES(0.005)EMVSGAR	At1g52780	1	S
AT1G70770	MTAIDS(1)DDDGVV	F5A18.5	1	S
AT1G70770	SNGYGDDGYDFDGS(1)DDEIATLK	F5A18.5	1	S
AT1G76850	LIT(0.008)ES(0.068)S(0.068)GS(0.79)PS(0.068)KAE K	SEC5A	1	S
AT1G80180	VS(1)PAVDPPS(1)PR		1	S
AT2G04410	S(0.001)DS(0.999)PGKDEPGYNK	At2g04410	1	S
AT2G30930	AT(0.003)S(0.995)ALS(0.002)EAK		1	S
AT2G42975	TQLDLLEQLTSTSDGYLS(0.992)DGGGS(0.008)R		1	S
AT3G27390	SSNAIS(0.051)AS(0.806)PPLT(0.142)ER		1	S
AT3G49590	IIT(0.042)DY(0.037)VGS(0.783)PAT(0.137)DPMR	T9C5.180	1	S
AT4G18070	SQGDKES(1)DDGVNER	At4g18070	1	S
AT5G40450	SSHTT(0.003)KPS(0.131)S(0.862)PT(0.004)	At5g40450	1	S
AT5G41950	NLS(0.958)GKAET(0.038)MS(0.002)T(0.001)NVER K	At5g41950	1	S
AT1G15400	VS(1)PAVDPPS(1)PR		2	S
AT1G15400	VS(1)PAVDPPS(1)PR		2	S
AT1G45688	T(0.005)DS(0.008)EVT(0.051)S(0.055)LAAS(0.424)S (0.472)PARS(0.985)PR		2	S
AT1G56230	S(0.003)LS(0.997)EIS(1)EVD AVR	At1g56230	2	S
AT1G56230	S(0.003)LS(0.997)EIS(1)EVD AVR	At1g56230	2	S
AT1G80180	VS(1)PAVDPPS(1)PR		2	S
AT1G80180	VS(1)PAVDPPS(1)PR		2	S
AT4G31130	S(1)IDGNS(0.511)S(0.424)S(0.065)RDVNK		2	S
AT4G32285	S(1)FGDVNEIGAREEK		1	S
AT1G15280	ATSEAEYES(1)DPEELNR	At1g15280	1	S
AT4G22670	SFVVEES(1)DDDMDETEEVKPK		1	S

## 7. Bibliography

- Alberts, B., Johnson, A., Lewis, J., Raff, M., Roberts, K., and Walter, P. (2002a). Signaling in plants. In *Molecular Biology of the Cell*. 4th edition (Garland Science).
- Alberts, B., Johnson, A., Lewis, J., Raff, M., Roberts, K., and Walter, P. (2002b). Signaling through enzyme-linked cell-surface receptors. In *Molecular Biology of the Cell*. 4th edition (Garland Science).
- Anderson, C.M., Wagner, T.A., Perret, M., He, Z.-H., He, D., and Kohorn, B.D. (2001). WAKs: cell wall-associated kinases linking the cytoplasm to the extracellular matrix. In *Plant Cell Walls* (Springer), pp. 197-206.
- Araya, T., Miyamoto, M., Wibowo, J., Suzuki, A., Kojima, S., Tsuchiya, Y.N., Sawa, S., Fukuda, H., Von Wirén, N., and Takahashi, H. (2014). CLE-CLAVATA1 peptide-receptor signaling module regulates the expansion of plant root systems in a nitrogen-dependent manner. *Proceedings of the National Academy of Sciences* 111, 2029-2034.
- Bai, L., Zhang, G., Zhou, Y., Zhang, Z., Wang, W., Du, Y., Wu, Z., and Song, C.P. (2009). Plasma membrane-associated proline-rich extensin-like receptor kinase 4, a novel regulator of Ca<sup>2+</sup> signalling, is required for abscisic acid responses in *Arabidopsis thaliana*. *The Plant Journal* 60, 314-327.
- Balagué, C., Gouget, A., Bouchez, O., Souriac, C., Haget, N., Boutet-Mercey, S., Govers, F., Roby, D., and Canut, H. (2017). The *Arabidopsis thaliana* lectin receptor kinase LecRK-I. 9 is required for full resistance to *Pseudomonas syringae* and affects jasmonate signalling. *Molecular plant pathology* 18, 937-948.
- Bartels, S., and Boller, T. (2015). Quo vadis, Pep? Plant elicitor peptides at the crossroads of immunity, stress, and development. *Journal of experimental botany* 66, 5183-5193.
- Bartels, S., Lori, M., Mbengue, M., van Verk, M., Klauser, D., Hander, T., Böni, R., Robotzek, S., and Boller, T. (2013). The family of Peps and their precursors in *Arabidopsis*: differential expression and localization but similar induction of pattern-triggered immune responses. *Journal of experimental botany* 64, 5309-5321.
- Becraft, P.W. (2002). Receptor kinase signaling in plant development. *Annual review of cell and developmental biology* 18, 163-192.
- Bemis, S.M., Lee, J.S., Shpak, E.D., and Torii, K.U. (2013). Regulation of floral patterning and organ identity by *Arabidopsis* ERECTA-family receptor kinase genes. *Journal of experimental botany* 64, 5323-5333.
- Boller, T., and Felix, G. (2009). A renaissance of elicitors: perception of microbe-associated molecular patterns and danger signals by pattern-recognition receptors. *Annual review of plant biology* 60, 379-406.
- Bradford, M.M. (1976). A rapid and sensitive method for the quantitation of microgram quantities of protein utilizing the principle of protein-dye binding. *Analytical biochemistry* 72, 248-254.
- Brand, U., Fletcher, J.C., Hobe, M., Meyerowitz, E.M., and Simon, R. (2000). Dependence of stem cell fate in *Arabidopsis* on a feedback loop regulated by CLV3 activity. *Science* 289, 617-619.
- Butenko, M.A., Vie, A.K., Brembu, T., Aalen, R.B., and Bones, A.M. (2009). Plant peptides in signalling: looking for new partners. *Trends in plant science* 14, 255-263.

- Butenko, M.A., Patterson, S.E., Grini, P.E., Stenvik, G.-E., Amundsen, S.S., Mandal, A., and Aalen, R.B. (2003). Inflorescence deficient in abscission controls floral organ abscission in *Arabidopsis* and identifies a novel family of putative ligands in plants. *The Plant Cell* 15, 2296-2307.
- Caspar, T., Huber, S.C., and Somerville, C. (1985). Alterations in growth, photosynthesis, and respiration in a starchless mutant of *Arabidopsis thaliana* (L.) deficient in chloroplast phosphoglucomutase activity. *Plant Physiology* 79, 11-17.
- Chakraborty, S., Nguyen, B., Wasti, S.D., and Xu, G. (2019). Plant leucine-rich repeat receptor kinase (LRR-RK): structure, ligand perception, and activation mechanism. *Molecules* 24, 3081.
- Chen, L.-J., Wuriyangan, H., Zhang, Y.-Q., Duan, K.-X., Chen, H.-W., Li, Q.-T., Lu, X., He, S.-J., Ma, B., and Zhang, W.-K. (2013). An S-domain receptor-like kinase, OsSIK2, confers abiotic stress tolerance and delays dark-induced leaf senescence in rice. *Plant Physiology* 163, 1752-1765.
- Chen, L.-Q., Qu, X.-Q., Hou, B.-H., Sosso, D., Osorio, S., Fernie, A.R., and Frommer, W.B. (2012). Sucrose efflux mediated by SWEET proteins as a key step for phloem transport. *Science* 335, 207-211.
- Chinchilla, D., Bauer, Z., Regenass, M., Boller, T., and Felix, G. (2006). The *Arabidopsis* receptor kinase FLS2 binds flg22 and determines the specificity of flagellin perception. *The Plant Cell* 18, 465-476.
- Clark, S.E., Williams, R.W., and Meyerowitz, E.M. (1997). The *CLAVATA1* gene encodes a putative receptor kinase that controls shoot and floral meristem size in *Arabidopsis*. *Cell* 89, 575-585.
- Clark, S.E., Jacobsen, S.E., Levin, J.Z., and Meyerowitz, E.M. (1996). The *CLAVATA* and *SHOOT MERISTEMLESS* loci competitively regulate meristem activity in *Arabidopsis*. *Development* 122, 1567-1575.
- Cock, J.M., Vanoosthuysse, V., and Gaude, T. (2002). Receptor kinase signalling in plants and animals: distinct molecular systems with mechanistic similarities. *Current opinion in cell biology* 14, 230-236.
- Cox, J., and Mann, M. (2008). MaxQuant enables high peptide identification rates, individualized ppb-range mass accuracies and proteome-wide protein quantification. *Nature biotechnology* 26, 1367-1372.
- Cox, J., Neuhauser, N., Michalski, A., Scheltema, R.A., Olsen, J.V., and Mann, M. (2011). Andromeda: a peptide search engine integrated into the MaxQuant environment. *Journal of proteome research* 10, 1794-1805.
- Cox, J., Hein, M.Y., Lubner, C.A., Paron, I., Nagaraj, N., and Mann, M. (2014). Accurate proteome-wide label-free quantification by delayed normalization and maximal peptide ratio extraction, termed MaxLFQ. *Molecular & cellular proteomics* 13, 2513-2526.
- Delay, C., Imin, N., and Djordjevic, M.A. (2013). CEP genes regulate root and shoot development in response to environmental cues and are specific to seed plants. *Journal of experimental botany* 64, 5383-5394.
- Demir, F., Horntrich, C., Blachutzyk, J.O., Scherzer, S., Reinders, Y., Kierszniowska, S., Schulze, W.X., Harms, G.S., Hedrich, R., and Geiger, D. (2013). *Arabidopsis* nanodomain-delimited ABA signaling pathway regulates the anion channel SLAH3. *Proceedings of the National Academy of Sciences* 110, 8296-8301.

- Diévar, A., and Clark, S.E. (2003). Using mutant alleles to determine the structure and function of leucine-rich repeat receptor-like kinases. *Current opinion in plant biology* 6, 507-516.
- Diévar, A., and Clark, S.E. (2004). LRR-containing receptors regulating plant development and defense. *Development* 131, 251-261.
- Dong, S., Lau, V., Song, R., Ierullo, M., Esteban, E., Wu, Y., Sivieng, T., Nahal, H., Gaudinier, A., and Pasha, A. (2019). Proteome-wide, structure-based prediction of protein-protein interactions/new molecular interactions viewer. *Plant physiology* 179, 1893-1907.
- Dunham, W.H., Mullin, M., and Gingras, A.C. (2012). Affinity-purification coupled to mass spectrometry: Basic principles and strategies. *Proteomics* 12, 1576-1590.
- Durek, P., Schmidt, R., Heazlewood, J.L., Jones, A., MacLean, D., Nagel, A., Kersten, B., and Schulze, W.X. (2010). PhosPhAt: the Arabidopsis thaliana phosphorylation site database. An update. *Nucleic acids research* 38, D828-D834.
- Endo, S., Betsuyaku, S., and Fukuda, H. (2014). Endogenous peptide ligand–receptor systems for diverse signaling networks in plants. *Current opinion in plant biology* 21, 140-146.
- Entzian, C., and Schubert, T. (2016). Studying small molecule–aptamer interactions using microscale thermophoresis (MST). *Methods* 97, 27-34.
- Escobar-Restrepo, J.-M., Huck, N., Kessler, S., Gagliardini, V., Gheyselinck, J., Yang, W.-C., and Grossniklaus, U. (2007). The FERONIA receptor-like kinase mediates male-female interactions during pollen tube reception. *Science* 317, 656-660.
- Escocard de Azevedo Manhães, A.M., Ortiz-Moreira, F.A., He, P., and Shan, L. (2021). Plant plasma membrane-resident receptors: Surveillance for infections and coordination for growth and development. *Journal of Integrative Plant Biology* 63, 79-101.
- Feng, L., Gao, Z., Xiao, G., Huang, R., and Zhang, H. (2014). Leucine-rich repeat receptor-like kinase FON1 regulates drought stress and seed germination by activating the expression of ABA-responsive genes in rice. *Plant molecular biology reporter* 32, 1158-1168.
- Fletcher, J.C., Brand, U., Running, M.P., Simon, R., and Meyerowitz, E.M. (1999). Signaling of cell fate decisions by CLAVATA3 in Arabidopsis shoot meristems. *Science* 283, 1911-1914.
- Flury, P., Klauser, D., Schulze, B., Boller, T., and Bartels, S. (2013). The anticipation of danger: microbe-associated molecular pattern perception enhances AtPep-triggered oxidative burst. *Plant Physiology* 161, 2023-2035.
- Fukuda, H., and Higashiyama, T. (2011). *Diverse functions of plant peptides: entering a new phase* (Oxford University Press).
- Gou, X., He, K., Yang, H., Yuan, T., Lin, H., Clouse, S.D., and Li, J. (2010). Genome-wide cloning and sequence analysis of leucine-rich repeat receptor-like protein kinase genes in Arabidopsis thaliana. *BMC genomics* 11, 1-15.
- Grisson, M.S., Kirk, P., Brault, M.L., Wu, X.N., Schulze, W.X., Benitez-Alfonso, Y., Immel, F., and Bayer, E.M. (2019). Plasma membrane-associated receptor-like kinases relocate to plasmodesmata in response to osmotic stress. *Plant physiology* 181, 142-160.
- Gully, K., Hander, T., Boller, T., and Bartels, S. (2015). Perception of Arabidopsis AtPep peptides, but not bacterial elicitors, accelerates starvation-induced senescence. *Frontiers in plant science* 6, 14.

- Hander, T., Fernández-Fernández, Á.D., Kumpf, R.P., Willems, P., Schatowitz, H., Rombaut, D., Staes, A., Nolf, J., Pottie, R., and Yao, P. (2019). Damage on plants activates Ca<sup>2+</sup>-dependent metacaspases for release of immunomodulatory peptides. *Science* 363.
- Hara, K., Kajita, R., Torii, K.U., Bergmann, D.C., and Kakimoto, T. (2007). The secretory peptide gene EPF1 enforces the stomatal one-cell-spacing rule. *Genes & development* 21, 1720-1725.
- Hartmann, J., Stührwohldt, N., Dahlke, R.I., and Sauter, M. (2013). Phytosulfokine control of growth occurs in the epidermis, is likely to be non-cell autonomous and is dependent on brassinosteroids. *The Plant Journal* 73, 579-590.
- Haruta, M., Sabat, G., Stecker, K., Minkoff, B.B., and Sussman, M.R. (2014). A peptide hormone and its receptor protein kinase regulate plant cell expansion. *Science* 343, 408-411.
- Hazak, O., and Hardtke, C.S. (2016). CLAVATA 1-type receptors in plant development. *Journal of experimental botany* 67, 4827-4833.
- He, Y., Zhou, J., Shan, L., and Meng, X. (2018). Plant cell surface receptor-mediated signaling—a common theme amid diversity. *Journal of cell science* 131.
- He, Z., Wang, Z.-Y., Li, J., Zhu, Q., Lamb, C., Ronald, P., and Chory, J. (2000). Perception of brassinosteroids by the extracellular domain of the receptor kinase BRI1. *Science* 288, 2360-2363.
- Heil, M. (2012). Damaged-self recognition as a general strategy for injury detection. *Plant Signaling & Behavior* 7, 576-580.
- Hobe, M., Müller, R., Grünwald, M., Brand, U., and Simon, R. (2003). Loss of CLE40, a protein functionally equivalent to the stem cell restricting signal CLV3, enhances root waving in *Arabidopsis*. *Development genes and evolution* 213, 371-381.
- Hohmann, U., Lau, K., and Hothorn, M. (2017). The structural basis of ligand perception and signal activation by receptor kinases. *Annual review of plant biology* 68, 109-137.
- Hohmann, U., Santiago, J., Nicolet, J., Olsson, V., Spiga, F.M., Hothorn, L.A., Butenko, M.A., and Hothorn, M. (2018). Mechanistic basis for the activation of plant membrane receptor kinases by SERK-family coreceptors. *Proceedings of the National Academy of Sciences* 115, 3488-3493.
- Hu, Z., Zhang, H., and Shi, K. (2018). Plant peptides in plant defense responses. *Plant signaling & behavior* 13, e1475175.
- Huffaker, A. (2015). Plant elicitor peptides in induced defense against insects. *Current opinion in insect science* 9, 44-50.
- Huffaker, A., and Ryan, C.A. (2007). Endogenous peptide defense signals in *Arabidopsis* differentially amplify signaling for the innate immune response. *Proceedings of the National Academy of Sciences* 104, 10732-10736.
- Huffaker, A., Pearce, G., and Ryan, C.A. (2006). An endogenous peptide signal in *Arabidopsis* activates components of the innate immune response. *Proceedings of the National Academy of Sciences* 103, 10098-10103.
- Huffaker, A., Dafoe, N.J., and Schmelz, E.A. (2011). ZmPep1, an ortholog of *Arabidopsis* elicitor peptide 1, regulates maize innate immunity and enhances disease resistance. *Plant physiology* 155, 1325-1338.
- Huffaker, A., Pearce, G., Veyrat, N., Erb, M., Turlings, T.C., Sartor, R., Shen, Z., Briggs, S.P., Vaughan, M.M., and Alborn, H.T. (2013). Plant elicitor peptides are conserved signals regulating direct and indirect antiherbivore defense. *Proceedings of the National Academy of Sciences* 110, 5707-5712.



- Iizasa, E.i., Mitsutomi, M., and Nagano, Y. (2010). Direct binding of a plant LysM receptor-like kinase, LysM RLK1/CERK1, to chitin in vitro. *Journal of Biological Chemistry* 285, 2996-3004.
- Janda, M., Lamparová, L., Zubíková, A., Burketová, L., Martinec, J., and Krčková, Z. (2019). Temporary heat stress suppresses PAMP-triggered immunity and resistance to bacteria in *Arabidopsis thaliana*. *Molecular plant pathology* 20, 1005-1012.
- Jerabek-Willemsen, M., Wienken, C.J., Braun, D., Baaske, P., and Duhr, S. (2011). Molecular interaction studies using microscale thermophoresis. *Assay and drug development technologies* 9, 342-353.
- Jerabek-Willemsen, M., André, T., Wanner, R., Roth, H.M., Duhr, S., Baaske, P., and Breitsprecher, D. (2014). MicroScale Thermophoresis: Interaction analysis and beyond. *Journal of Molecular Structure* 1077, 101-113.
- Jing, Y., Shen, N., Zheng, X., Fu, A., Zhao, F., Lan, W., and Luan, S. (2020). Danger-associated peptide regulates root immune responses and root growth by affecting ros formation in *Arabidopsis*. *International journal of molecular sciences* 21, 4590.
- Jing, Y., Zheng, X., Zhang, D., Shen, N., Wang, Y., Yang, L., Fu, A., Shi, J., Zhao, F., and Lan, W. (2019). Danger-associated peptides interact with PIN-dependent local auxin distribution to inhibit root growth in *Arabidopsis*. *The Plant Cell* 31, 1767-1787.
- Jinn, T.-L., Stone, J.M., and Walker, J.C. (2000). HAESA, an *Arabidopsis* leucine-rich repeat receptor kinase, controls floral organ abscission. *Genes & development* 14, 108-117.
- Jun, J.H., Fiume, E., and Fletcher, J. (2008). The CLE family of plant polypeptide signaling molecules. *Cellular and Molecular Life Sciences* 65, 743-755.
- Kapila, J., De Rycke, R., Van Montagu, M., and Angenon, G. (1997). An *Agrobacterium*-mediated transient gene expression system for intact leaves. *Plant science* 122, 101-108.
- Keilhauer, E.C., Hein, M.Y., and Mann, M. (2015). Accurate protein complex retrieval by affinity enrichment mass spectrometry (AE-MS) rather than affinity purification mass spectrometry (AP-MS). *Molecular & Cellular Proteomics* 14, 120-135.
- Klauser, D., Desurmont, G.A., Glauser, G., Vallat, A., Flury, P., Boller, T., Turlings, T.C., and Bartels, S. (2015). The *Arabidopsis* Pep-PEPR system is induced by herbivore feeding and contributes to JA-mediated plant defence against herbivory. *Journal of Experimental Botany* 66, 5327-5336.
- Krol, E., Mentzel, T., Chinchilla, D., Boller, T., Felix, G., Kemmerling, B., Postel, S., Arents, M., Jeworutzki, E., and Al-Rasheid, K.A. (2010). Perception of the *Arabidopsis* danger signal peptide 1 involves the pattern recognition receptor AtPEPR1 and its close homologue AtPEPR2. *Journal of Biological Chemistry* 285, 13471-13479.
- Lease, K.A., and Walker, J.C. (2006). The *Arabidopsis* unannotated secreted peptide database, a resource for plant peptidomics. *Plant physiology* 142, 831-838.
- Lee, J.S., Kuroha, T., Hnilova, M., Khatayevich, D., Kanaoka, M.M., McAbee, J.M., Sarikaya, M., Tamerler, C., and Torii, K.U. (2012). Direct interaction of ligand-receptor pairs specifying stomatal patterning. *Genes & development* 26, 126-136.
- Lemoine, R. (2000). Sucrose transporters in plants: update on function and structure. *Biochimica et Biophysica Acta (BBA)-Biomembranes* 1465, 246-262.
- Lemoine, R., La Camera, S., Atanassova, R., Dédaldéchamp, F., Allario, T., Pourtau, N., Bonnemain, J.-L., Laloi, M., Coutos-Thévenot, P., and Maurousset, L. (2013). Source-to-sink transport of sugar and regulation by environmental factors. *Frontiers in plant science* 4, 272.

- Li, J., and Chory, J. (1997). A putative leucine-rich repeat receptor kinase involved in brassinosteroid signal transduction. *Cell* 90, 929-938.
- Lim, C.W., Yang, S.H., Shin, K.H., Lee, S.C., and Kim, S.H. (2015). The AtLRK10L1. 2, Arabidopsis ortholog of wheat LRK10, is involved in ABA-mediated signaling and drought resistance. *Plant cell reports* 34, 447-455.
- Lindsey, K., Casson, S., and Chilley, P. (2002). Peptides: new signalling molecules in plants. *Trends in plant science* 7, 78-83.
- Liu, T., Liu, Z., Song, C., Hu, Y., Han, Z., She, J., Fan, F., Wang, J., Jin, C., and Chang, J. (2012). Chitin-induced dimerization activates a plant immune receptor. *science* 336, 1160-1164.
- Lori, M., Van Verk, M.C., Hander, T., Schatowitz, H., Klauser, D., Flury, P., Gehring, C.A., Boller, T., and Bartels, S. (2015). Evolutionary divergence of the plant elicitor peptides (Peps) and their receptors: interfamily incompatibility of perception but compatibility of downstream signalling. *Journal of experimental botany* 66, 5315-5325.
- Ma, Y., Zhao, Y., Walker, R.K., and Berkowitz, G.A. (2013). Molecular steps in the immune signaling pathway evoked by plant elicitor peptides: Ca<sup>2+</sup>-dependent protein kinases, nitric oxide, and reactive oxygen species are downstream from the early Ca<sup>2+</sup> signal. *Plant Physiology* 163, 1459-1471.
- Mahmood, T., and Yang, P.-C. (2012). Western blot: technique, theory, and trouble shooting. *North American journal of medical sciences* 4, 429.
- Marček, T., Hamow, K.Á., Véghe, B., Janda, T., and Darko, E. (2019). Metabolic response to drought in six winter wheat genotypes. *PloS one* 14, e0212411.
- Marshall, A., Aalen, R.B., Audenaert, D., Beeckman, T., Broadley, M.R., Butenko, M.A., Caño-Delgado, A.I., de Vries, S., Dresselhaus, T., and Felix, G. (2012). Tackling drought stress: receptor-like kinases present new approaches. *The Plant Cell* 24, 2262-2278.
- Matsubayashi, Y. (2003). Ligand-receptor pairs in plant peptide signaling. *Journal of cell science* 116, 3863-3870.
- Matsubayashi, Y. (2011). Small post-translationally modified peptide signals in Arabidopsis. *The Arabidopsis book/American Society of Plant Biologists* 9.
- Matsubayashi, Y. (2014). Posttranslationally modified small-peptide signals in plants. *Annual review of plant biology* 65, 385-413.
- Matsubayashi, Y., and Sakagami, Y. (1996). Phytosulfokine, sulfated peptides that induce the proliferation of single mesophyll cells of *Asparagus officinalis* L. *Proceedings of the National Academy of Sciences* 93, 7623-7627.
- Matsubayashi, Y., Ogawa, M., Morita, A., and Sakagami, Y. (2002). An LRR receptor kinase involved in perception of a peptide plant hormone, phytosulfokine. *Science* 296, 1470-1472.
- Michel, B.E., and Kaufmann, M.R. (1973). The osmotic potential of polyethylene glycol 6000. *Plant physiology* 51, 914-916.
- Money, N.P. (1989). Osmotic pressure of aqueous polyethylene glycols: relationship between molecular weight and vapor pressure deficit. *Plant physiology* 91, 766-769.
- Moore, J.P., Vicré-Gibouin, M., Farrant, J.M., and Driouich, A. (2008). Adaptations of higher plant cell walls to water loss: drought vs desiccation. *Physiologia plantarum* 134, 237-245.

- Nakaminami, K., Okamoto, M., Higuchi-Takeuchi, M., Yoshizumi, T., Yamaguchi, Y., Fukao, Y., Shimizu, M., Ohashi, C., Tanaka, M., and Matsui, M. (2018). AtPep3 is a hormone-like peptide that plays a role in the salinity stress tolerance of plants. *Proceedings of the National Academy of Sciences* 115, 5810-5815.
- Ni, J., and Clark, S.E. (2006). Evidence for functional conservation, sufficiency, and proteolytic processing of the CLAVATA3 CLE domain. *Plant physiology* 140, 726-733.
- Niittylä, T., Fuglsang, A.T., Palmgren, M.G., Frommer, W.B., and Schulze, W.X. (2007). Temporal analysis of sucrose-induced phosphorylation changes in plasma membrane proteins of Arabidopsis. *Molecular & Cellular Proteomics* 6, 1711-1726.
- Nimchuk, Z.L. (2017). CLAVATA1 controls distinct signaling outputs that buffer shoot stem cell proliferation through a two-step transcriptional compensation loop. *PLoS genetics* 13, e1006681.
- Oertli, J. (1985). The response of plant cells to different forms of moisture stress. *Journal of plant physiology* 121, 295-300.
- Ogawa, M., Shinohara, H., Sakagami, Y., and Matsubayashi, Y. (2008). Arabidopsis CLV3 peptide directly binds CLV1 ectodomain. *Science* 319, 294-294.
- Ohyama, K., Ogawa, M., and Matsubayashi, Y. (2008). Identification of a biologically active, small, secreted peptide in Arabidopsis by in silico gene screening, followed by LC-MS-based structure analysis. *The Plant Journal* 55, 152-160.
- Okuda, S., Tsutsui, H., Shiina, K., Sprunck, S., Takeuchi, H., Yui, R., Kasahara, R.D., Hamamura, Y., Mizukami, A., and Susaki, D. (2009). Defensin-like polypeptide LUREs are pollen tube attractants secreted from synergid cells. *Nature* 458, 357-361.
- Osakabe, Y., Yamaguchi-Shinozaki, K., Shinozaki, K., and Tran, L.-S.P. (2013). Sensing the environment: key roles of membrane-localized kinases in plant perception and response to abiotic stress. *Journal of experimental botany* 64, 445-458.
- Ouyang, S.Q., Liu, Y.F., Liu, P., Lei, G., He, S.J., Ma, B., Zhang, W.K., Zhang, J.S., and Chen, S.Y. (2010). Receptor-like kinase OsSIK1 improves drought and salt stress tolerance in rice (*Oryza sativa*) plants. *The Plant Journal* 62, 316-329.
- Pearce, G., Strydom, D., Johnson, S., and Ryan, C.A. (1991). A polypeptide from tomato leaves induces wound-inducible proteinase inhibitor proteins. *Science* 253, 895-897.
- Pearce, G., Moura, D.S., Stratmann, J., and Ryan, C.A. (2001). RALF, a 5-kDa ubiquitous polypeptide in plants, arrests root growth and development. *Proceedings of the National Academy of Sciences* 98, 12843-12847.
- Péret, B., Li, G., Zhao, J., Band, L.R., Voß, U., Postaire, O., Luu, D.-T., Da Ines, O., Casimiro, I., and Lucas, M. (2012). Auxin regulates aquaporin function to facilitate lateral root emergence. *Nature cell biology* 14, 991-998.
- Pertl, H., Himly, M., Gehwolf, R., Kriechbaumer, R., Strasser, D., Michalke, W., Richter, K., Ferreira, F., and Obermeyer, G. (2001). Molecular and physiological characterisation of a 14-3-3 protein from lily pollen grains regulating the activity of the plasma membrane H<sup>+</sup> ATPase during pollen grain germination and tube growth. *Planta* 213, 132-141.
- Petutschnig, E.K., Jones, A.M., Serazetdinova, L., Lipka, U., and Lipka, V. (2010). The lysin motif receptor-like kinase (LysM-RLK) CERK1 is a major chitin-binding protein in Arabidopsis thaliana and subject to chitin-induced phosphorylation. *Journal of Biological Chemistry* 285, 28902-28911.

- Pillitteri, L.J., and Torii, K.U. (2012). Mechanisms of stomatal development. *Annual review of plant biology* 63, 591-614.
- Pinheiro, C., and Chaves, M. (2011). Photosynthesis and drought: can we make metabolic connections from available data? *Journal of experimental botany* 62, 869-882.
- Poole, R.L. (2005). The TAIR database. In *Plant Bioinformatics* (Springer), pp. 179-212.
- Postel, S., Küfner, I., Beuter, C., Mazzotta, S., Schwedt, A., Borlotti, A., Halter, T., Kemmerling, B., and Nürnberger, T. (2010). The multifunctional leucine-rich repeat receptor kinase BAK1 is implicated in Arabidopsis development and immunity. *European journal of cell biology* 89, 169-174.
- Prak, S., Hem, S., Boudet, J., Viennois, G., Sommerer, N., Rossignol, M., Maurel, C., and Santoni, V. (2008). Multiple phosphorylations in the C-terminal tail of plant plasma membrane aquaporins: role in subcellular trafficking of AtPIP2; 1 in response to salt stress. *Molecular & Cellular Proteomics* 7, 1019-1030.
- Qian, P., Song, W., Yokoo, T., Minobe, A., Wang, G., Ishida, T., Sawa, S., Chai, J., and Kakimoto, T. (2018). The CLE9/10 secretory peptide regulates stomatal and vascular development through distinct receptors. *Nature plants* 4, 1071-1081.
- Rappsilber, J., Ishihama, Y., and Mann, M. (2003). Stop and go extraction tips for matrix-assisted laser desorption/ionization, nanoelectrospray, and LC/MS sample pretreatment in proteomics. *Analytical chemistry* 75, 663-670.
- Ryan, C.A., Pearce, G., Scheer, J., and Moura, D.S. (2002). Polypeptide hormones. *The Plant Cell* 14, S251-S264.
- Ryu, K.H., Huang, L., Kang, H.M., and Schiefelbein, J. (2019). Single-cell RNA sequencing resolves molecular relationships among individual plant cells. *Plant physiology* 179, 1444-1456.
- Saibo, N.J., Lourenço, T., and Oliveira, M.M. (2009). Transcription factors and regulation of photosynthetic and related metabolism under environmental stresses. *Annals of botany* 103, 609-623.
- Santiago, J., Henzler, C., and Hothorn, M. (2013). Molecular mechanism for plant steroid receptor activation by somatic embryogenesis co-receptor kinases. *Science* 341, 889-892.
- Santiago, J., Brandt, B., Wildhagen, M., Hohmann, U., Hothorn, L.A., Butenko, M.A., and Hothorn, M. (2016). Mechanistic insight into a peptide hormone signaling complex mediating floral organ abscission. *Elife* 5, e15075.
- Scheer, J.M., and Ryan, C.A. (1999). A 160-kD systemin receptor on the surface of *Lycopersicon peruvianum* suspension-cultured cells. *The plant cell* 11, 1525-1535.
- Schlesier, B., Bréton, F., and Mock, H.-P. (2003). A hydroponic culture system for growing *Arabidopsis thaliana* plantlets under sterile conditions. *Plant Molecular Biology Reporter* 21, 449-456.
- Seidel, S.A., Dijkman, P.M., Lea, W.A., van den Bogaart, G., Jerabek-Willemsen, M., Lazic, A., Joseph, J.S., Srinivasan, P., Baaske, P., and Simeonov, A. (2013). Microscale thermophoresis quantifies biomolecular interactions under previously challenging conditions. *Methods* 59, 301-315.
- Shatil-Cohen, A., Sibony, H., Draye, X., Chaumont, F., Moran, N., and Moshelion, M. (2014). Measuring the osmotic water permeability coefficient (Pf) of spherical cells: isolated plant protoplasts as an example. *JoVE (Journal of Visualized Experiments)*, e51652.
- She, J., Han, Z., Kim, T.-W., Wang, J., Cheng, W., Chang, J., Shi, S., Wang, J., Yang, M., and Wang, Z.-Y. (2011). Structural insight into brassinosteroid perception by BRI1. *Nature* 474, 472-476.

- Shen, N., Jing, Y., Tu, G., Fu, A., and Lan, W. (2020). Danger-Associated Peptide Regulates Root Growth by Promoting Protons Extrusion in an AHA2-Dependent Manner in Arabidopsis. *International journal of molecular sciences* 21, 7963.
- Shen, W., Liu, J., and Li, J.-F. (2019). Type-II metacaspases mediate the processing of plant elicitor peptides in Arabidopsis. *Molecular plant* 12, 1524-1533.
- Shinohara, H., Mori, A., Yasue, N., Sumida, K., and Matsubayashi, Y. (2016). Identification of three LRR-RKs involved in perception of root meristem growth factor in Arabidopsis. *Proceedings of the National Academy of Sciences* 113, 3897-3902.
- Shiu, S.-H., and Bleecker, A.B. (2001a). Plant receptor-like kinase gene family: diversity, function, and signaling. *Science's STKE* 2001, re22-re22.
- Shiu, S.-H., and Bleecker, A.B. (2001b). Receptor-like kinases from Arabidopsis form a monophyletic gene family related to animal receptor kinases. *Proceedings of the National Academy of Sciences* 98, 10763-10768.
- Shiu, S.-H., and Bleecker, A.B. (2003). Expansion of the receptor-like kinase/Pelle gene family and receptor-like proteins in Arabidopsis. *Plant physiology* 132, 530-543.
- Shpak, E.D., McAbee, J.M., Pillitteri, L.J., and Torii, K.U. (2005). Stomatal patterning and differentiation by synergistic interactions of receptor kinases. *Science* 309, 290-293.
- Shulse, C.N., Cole, B.J., Ciobanu, D., Lin, J., Yoshinaga, Y., Gouran, M., Turco, G.M., Zhu, Y., O'Malley, R.C., and Brady, S.M. (2019). High-throughput single-cell transcriptome profiling of plant cell types. *Cell reports* 27, 2241-2247. e2244.
- Sommer, A., Mählknecht, G., and Obermeyer, G. (2007). Measuring the osmotic water permeability of the plant protoplast plasma membrane: implication of the nonosmotic volume. *Journal of Membrane Biology* 215, 111-123.
- Song, W., Han, Z., Wang, J., Lin, G., and Chai, J. (2017). Structural insights into ligand recognition and activation of plant receptor kinases. *Current opinion in structural biology* 43, 18-27.
- Sorensen, K., and Brodbeck, U. (1986). A sensitive protein assay method using micro-titer plates. *Experientia* 42, 161-162.
- Stegmann, M., Monaghan, J., Smakowska-Luzan, E., Rovenich, H., Lehner, A., Holton, N., Belkhadir, Y., and Zipfel, C. (2017). The receptor kinase FER is a RALF-regulated scaffold controlling plant immune signaling. *Science* 355, 287-289.
- Stenvik, G.-E., Tandstad, N.M., Guo, Y., Shi, C.-L., Kristiansen, W., Holmgren, A., Clark, S.E., Aalen, R.B., and Butenko, M.A. (2008). The EPIP peptide of INFLORESCENCE DEFICIENT IN ABSCISSION is sufficient to induce abscission in Arabidopsis through the receptor-like kinases HAESA and HAESA-LIKE2. *The Plant Cell* 20, 1805-1817.
- Sun, Y., Li, L., Macho, A.P., Han, Z., Hu, Z., Zipfel, C., Zhou, J.-M., and Chai, J. (2013). Structural basis for flg22-induced activation of the Arabidopsis FLS2-BAK1 immune complex. *Science* 342, 624-628.
- Szklarczyk, D., Franceschini, A., Wyder, S., Forslund, K., Heller, D., Huerta-Cepas, J., Simonovic, M., Roth, A., Santos, A., and Tsafou, K.P. (2015). STRING v10: protein-protein interaction networks, integrated over the tree of life. *Nucleic acids research* 43, D447-D452.

- Szymanski, W.G., Kierszniowska, S., and Schulze, W.X. (2013). Metabolic labeling and membrane fractionation for comparative proteomic analysis of *Arabidopsis thaliana* suspension cell cultures. *Journal of visualized experiments: JoVE*.
- Szymanski, W.G., Zauber, H., Erban, A., Gorka, M., Wu, X.N., and Schulze, W.X. (2015). Cytoskeletal components define protein location to membrane microdomains. *Molecular & Cellular Proteomics* 14, 2493-2509.
- Tabata, R., Sumida, K., Yoshii, T., Ohyama, K., Shinohara, H., and Matsubayashi, Y. (2014). Perception of root-derived peptides by shoot LRR-RKs mediates systemic N-demand signaling. *Science* 346, 343-346.
- Tang, J., Han, Z., Sun, Y., Zhang, H., Gong, X., and Chai, J. (2015). Structural basis for recognition of an endogenous peptide by the plant receptor kinase PEPR1. *Cell research* 25, 110-120.
- Tanz, S.K., Castleden, I., Hooper, C.M., Vacher, M., Small, I., and Millar, H.A. (2012). SUBA3: a database for integrating experimentation and prediction to define the SUB cellular location of proteins in *A. thaliana*. *Nucleic acids research* 41, D1185-D1191.
- Tavormina, P., De Coninck, B., Nikonorova, N., De Smet, I., and Cammue, B.P. (2015). The plant peptidome: an expanding repertoire of structural features and biological functions. *The Plant Cell* 27, 2095-2118.
- Tenhaken, R. (2015). Cell wall remodeling under abiotic stress. *Frontiers in plant science* 5, 771.
- Thimm, O., Bläsing, O., Gibon, Y., Nagel, A., Meyer, S., Krüger, P., Selbig, J., Müller, L.A., Rhee, S.Y., and Stitt, M. (2004). MAPMAN: a user-driven tool to display genomics data sets onto diagrams of metabolic pathways and other biological processes. *The Plant Journal* 37, 914-939.
- Tichtinsky, G., Vanoosthuysse, V., Cock, J.M., and Gaude, T. (2003). Making inroads into plant receptor kinase signalling pathways. *Trends in plant science* 8, 231-237.
- Torii, K.U. (2004). Leucine-rich repeat receptor kinases in plants: structure, function, and signal transduction pathways. *Int Rev Cytol* 234, 1-46.
- Torii, K.U. (2012). Mix-and-match: ligand–receptor pairs in stomatal development and beyond. *Trends in plant science* 17, 711-719.
- Torii, K.U., Mitsukawa, N., Oosumi, T., Matsuura, Y., Yokoyama, R., Whittier, R.F., and Komeda, Y. (1996). The *Arabidopsis* ERECTA gene encodes a putative receptor protein kinase with extracellular leucine-rich repeats. *The Plant Cell* 8, 735-746.
- Törnroth-Horsefield, S., Wang, Y., Hedfalk, K., Johanson, U., Karlsson, M., Tajkhorshid, E., Neutze, R., and Kjellbom, P. (2006). Structural mechanism of plant aquaporin gating. *Nature* 439, 688-694.
- Trivilin, A., Hartke, S., and Moraes, M. (2014). Components of different signalling pathways regulated by a new orthologue of *A. t* PROPEP 1 in tomato following infection by pathogens. *Plant Pathology* 63, 1110-1118.
- Trotochaud, A.E., Jeong, S., and Clark, S.E. (2000). CLAVATA3, a multimeric ligand for the CLAVATA1 receptor-kinase. *Science* 289, 613-617.
- Trotochaud, A.E., Hao, T., Wu, G., Yang, Z., and Clark, S.E. (1999). The CLAVATA1 receptor-like kinase requires CLAVATA3 for its assembly into a signaling complex that includes KAPP and a Rho-related protein. *The Plant Cell* 11, 393-405.
- Tyanova, S., Temu, T., and Cox, J. (2016a). The MaxQuant computational platform for mass spectrometry-based shotgun proteomics. *Nature protocols* 11, 2301.

- Tyanova, S., Temu, T., Sinitcyn, P., Carlson, A., Hein, M.Y., Geiger, T., Mann, M., and Cox, J. (2016b). The Perseus computational platform for comprehensive analysis of (prote) omics data. *Nature methods* 13, 731.
- Ullrich, A., and Schlessinger, J. (1990). Signal transduction by receptors with tyrosine kinase activity. *Cell* 61, 203-212.
- Van der Weele, C.M., Spollen, W.G., Sharp, R.E., and Baskin, T.I. (2000). Growth of *Arabidopsis thaliana* seedlings under water deficit studied by control of water potential in nutrient-agar media. *Journal of Experimental Botany* 51, 1555-1562.
- Verslues, P.E., Agarwal, M., Katiyar-Agarwal, S., Zhu, J., and Zhu, J.K. (2006). Methods and concepts in quantifying resistance to drought, salt and freezing, abiotic stresses that affect plant water status. *The Plant Journal* 45, 523-539.
- Walhout, M., Vidal, M., and Dekker, J. (2012). *Handbook of systems biology: concepts and insights.* (Academic Press).
- Wang, J., Lin, G., Ma, R., Han, Z., and Chai, J. (2018a). Structural Insight into Recognition of Plant Peptide Hormones by Plant Receptor Kinases. In *Plant Structural Biology: Hormonal Regulations* (Springer), pp. 31-46.
- Wang, J., Li, H., Han, Z., Zhang, H., Wang, T., Lin, G., Chang, J., Yang, W., and Chai, J. (2015). Allosteric receptor activation by the plant peptide hormone phytosulfokine. *Nature* 525, 265-268.
- Wang, J., Xi, L., Wu, X.N., König, S., Schulze, W.X. (unpublished). PEP7 is a ligand for receptor kinase SIRK1 to regulate aquaporins and root growth.
- Wang, L., Einig, E., Almeida-Trapp, M., Albert, M., Fliegmann, J., Mithöfer, A., Kalbacher, H., and Felix, G. (2018b). The systemin receptor SYR1 enhances resistance of tomato against herbivorous insects. *Nature plants* 4, 152-156.
- Wang, Z.-Y. (2012). Brassinosteroids modulate plant immunity at multiple levels. *Proceedings of the National Academy of Sciences* 109, 7-8.
- Wang, Z.-Y., Seto, H., Fujioka, S., Yoshida, S., and Chory, J. (2001). BRI1 is a critical component of a plasma-membrane receptor for plant steroids. *Nature* 410, 380-383.
- Wienken, C.J., Baaske, P., Rothbauer, U., Braun, D., and Duhr, S. (2010). Protein-binding assays in biological liquids using microscale thermophoresis. *Nature communications* 1, 1-7.
- Witte, C.-P., Noël, L., Gielbert, J., Parker, J., and Romeis, T. (2004). Rapid one-step protein purification from plant material using the eight-amino acid StrepII epitope. *Plant molecular biology* 55, 135-147.
- Wong, J.E., Midtgaard, S.R., Gysel, K., Thygesen, M.B., Sørensen, K.K., Jensen, K.J., Stougaard, J., Thirup, S., and Blaise, M. (2015). An intermolecular binding mechanism involving multiple LysM domains mediates carbohydrate recognition by an endopeptidase. *Acta Crystallographica Section D: Biological Crystallography* 71, 592-605.
- Wu, X.N., Rodriguez, C.S., Pertl-Obermeyer, H., Obermeyer, G., and Schulze, W.X. (2013). Sucrose-induced receptor kinase SIRK1 regulates a plasma membrane aquaporin in *Arabidopsis*. *Molecular & Cellular Proteomics* 12, 2856-2873.
- Wu, X.N., Xi, L., Pertl-Obermeyer, H., Li, Z., Chu, L.-C., and Schulze, W.X. (2017). Highly efficient single-step enrichment of low abundance phosphopeptides from plant membrane preparations. *Frontiers in plant science* 8, 1673.

- Wu, X.N., Chu, L., Xi, L., Pertl-Obermeyer, H., Li, Z., Sklodowski, K., Sanchez-Rodriguez, C., Obermeyer, G., and Schulze, W.X. (2019). Sucrose-Induced Receptor Kinase 1 is modulated by an interacting kinase with short extracellular domain. *Molecular & Cellular Proteomics* 18, 1556-1571.
- Xi, L., Wu, X.N., Gilbert, M., and Schulze, W.X. (2019). Classification and interactions of LRR receptors and co-receptors within the Arabidopsis plasma membrane—an overview. *Frontiers in plant science* 10, 472.
- Xi, L., Wu, X.N., Wang, J., Zhang, Z., Schulze, W.X. (unpublished). Receptor kinase signaling of BRI1 and SIKK1 is tightly balanced by their interactomes as revealed from domain-swap chimaera in AE-MS approaches.
- Xiao, Y., Stegmann, M., Han, Z., DeFalco, T.A., Parys, K., Xu, L., Belkhadir, Y., Zipfel, C., and Chai, J. (2019). Mechanisms of RALF peptide perception by a heterotypic receptor complex. *Nature* 572, 270-274.
- Yamaguchi, Y., Pearce, G., and Ryan, C.A. (2006). The cell surface leucine-rich repeat receptor for AtPep1, an endogenous peptide elicitor in Arabidopsis, is functional in transgenic tobacco cells. *Proceedings of the National Academy of Sciences* 103, 10104-10109.
- Yamaguchi, Y., Huffaker, A., Bryan, A.C., Tax, F.E., and Ryan, C.A. (2010). PEPR2 is a second receptor for the Pep1 and Pep2 peptides and contributes to defense responses in Arabidopsis. *The Plant Cell* 22, 508-522.
- Yang, X., Deng, F., and Ramonell, K.M. (2012). Receptor-like kinases and receptor-like proteins: keys to pathogen recognition and defense signaling in plant innate immunity. *Frontiers in Biology* 7, 155-166.
- Yekondi, S., Liang, F.C., Okuma, E., Radziejowski, A., Mai, H.W., Swain, S., Singh, P., Gauthier, M., Chien, H.C., and Murata, Y. (2018). Nonredundant functions of Arabidopsis Lec RK-V. 2 and Lec RK-VII. 1 in controlling stomatal immunity and jasmonate-mediated stomatal closure. *New Phytologist* 218, 253-268.
- Yu, M., Li, R., Cui, Y., Chen, W., Li, B., Zhang, X., Bu, Y., Cao, Y., Xing, J., and Jewaria, P.K. (2020). The RALF1-FERONIA interaction modulates endocytosis to mediate control of root growth in Arabidopsis. *Development* 147.
- Zhang, H., Han, Z., Song, W., and Chai, J. (2016a). Structural insight into recognition of plant peptide hormones by receptors. *Molecular plant* 9, 1454-1463.
- Zhang, H., Lin, X., Han, Z., Wang, J., Qu, L.-J., and Chai, J. (2016b). SERK family receptor-like kinases function as co-receptors with PXY for plant vascular development. *Molecular plant* 9, 1406-1414.
- Zhang, X., Yang, Z., Wu, D., and Yu, F. (2020). RALF-FERONIA signaling: linking plant immune response with cell growth. *Plant communications*, 100084.
- Zimmermann, M.H., and Milburn, J.A. (2012). *Transport in plants I: phloem transport*. (Springer Science & Business Media).
- Zipfel, C., Kunze, G., Chinchilla, D., Caniard, A., Jones, J.D., Boller, T., and Felix, G. (2006). Perception of the bacterial PAMP EF-Tu by the receptor EFR restricts Agrobacterium-mediated transformation. *Cell* 125, 749-760.
- Zulawski, M., Schulze, G., Braginet, R., Hartmann, S., and Schulze, W.X. (2014). The Arabidopsis Kinome: phylogeny and evolutionary insights into functional diversification. *BMC genomics* 15, 1-15.



## 8. Acknowledgments

My first thanks must go to China Scholarship Council (CSC), for sponsoring me to live and study in Germany for 40 months.

I would like to express my deepest gratitude to my supervisor Prof. Dr. Waltraud Schulze. She accepted me despite the fact that I initially knew nothing about this academic field. She gave me time and patience, and guided me most wisely in my studies and beyond. She was always available to discuss ideas with me and provided valuable feedback on conceptual and technical aspects. I learned a lot from her, not only about the qualities necessary to be a proper scientific researcher, but also about everything it takes to be an independent, courageous, open-minded person.

I would like to sincerely thank my colleagues who work with me and those who have worked with me. We discussed academic issues and shared happiness and sorrow. They are Dr. Lin Xi, Dr. Xuna Wu, Dr. Thorsten Stefan, Dr. Zhi Li, Dr. Liangcui Chu, Max Gilbert, Sven Gombos, Mingjie He, Matthias Mayer, and many others. I will remember every single favor they gave me, including those whiteboard lectures and hands-on teaching. I am truly grateful to our technicians Susanne Liner, Zhaoxia Zhang and Sandra Herold for their help and family-like warmth. I am also grateful to our secretary, Frau Melina Effner, for her help in all administrative matters. I feel much honored to work in this team.

Special thanks to Prof. Dr. Andreas Schaller, Eric Bühler, Dr. Nils Stührwohldt, and other members of the Department of Plant Physiology and Biotechnology (190c). Thanks to Eric for teaching me to use the 'Monolith NT.115' and making appointments for me to use it, and to Dr. Nils Stührwohldt and Prof. Dr. Andreas Schaller for their guidance in this regard.

I am grateful for all the friends I met in Germany. Your company has brightened my lonely journey abroad, and I will always miss the time I spent with you. I wish you all the best in life.

Finally, I would like to thank my family and friends from far away in China for their support and inspiration over the past four years. I would especially like to thank my fiancé Dr. Shoubing Huang, for always encouraging, sustaining, caring and accommodating with love.

## 9. Declaration

**According to Sec. 18(3) sentence 5 of the University of Hohenheim's Doctoral Regulations for the Faculties of Agricultural Sciences, Natural Sciences, and Business, Economics and Social Sciences**

1. The dissertation submitted on the topic 'PEP7 is a ligand for receptor kinase SIRK1 to regulate aquaporins and root growth' is work done independently by me.
2. I only used the sources and aids listed and did not make use of any impermissible assistance from third parties. In particular, I marked all content taken word-for-word or paraphrased from other works.
3. I did not use the assistance of a commercial doctoral placement or advising agency.
4. I am aware of the importance of the declaration in lieu of oath and the criminal consequences of false or incomplete declarations in lieu of oath.

I confirm that the declaration above is correct. I declare in lieu of oath that I have declared only the truth to the best of my knowledge and have not omitted anything.

Stuttgart, 30. Jun. 2021

---

Place, Date

*Jinhu-Wang.*

---

Signature

## 10. Curriculum Vitae

### Personal information

Name: Jiahui Wang

Sex: Female

Date of Birth: 10 November 1992

Place of birth: Shanxi, China

Nationality: Chinese

Contact: [Jiahui.Wang@uni-hohenheim.de](mailto:Jiahui.Wang@uni-hohenheim.de)

### Education

- 2017.10 – present    Ph.D. candidate (Plant Systems Biology)  
Institute of Biology, Faculty of Natural Science, University of Hohenheim  
Stuttgart, Germany
- 2015.09 – 2017. 09    M.Sc. (Crop Physiology)  
College of Agronomy and Biotechnology, China Agricultural University  
Beijing, China
- 2011.09 – 2015.09    B.Sc. (Agronomy)  
College of Agronomy, Shan Dong Agricultural University  
Shandong, China

### Workshop, summer school and conference

- Sep. 2019            4th Summer Academy in Molecular Plant Biology  
Heiligkreuztal, Germany
- Mar. 2019            11th RegioPlantScience Meeting  
Stuttgart, Germany
- Feb. 2018            10th RegioPlantScience Meeting  
Tübingen, Germany

*Jiahui Wang.*